

ROLE OF ACTIVATING TRANSCRIPTION FACTOR 4 IN GUIDING THE LIVER
RESPONSE TO AMINO ACID DEPLETION BY ASPARAGINASE

By

RANA JABER TARISH AL-BAGHDADI

A dissertation submitted to the

Graduate School-New Brunswick

Rutgers, The State University of New Jersey

In partial fulfillment of the requirements

For the degree of

Doctor of Philosophy

Graduate Program in Endocrinology and Animal Biosciences

Written under the direction of

Tracy G Anthony

And approved by

New Brunswick, New Jersey

October 2016

ABSTRACT OF THE DISSERTATION

Role of Activating Transcription Factor 4 in Guiding the Liver Response to Amino

Acid Depletion by Asparaginase

By RANA JABER TARISH AL-BAGHDADI

Dissertation Director:

Tracy G Anthony

Asparaginase (ASNase) is widely used to treat acute lymphoblastic leukemia (ALL) in children but it causes metabolic complications related to liver toxicity. ASNase depletes circulating asparagine and glutamine, activating the homeostatic amino acid response (AAR) via phosphorylation of eukaryotic initiation factor 2 (eIF2) and resultant synthesis of activating transcription factor 4 (ATF4). The eIF2-ATF4 pathway is essential for cell survival during amino acid starvation conditions. Activation of the AAR in liver requires the eIF2 kinase called general control nonderepressible 2 kinase (GCN2). This pathway is vital to prevent hepatic failure during ASNase treatment. To what extent activation of the GCN2-eIF2-AAR is mediated by ATF4 is unknown. My dissertation objective is to assess the role of ATF4 in directing the hepatic response to ASNase. The

overarching hypothesis is that the AAR protects the liver during ASNase treatment. My objective and hypothesis are addressed in three aims: (1) Describe the liver response to ASNase in mice deleted for *Atf4*; (2) Determine if *Atf4* heterozygosity alters the liver response to ASNase; (3) Examine the hepatic response to ASNase in mice with a liver-specific deletion of *Atf4*. RNA sequencing alongside complementary biochemical and histological approaches were performed in the livers of mice treated with 8 daily injections of ASNase or saline excipient. Cellular pathways examined in detail included the AAR, endoplasmic reticulum (ER) stress response, and the mammalian target of rapamycin complex 1 (mTORC1) signaling pathway. In Aim 1, I discovered that global hepatic gene expression patterns in *Atf4* knockout mice overlapped with *Gcn2* knockout mice. Shared hepatic pathways or processes altered during ASNase included nuclear receptor activation, mTOR signaling, and xenobiotic metabolism. On the other hand, loss of *Atf4* during ASNase uniquely altered gene expression signatures reflecting signaling via eIF2 and ER stress. Further exploration at the level of protein expression and activity in liver revealed that during ASNase *Gcn2* deletion stimulated mTORC1 activity whereas *Atf4* deletion induced ER stress. In Aim 2, I found that *Atf4* heterozygosity compromised the hepatic AAR to ASNase, resulting in greater DNA fragmentation and hepatotoxicity. In Aim 3, I discovered that global hepatic gene expression patterns in nonstressed *Atf4* knockout mice reflected many of the same processes and pathways altered in

nonstressed mice with a liver-specific deletion of *Atf4*. Furthermore, the AAR and ER stress profiles in ASNase-treated mice with liver specific deletion of *Atf4* were similar in pattern and direction to whole body *Atf4* deletion, supporting a role for hepatic ATF4 in directing the adaptive AAR and preventing maladaptive ER stress to ASNase. This research provides insight into the importance of genetic background of patients in choosing ASNase as a treatment. These findings may be used to help predict which patients diagnosed with ALL may be susceptible to adverse metabolic events during ASNase. Alongside that, I established that global or partial loss of ATF4 influences liver toxicity in ASNase-treated mice.

ACKNOWLEDGMENTS

I would like to first thank my advisor, and mentor, Dr. Tracy G. Anthony for her guidance and support through the years of my research project. I am really grateful for your professional guidance and endless support. Thank you for giving me the opportunity to be a student in your laboratory. I am fully appreciative for your support during all the difficult moments I faced during the previous years. I would like to acknowledge my committee members, Dr. Terri G. Kinzy, Dr. Wendie S. Cohick, and Dr. William J. Belden, for their expertise, support, and encouragement. I really appreciate all your feedback and advice during the years of my dissertation project.

Great thanks to Dr. William Belden who guided me through the RNA-Seq analyses and for the space he gave me in his lab during the bioinformatics analyses. Thank you to Dr. Tammy Joska who taught me how to use the IPA pathway analysis software and for the use of her lab computer during my RNA-Seq analyses. I am so grateful to Jinhee Park, Dr. Belden's PhD student, who helped me during my time in Dr. Belden's lab.

Sincere thanks to Emily Mirek. Your friendship, technical expertise, help, and support all the time made my lab life much easier. I was greatly fortunate that you were the lab manager and the mouse whisper (as Lindsey used to call you) and most importantly a great friend. I would like to thank you for always being there at the end of a hard day. Those late times in the lab and the mouse room would have been much more difficult without your help.

I would also like to thank Dr. Yongping Wang for helping with the TUNEL assay and the RNA-seq samples preparation. Thank you Dr. Inna Nikonorova, and Dr. Ashley Pettit for the technical help and science discussion. Thank you for your friendship and great advice. Thank you Lindsey Philipson-Weiner for being such a great friend and for hydrating me especially during the long days of western blotting. I am so happy and appreciative that we were graduate students in the same. You are very intelligent, and have bright ideas, and I am always so impressed with your knowledge and great thinking.

I have to thank Dr. Gabe Wilson who showed me how to do western blots and analyze qPCR data.

Great appreciation and Thanks to our previous undergraduate student Casey Fannell who put lots of time and effort toward the age study especially conducting western blots and qPCR. Thank you to our previous and current undergrads, Brittany Leigh Lennox, Chris De Oliveira and Shadi Rajeh for maintaining an efficient workspace in the lab.

I would like to acknowledge the enormous effort that the Higher Committee for Educational Development in Iraq (HCED) has done to confer the Iraqi students this great opportunity to study in the United States. I highly appreciate the HCED scholarship moral and financial support.

Importantly, a great gratitude to all the faculty and staff in the Veterinary Medicine College/ Al-Qadisiya University for the recognizable efforts they have done to help me to be able to study in the United States. Specifically, enormous acknowledgements to Dr. Jabbar Abbass Al-sa`adi, Dr. No`man Naji, Dr. Eman

Faisal, Dr. Amer Ibrahim, Dr. Tha`r Alwan, Dr. Dhia Al-Dolaimi, Dr. Abudlstar Alalwani, and Dr. Hassan Khalaf.

A sincere thank you to my family; my mother, father, brothers, sisters, nieces, and nephews, without whom I would not have made it this far. Thank you for your love, support, and patience. Thank you for supporting me as I decided to study abroad and for your fabulous emotional support through all the time. I love you all and I am so grateful to have the greatest family. Words cannot express my gratitude to all of you.

I would like to thank my husband, Ali who believes in me and supports me strongly. I am thankful for your patience and self-sacrifice over the past years. No matter what I say it would not be enough to express my gratitude.

Thank you to my absolutely wonderful son, Mohammed. I love you infinity as you always say to me. I am so thankful for your endless love.

Finally, I would like to dedicate this to my mother who died of lymphoblastic leukemia in 1998. I wish this work would help in any way patients of this disease.

TABLE OF CONTENTS

	Page
Abstract	ii
Acknowledgments	v
Table of Contents	viii
List of Figures	xviii
 Introduction	 1
CHAPTER ONE: Literature Review	4
ASNase as Chemotherapy for ALL.....	4
ASNase Mechanism of Action	5
Integrated Stress Response	6
ASNase Activates the Amino Acid Response	8
Loss of GCN2 Aggravate ASNase-induced Hepatotoxicity	10
ER stress and the Unfolded Protein Response.....	11
mTORC1 Signaling	14
ATF4 Is a Master Regulator.....	16
Summary	20
Literature Cited	22
Common Abbreviations.....	39
Figures.....	42
Research Objectives and Hypotheses.....	45

CHAPTER TWO: Roles of ATF4 in the Murine Response to ASNase in Liver.

Abstract	47
Introduction.....	48
Materials and Methods	51
Results.....	58
Discussion	65
Literature Cited	70
Figures Caption	75
Figures.....	79

CHAPTER THREE: Hepatic ATF4 Regulates the AAR to ASNase in Mice.

Abstract	93
Introduction.....	95
Materials and Methods	97
Results.....	101
Discussion	106
Literature Cited	108
Figure Captions	112
Figures.....	115
Overall Summary	123
Literature Cited.....	128

LIST OF FIGURES

CHAPTER ONE

Figure 1. The ISR. In mammals, Eif2 is phosphorylated by four different kinases in response to various environmental stresses.....43

Figure 2. Hypothesized model of amino acid response (AAR) pathway activated by ASNase in liver. ASNase induces eIF2 phosphorylation and subsequent activation of the AAR. These events correspond with hepatic adaptive recovery in intact GCN2 mice. Mice lacking *Atf4* fails to activate the homeostatic AAR and this corresponds with ASNase-induced hepatotoxicity.....44

CHAPTER TWO

Figure 1. Whole body and tissue responses to ASNase. (A) Percent of body fat mass and percent of body lean mass was measured by EchoMRI before the treatment (day 0) in wildtype (WT), *Gcn2*^{-/-} and *Atf4*^{-/-} mice. (B) Percent of body fat mass change after 8 d of i.p. injection of PBS or ASNase. (C) Percent of body lean mass change after 8 d of i.p. injection of PBS or ASNase. (D) Percent body weight (BW) change in wildtype (WT), *Gcn2*^{-/-} and *Atf4*^{-/-} mice treated with 8 daily i.p. injections of PBS or ASNase (3 IU/g BW) and euthanized 8 h after the last injection. (E) Percent weight change of liver, pancreas, and spleen relative to

BW. Data were analyzed by two-factor ANOVA, n=4-6 animals per group. Means without a common letter are statistically different (P<0.05).....79

Figure 2. Transcriptional profiling of livers from WT, *Gcn2*^{-/-} and *Atf4*^{-/-} mice treated with PBS or ASNase. Deletion of *Gcn2* and *Atf4* genes in mice. (A, B) Integrity Genome Viewer (IGV) plots show the absence of *Gcn2* and *Atf4* exons in *Gcn2*^{-/-} and *Atf4*^{-/-} mice respectively after being aligned to the mouse genome mm10. (C) Gene expression of *Atf4* measured by using RT-qPCR. Data represent n=3 per group. *Atf4* gene expression was analyzed by two-factor ANOVA, Means not sharing a common letter are different, P<0.05. (D) Volcano plot shows the genes that differ significantly (highlighted in red) among PBS and ASNase treatment conditions in wildtype (WT), *Gcn2*^{-/-} and *Atf4*^{-/-} mice treated with 8 daily intraperitoneal injections of PBS or ASNase (3 IU/g BW) and euthanized 8 h after the last injection (P<0.05). X-axis represents Log2 (fold change) and Y axis represents the -log(P-value). (E) Principle Component Analysis (PCA) plot with X-axis represents PC1, the first component points in the direction of highest variance. The Y-axis represents PC2, the second component points in the direction of highest variance. (F) Venn diagram showing altered basal gene expression divided into three categories: unique to *Gcn2* deletion [A], unique to *Atf4* deletion [C] or common to deletion of either [B]. (G) Venn diagram showing categories of gene expression altered by ASNase including gene changes independent of the GCN2-ATF4-AAR [D]; those unique to *Gcn2*^{-/-} [E]; those unique to *Atf4*^{-/-} [G]; and those common to *Gcn2*^{-/-} and *Atf4*^{-/-} [F]. (H) IPA of

basal gene expression categories A-C in above Venn diagram. (I) IPA of ASNase-induced gene expression categories D-G in the above Venn diagram. (J) Heat map of nuclear receptor gene expression. Data represent n=3 per group. All differentially expressed genes shown were statistically significant (q value or FDR < 0.1; unadjusted p < 0.017).....81

Figure 3. Loss of *Gcn2* or *Atf4* differentially alters the hepatic AAR to ASNase.

(A) Phosphorylation of eIF2 in liver by immunoblot analysis. (B) RNA-Seq expression data presented in a heat map clusters the hepatic AAR to ASNase into three categories: stable or increased gene expression in both *Gcn2*^{-/-} and *Atf4*^{-/-}, represented by *Sesn2* (C), elevated gene expression in *Atf4*^{-/-} but not in *Gcn2*^{-/-}, represented by *Asns* (D), and reduced expression in both *Gcn2*^{-/-} and *Atf4*^{-/-}, represented by *Fgf21* (E) Color scale shows genes with increased expression (dark brown range) and decreased expression (light yellow range). Gene expression in C-E measured by RT-qPCR. Data were analyzed by two-factor ANOVA, n=3 per group. Means without a common letter are different, P<0.05.....85

Figure 4. Whole body deletion of *Atf4* induces genetic markers of hepatic ER stress following 8 d ASNase. (A) Phosphorylation of PERK in liver by immunoblot analysis. (B) Gene expression of spliced (*sXbp1*) and unspliced (*uXbp1*) Xbp1 measured by RT-qPCR. (C) Gene expression of *Atf6* measured by RT-qPCR. (D) Gene expression of *Ddit3* measured by RT-qPCR. Data were analyzed by two-

factor ANOVA, n=3 per group. Means without a common letter are different, P<0.05..... 86

Figure 5. Hepatic mTORC1 signaling is hyperactivated in response to ASNase in *Gcn2*^{-/-} but not *Atf4*^{-/-} mice. Densitometry of immunoblots for (A) Phospho-S6K1 at threonine 389 B) Phospho-4E-BP1 C) Phospho Akt at threonine 308 and D) Phospho Sestrin2. E) Representative immunoblots for panels A-D..... 87

Figure 6. Heterozygous deletion of *Atf4* alters hepatic AAR and promotes cell death in response to ASNase. (A) Percentage of body fat and lean mass before the treatment (day 0) in wildtype (*Atf4*^{+/+}), *Atf4*^{+/-} and *Atf4*^{-/-} mice as measures by EchoMRI. (B) Percent of body fat mass change after 8 d of i.p. injection of PBS or ASNase. (C) Percent of body lean mass change after 8 d of intraperitoneal injection of PBS or ASNase (D) Percent body weight (BW) change in *Atf4*^{+/+}, *Atf4*^{+/-} and *Atf4*^{-/-} mice treated with PBS or ASNase (daily i.p. injections of 3 IU/g BW for 8 days) and sacrificed 8 h after the last injection. (E) Percent weight change of liver, pancreas, and spleen relative to body weight. (F) Oil Red O stained liver sections (5μm) show neutral lipid accumulations, red dots. (G) Triglyceride concentrations in the livers of *Atf4*^{+/+}, *Atf4*^{+/-} and *Atf4*^{-/-} mice as measured by Triglyceride Quantification Colorimetric/Fluorometric assay. (H) Fragmented DNA visualization using TUNEL assay in liver sections (10μm). Images show visual features determined in 3-5 mice per group using X 20 objective in *Atf4*^{+/+}, *Atf4*^{+/-} and *Atf4*^{-/-} mice. (I) Apoptosis was ascertained by

manual counting of TUNEL-positive nuclei using Image J software. (J) Phospho-eIF2 was measure by immunoblot analysis and quantified relative to total eIF2. (K) Gene expression of *Atf4* in liver as measured by RT-qPCR. (L) Gene expression of AAR genes *Asns*, *Atf3*, *Atf5*, *Fgf21*, *Elf4ebp1*, *Ppp1r15a* in *Atf4*^{+/+}, *Atf4*^{+/-} and *Atf4*^{-/-} mice. Data were analyzed by two-factor ANOVA, n=4-8 per group. Means not sharing a common letter are different, P<0.05..... 88

Figure 7. Heterozygous loss of *Atf4* predisposes mice to ER stress when treated with ASNase. Expression of ER stress genes A) *Ddit3* (*Chop*) B) *Xbp1* splicing C) *Hspa5* and *Atf6* in liver was measured by RT-qPCR. D) Expression of oxidative stress marker *Nrf2* in liver was measured by RT-qPCR. Data were analyzed by two-factor ANOVA, n=4-8 per group. Means not sharing a common letter are different, P<0.05 92

CHAPTER THREE

Figure 1. Body and tissue responses to ASNase in mice with Cre recombinase-mediated deletion of *Atf4* in liver. (A-C) Body fat mass and percent of body lean mass was measured by EchoMRI before the treatment (day 0) in Cre- and Cre+ mice. (D) Percent body weight (BW) change in Cre- (*Atf4*^{flox/flox}), and Alb-Cre+ (liver-specific *Atf4*^{-/-}) mice treated with 8 daily i.p. injections of ASNase (3 IU/g BW) or saline excipient and killed 8 h after the last injection. (E) Percent weight change of liver, pancreas, and spleen relative to body weight. Data were

analyzed by two-factor ANOVA, n=6-8 animals per group. Means not sharing a common letter are different, $P < 0.05$115

Figure 2. Global discovery of genes altered by *IsAtf4^{-/-}* (Cre+) mice basally. (A) *Atf4* gene expression by RT-qPCR. (B) Volcano plot shows the genes that differ significantly (highlighted in red) between 2 conditions ($P < 0.05$). X-axis represents Log2 (fold change) and Y axis represents the negative log(P value). (C) Principle Component Analysis (PCA) plot was conducted to explore the relationship between the two strains, with X-axis represents PC1, the first component points in the direction of highest variance. The Y-axis represents PC2, the second component points in the direction of highest variance. Cre-, Cre+, WT, whole body *Atf4^{-/-}* mice, n=3 per group ($P < 0.03$, FDR<0.1). (D) Venn diagram shows number of genes altered basally can be divided into three categories, unique to Cre+ deletion [A], unique to whole body *Atf4* deletion [C] or common to deletion of either [B]. (E) IPA of biological changes in gene expression as categorized above within the Venn diagram. Samples went through RNA-Seq analyses are livers of Cre-, Cre+, WT and whole body *Atf4^{-/-}* mice FDR<0.1, n=3 per group. Means not sharing a common letter are different, $P < 0.05$117

Figure 3. Hepatic deletion of *Atf4* alters AAR and promotes cell death in response to ASNase. (A) Fragmented DNA evaluation as a marker of apoptosis level was measured by TUNEL staining of liver sections (10µm), and ascertained by manual counting of the staining-positive nuclei using Image J software. n=3

per group. (B) Phospho-eIF2 was measure by immunoblot analysis and quantified relative to total eIF2. (C) Gene expression of AAR genes *Asns*, *Atf3*, *Atf5*, *Fgf21*, *Eif4ebp1*, and *Ppp1r15a* in Cre- and Cre+ mice. Data were analyzed by two-factor ANOVA, n=6-8 per group. Means not sharing a common letter are different, P<0.05.....120

Figure 4. Hepatic *Atf4* deletion promotes ER stress to ASNase. Gene expression of (A) *Ddit3*, (B) spliced (s*Xbp1*) and unspliced (u*Xbp1*) Xbp1, (C) *Hspa5* and *Atf6*, (D) *Nrf2* measured by RT-PCR. Data were analyzed by two-factor ANOVA, n=6-8 per group. Means not sharing a common letter are different, P<0.05..... 121

Figure 5. Nonstressed Cre+ mice demonstrate elevated mTORC1signaling that is downregulated in response to ASNase independent of Akt phosphorylation and Sestrin2 phosphorylation. (A) Phospho-S6K1 at threonine 389, (B) Phospho-4E-BP1, and (C) Phospho-Akt at threonine 308 was assessed by immunoblot analysis while (D) Phospho-Sestrin2 was assessed by electrophoretic mobility shift. (Data were analyzed by two-factor ANOVA, n=6-8 per group. Means not sharing a common letter are different, P<0.05.....122

INTRODUCTION

Acute lymphoblastic leukemia (ALL) is the most common type of cancer in children and adolescents, and it is a frequent cause of death in those under age 20. Asparaginase (ASNase) is a drug that is used to treat ALL (Pui et al., 2008; Patil et al., 2010; Raetz and Salzer, 2010; Hill et al., 1967), and it is widely recommended as it improves remission induction rate (Landau and Lamanna, 2006). Nevertheless, ASNase has many deleterious side effects such as coagulopathy and thromboembolism (Wani et al., 2010; Pui and Evans, 2006; Payne and Vora, 2007), neurological and cardiovascular complications (Kieslich et al., 2003), hyperglycemia and pancreatitis (Knoderer et al., 2007; Spinola-Castro et al., 2009). Liver failure is one of the main metabolic complications of ASNase leading to treatment abandonment particularly in adolescents who suffer greater complications (Appel et al., 2008). Importantly, the exact mechanisms underlying ASNase-induced toxicity remain incompletely understood. Acquiring an improved understanding of the mechanism of these toxicities may improve treatment options.

ASNase works by depleting blood levels of the amino acids asparagine and glutamine, causing amino acid deprivation. Our laboratory was the first to demonstrate that ASNase reduces liver protein synthesis by increasing phosphorylation of eukaryotic initiation translation factor 2 (eIF2) (Reinert et al., 2006) via the general control nonderepressible 2 kinase (GCN2) (Bunpo et al., 2009). Phosphorylation of eIF2 by GCN2 dampens global protein synthesis rates

while simultaneously promoting gene-specific translation of protein factors such as activating transcription factor 4 (ATF4). Subsequent binding of ATF4 to specific cis-elements called CARE (for CAAT enhancer binding protein-ATF response element; also referred to as amino acid response elements or AARE) in genes alters the transcriptome to promote survival and regain homeostasis. This GCN2-eIF2-ATF4-driven adaptive mechanism is described as the amino acid response (AAR) (Kilberg et al., 2009). Our laboratory previously described how GCN2 is necessary for hepatic adaptation to ASNase through activating the GCN2-eIF2-ATF4-AAR (Wilson et al., 2013; Wilson et al., 2015). In these studies, the role of GCN2 in minimizing ASNase hepatotoxicity is revealed. However, the downstream modulators are yet to be elucidated, in particular the role of ATF4.

ATF4 is described in many research articles as a master regulator of metabolism in response to many cellular stressors. It was found to play critical role in amino acid deficiency as a member of the GCN2-eIF2-ATF4 AAR pathway (Kilberg et al., 2012). ATF4 also plays a fundamental role in oxidative, heat shock and endoplasmic reticulum stress in response to activation of multiple eIF2 kinases in a process known as integrated stress response (Harding et al., 2003). ATF4 acts as a key point that help the cell to survive stress through activation of survival pathways such as enhancing amino acids synthesis by providing amino acids supply as a result of inducing amino acid synthetases (Gjymishka et al., 2009) and transporters (Luo et al., 2013). ATF4 regulates lipid and glucose metabolism due to its ability to activate fibroblast growth factor 21 (Seo et al.,

2009), a hormone that is known to have a main role in lipid and glucose metabolism. ATF4 also induces autophagy and antioxidants in response to ER stress and/or oxidative stress (Rzymiski et al., 2010; Malhi and Kaufman, 2011). However, it directs the cell towards apoptosis through activation of cell cycle arrest and preapoptotic proteins such as C/EBP homologous protein (CHOP), activating transcription factor 3 (ATF3), and cation transport regulator-like protein 1 (CHAC1) in response to chronic or irrecoverable stress (Jiang et al., 2004; Mungrue et al., 2009; Szegezdi et al., 2006). It was found that deletion of the *Atf4* from mouse embryonic fibroblast (MEF) cells causes oxidative stress under nonstressed conditions (Harding et al., 2003) which supports that ATF4 is very important for health even in its basal level and during normal conditions.

The goal of this dissertation project is to evaluate the role of whole body versus hepatic ATF4 in mitigating ASNase hepatotoxicity. Assessing ATF4 deletion effects will determine whether the role of GCN2 is fully mediated by ATF4 or shared with other factors. This will help to better identify the causes of drug toxicity and perhaps reveal new treatment and prevention approaches.

The overarching hypothesis of my dissertation is that the AAR protects the liver during ASNase. The objective of my dissertation project is to assess the role of ATF4 in directing the hepatic AAR during ASNase treatment.

CHAPTER ONE: Literature Review

ASNase as Chemotherapy for ALL

ALL is the most common type of cancer in children from infancy to under age 20, although it can occur at any age. According to the National Cancer Institute, overall survival statistics for people with ALL (all ages) is 66.4% whereas survival in children under 5 years old is 90.8% (Howlader et al., 2016). According to the 2013 data of the Surveillance, Epidemiology, and End Results Program, an estimated 77,855 people in United States were living with ALL (www.seer.cancer.gov/statfacts/html/alyt.html). ASNase has been used in the treatment of ALL for decades (Pui et al., 2008; Patil et al., 2010; Raetz and Salzer, 2010; Hill et al., 1967). ASNase is purified from different microbial sources including *Escherichia coli*, and *Erwinia chrysanthemi*. The enzyme can also be conjugated with polyethylene glycol to increase half-life in the blood and reduce allergic response (Rytting, 2012; Ramya et al., 2012, Lubkowski et al., 1996).

Even today, patients receiving ASNase suffer severe deleterious side effects such as coagulopathy and thromboembolism (Wani et al., 2010; Pui and Evans 2006; Payne and Vora, 2007), neurological and cardiovascular complications (Kieslich et al., 2003), steatosis, hyperglycemia and pancreatitis (Knoderer et al., 2007; Spinola-Castro et al., 2009). Liver toxicity is the basis for many metabolic complications associated with ASNase. Liver dysfunction markers such as elevations in transaminase and bilirubin levels, decreases in

serum albumin, fibrinogen and lipoprotein levels are documented in significant numbers of patients receiving ASNase (Payne and Vora, 2007, Parsons et al., 1997). Moreover, fatty infiltrations of the liver and antithrombin III deficiency are consistently reported (Sahoo and Hart, 2003; Pratt and Johnson, 1971).

Although ASNase has been used as a chemotherapy for decades, the molecular mechanism(s) implicated in these adverse events remain unknown. Pharmacokinetic and pharmacodynamic studies have been unsuccessful in providing knowledge as to who is at risk and why age influences toxicity. Thus, there exists a critical need to develop therapies that prevent or mitigate the adverse metabolic effects of ASNase based on its molecular mechanism of action in affected tissues. Our lab studies the molecular mechanism of ASNase hepatotoxicity and has identified the GCN2-directed AAR as critically important to minimizing ASNase-induced hepatotoxicity (Reinert et al., 2006, Bunpo et al., 2009; Bunpo et al., 2010, Wilson et al., 2013; Wilson et al., 2015). This dissertation project sought to determine the role of the GCN2 downstream effector ATF4 and particularly the influence of global versus partial loss of ATF4 on liver toxicity in ASNase-treated mice.

ASNase Mechanism of Action

ASNase is an enzyme that works by catalyzing the hydrolysis of asparagine to yield aspartate and ammonia, which ultimately depletes the body's pool of this non-essential amino acid. When utilized as chemotherapy, the rationale is that leukemic lymphoblasts are unable to synthesize asparagine due to low or absent levels of asparagine synthetase (ASNS) (Leslie et al., 2006;

Aslanian et al., 2001; Broome, 1968). This means that asparagine is an essential amino acid for leukemic lymphoblasts to grow and proliferate so when circulating levels of asparagine are depleted leukemic cell death occurs due to amino acid starvation (Asselin et al., 1989).

The intrinsic glutaminase activity of ASNase potentiates its efficacy to induce cell death by lowering the level of glutamine, a conditionally essential amino acid that is required to synthesize asparagine by ASNS (Panosyan et al., 2004; Offman et al., 2011). However, glutamine deficiency is also cytotoxic to the liver and other tissues (Reinert et al., 2006). Indeed, our laboratory finds that clinically-used forms of ASNase diminish glutamine levels in the blood stream whereas an experimental, glutaminase-free form of ASNase does not (Reinert *et al.*, 2006). Liver protein synthesis and mammalian target of rapamycin complex 1 (mTORC1) signaling are both reduced upon glutaminase-containing ASNase but not glutaminase-free ASNase (Reinert *et al.*, 2006). These data show that glutamine-depleting forms of ASNase inflict a severe form of amino acid starvation to mammalian tissues. That is why our laboratory uses ASNase as it represents a clinically-relevant model of amino acid depletion to both tumor and normal tissues.

Integrated Stress Response

Activation of the eIF2-ATF4 pathway by a family of eIF2 kinases is named the Integrated Stress Response (ISR) (Harding et al., 2003) to describe how multiple eIF2 kinases sense different environmental stressors and integrate this

information at the level of eIF2 phosphorylation to simultaneously control both protein synthesis and gene expression. There are four eIF2 kinases that phosphorylate eIF2 in response to various types of stress.

First, general control nonderepressible 2 (GCN2; also known as eukaryotic translation initiation factor 2 alpha kinase 4 or EIF2AK4) is activated by binding uncharged tRNA which accumulate in response to inadequate amounts of amino acids in the cellular environment (Hinnebusch, 2005; Chaveroux et al., 2010; Baird and Wek, 2012). Second, PKR-like endoplasmic reticulum kinase (PERK; also known as eukaryotic translation initiation factor 2 alpha kinase 3 or EIF2AK3) phosphorylates eIF2 in response to accumulation of misfolded or unfolded proteins in the endoplasmic reticulum (ER) resulting in ER stress (Harding et al., 1999; Harding et al., 2000; Sood et al., 2000b). Third, protein kinase RNA-activated (PKR; also known as eukaryotic translation initiation factor 2 alpha kinase 2 or EIF2AK2) is activated in response to double stranded RNA as in viral infection to support host defense mechanisms by shutting down the host's protein synthesis machinery to interfere and disturb the viral infections (Clemens and Elia, 1997). Finally, heme-regulated inhibitor (HRI; also known as eukaryotic translation initiation factor 2 alpha kinase 1 or EIF2AK1) is activated by low levels of heme or by heat shock stress (Chen et al., 2000; Lu et al., 2001). Phosphorylation of eIF2 by any of these kinases reduces general protein synthesis while enhancing mRNA translation of specific genes that contain upstream open reading frames (uORFs) in the 5' untranslated region. The best characterized preferentially synthesized ISR gene is ATF4. As part of

the adaptive response to multiple environmental stresses that activate ISR, ATF4 facilitates expression of genes that are responsible for alleviating cellular stress and regaining homeostasis. If the stress is chronic or of severe intensity that the cell cannot tolerate, ATF4 guides the cell to alter the transcriptional profile from survival attempts to programmed cell death. In such case, ATF4 activates cell death pathways via genes such as *Ddit3* (DNA damage-inducible transcript 3) encoding the protein CHOP (also known as GADD153) (Su and Kilberg, 2008).

It is suggested that amino acid depletion may promote ER stress (Cao and Kaufman, 2012). However, ER stress is not induced in the livers of *Gcn2*^{+/+} or *Gcn2*^{-/-} mice by ASNase (Wilson et al., 2013). Whether or not ER stress is activated by ASNase in the absence of ATF4 is unknown. The ISR signaling is summarized in Figure 1.

ASNase Activates the AAR

An expansion of the ISR concept specific for amino acid deprivation is coined by the Kilberg lab as the Amino Acid Response (AAR) (Kilberg et al., 2012) and is defined as a collection of signal transduction pathways that terminate in specific transcriptional programs aimed toward adaptation to amino acid stress. These pathways include the GCN2-eIF2-ATF4 pathway as well as MAP kinase signal transduction pathways.

ASNase deleterious outcomes are suggested to be consequential to inhibition of global protein synthesis. The low levels of asparagine and glutamine limit availability of asparaginyl-tRNA and/or glutamyl-tRNA which activates GCN2

by the binding of these uncharged tRNAs to a domain related to histidyl-tRNA synthetase. This binding event activates GCN2 kinase activity (Qiu et al., 2001) toward its substrate, eIF2 (Sood et al., 2000a). Phosphorylation of eIF2 on its alpha subunit at serine 51 increases its affinity for the guanine nucleotide exchange factor eIF2B. This reduces GDP-GTP exchange on eIF2, inhibiting ternary initiation complex formation. As a result, global translation initiation rates decline (Wek et al., 2006).

A slowing of initiation, and particularly reinitiation, favors the translation of genes containing uORFs (Morris and Geballe, 2000, Wek et al., 2006). One of the best characterized in this regard is ATF4 (Harding et al., 2000; Vattem and Wek, 2004) which has two uORFs. The uORF1 is an activating element and allows for ribosomal reinitiation at the downstream ATF4 coding region (Hiraishi et al., 2014; Krishna et al., 2004). In contrast, the uORF 2 is an inhibitory element because it overlaps the ATF4 coding region preventing ribosomal reinitiation at the ATF4 start codon and subsequently blocking ATF4 translation (Krishna et al., 2004, Wek et al., 2006). Stress conditions that cause ternary initiation complex depletion slows down the rate of ribosomal reinitiation resulting in the bypassing of the inhibitory uORFs and engagement of the ATF4 ORF (Kilberg et al., 2009, Harding et al., 2003). ATF4 protein then locates to the nucleus where it binds to CARE/AARE elements in DNA and functions to reconfigure gene expression in order to alleviate cell stress (Kilberg et al., 2012). Although ATF4 is a key, canonical point in regulating the AAR, little is known concerning the *in vivo* contribution of ATF4 to the GCN2-activated AAR during ASNase.

As defined by Kilberg et al. 2012, the AAR results in altered gene expression driven by ATF4 and other transcription factors binding to CARE/AARE during amino acid stress. Examples of genes regulated by ATF4 include Activating Transcription Factor 5 (*Atf5*), a transcription factor enriched in liver, and Growth arrest and DNA damage Inducible 34 (*Ppp1r15a*), an eIF2 phosphatase that serves in part to restore global translation efficiency (Kilberg et al. 2012). While ATF4 is proposed to regulate the AAR, there is no definitive list of all genes belonging to this signaling pathway. And while ATF4 is considered the key point in cellular decision making during ISR (Harding et al., 2003; Fusakio et al., 2016), little is known concerning the *in vivo* contribution of ATF4 to the GCN2-activated AAR during ASNase.

Loss of GCN2 Aggravates ASNase-induced Hepatotoxicity

Although GCN2 is conserved throughout eukaryotes and is ubiquitously expressed, loss of GCN2 function in the whole body is without effect when nutrient supply is adequate. Yet under conditions of amino acid insufficiency, maladaptive outcomes manifest (She et al., 2013). Indeed, upon ASNase treatment mice deleted for *Gcn2* (*Gcn2*^{-/-}) express dysfunctional phenotypes such as immunosuppression, hepatic steatosis, pancreatitis and increased mortality rate (Bunpo et al., 2010, Wilson et al., 2013, Wilson et al., 2015; Phillipson-Weiner et al 2016). Previous studies examining leucine starvation suggest that liver steatosis in *Gcn2*^{-/-} mice is due to the failure of these animals to downregulate the expression of lipogenic genes (Guo and Cavener, 2007).

However, our laboratory found that fatty liver in ASNase-treated *Gcn2*^{-/-} mice resulted from reduced expression of apolipoprotein B100 resulting in an inability of the liver to secrete triglycerides into the circulation (Wilson et al., 2015).

The rationale to study the effect of ASNase in *Gcn2*^{-/-} mice was initially based on the pathology resulting from feeding leucine-devoid diets to *Gcn2*^{-/-} mice (Zhang et al., 2002). Based on these data, it was reasonable to suggest that metabolic derangements by ASNase may be related to GCN2 deficiency or defects in the GCN2-eIF2-ATF4-AAR. Our previously published data suggest that ASNase is not the ideal chemotherapy to treat patients who are defective in inducing GCN2. This project aims to follow the GCN2-eIF2-ATF4 AAR pathway by studying the role of ATF4 in the hepatic response to ASNase. I propose to identify the role of ATF4 in guiding the liver response to amino acid depletion by ASNase. The effect of ASNase on the GCN2-eIF2-ATF4-AAR is summarized in Figure 2.

ER Stress and the Unfolded Protein Response

Protein synthesis, processing and folding occurs in the endoplasmic reticulum (ER). The process of protein folding by the cell is endangered by different factors that affect the normality of this process such as energy deprivation, oxidative stress, hypoxia, Ca₂⁺ depletion, amino acid deprivation, altered glycosylation, inflammation, and the accumulation of misprocessed proteins in the ER (reviewed in Cao and Kaufman, 2012). Cellular stress resulting in an accumulation of misfolded proteins in the ER activates the unfolded protein

response (UPR), an assembly of signal transduction events guarded by three ER transmembrane proteins: the eIF2 kinase PERK, inositol-requiring kinase 1 (IRE1), and ATF6 (Tirasophon *et al.*, 1998; Harding *et al.*, 1999; Chakrabarti *et al.*, 2011). Normally, the N-terminal domains of IRE1, PERK, and ATF6 proteins are bound to a molecular chaperone, B cell immunoglobulin protein (BIP, also known as glucose regulatory protein 78 or Grp78) (Shen *et al.*, 2002). Upon accumulation of misfolded proteins in the ER, BIP releases PERK, IRE1 and ATF6 allowing for their activation (Shen *et al.*, 2002). After being detached from BIP, PERK dimerizes and activates its own kinase activity by autophosphorylation, resulting in ATF4 synthesis via preferential mRNA translation (Vattem and Wek, 2004).

To cope with ER stress, ATF4 functions in two ways. First, ATF4 elevates expression of genes involved in ER folding capacity, oxidative stress, cell cycle control, and amino acid metabolism (Malhi and Kaufman, 2011). ATF4 activates a negative feedback loop by stimulating the expression of growth arrest and DNA damage-inducible protein 34 (GADD34). GADD34 dephosphorylates eIF2 to return translation levels to normal in an effort to restore homeostasis (Fels and Koumenis, 2006). Second, during irrecoverable or chronic stress, ATF4 directs cell fate toward programmed cell death by inducing CHOP and other factors (Teske *et al.*, 2013; Han *et al.*, 2013).

Similarly, IRE1 oligomerizes and autophosphorylates itself activating its dual kinase and endoribonuclease activities. The RNase activity of IRE1 degrades some of the mRNAs in the cell by a process called IRE1-dependent

decay (Hollien and Weissman, 2006; Hollien et al., 2009). This activity also splices X Box Binding Protein 1 (XBP1) (Kober et al., 2012), a transcription factor that helps the cell to restore normal protein folding capacity by inducing protein folding chaperones and ER-associated degradation (Yoshida et al., 2001).

Upon its release from BiP, ATF6 moves from the ER to the Golgi apparatus where it is cleaved by site 1 and site 2 proteases to produce ATF6 active form, a transcription factor that translocates to the nucleus to increase the gene expression of XBP1 and other genes that function to help the ER overcome and recover from the stress condition (Lee et al., 2002; Chen et al., 2002). These three signaling events can work together or independently to promote ER folding ability, decrease protein synthesis, and increase degradation of improperly folded proteins (Malhi and Kaufman, 2011).

It is suggested that GCN2 might serve to activate the ISR in response to ER stress in the absence of PERK. In *Perk*^{-/-} cells, GCN2 enhances eIF2 phosphorylation upon ER stress by hypoxia (Liu et al., 2010). As is revealed by our previous studies, mice lacking *Gcn2* do not show evidence of hepatic ER stress to ASNase (Wilson et al., 2013, Wilson et al., 2015). Due to the importance of ATF4 in managing ER stress, whether loss of ATF4 provokes ER stress to ASNase is yet to be addressed.

mTORC1 Signaling

In mammalian cells, there are two amino acid supply sensors; GCN2 and mechanistic target of rapamycin complex 1 (mTORC1). mTORC1 consists of mTOR, Regulatory associated protein of mTOR (Raptor), mammalian lethal with SEC13 protein 8 (MLST8), proline-rich AKT substrate (PRAS40) and DEP domain-containing mTOR-interacting protein (DEPTOR) (Kim et al., 2002; Kim et al., 2003; Wullschleger et al., 2006). GCN2 senses amino acid insufficiency whereas mTORC1 senses amino acid sufficiency or abundance leading to decreases or increases in protein synthesis, respectively. A wide variety of environmental signals such as nutrients, growth factors, oxygen, and stress induce mTORC1 to regulate protein synthesis, metabolism, and cell growth (Laplane and Sabatini 2012; Jewell et al. 2013; Shimobayashi and Hall 2014). However, amino acid sufficiency is indispensable for complete activation of mTORC1, even in the presence of growth factor activation (Ye et al., 2015). In amino acid abundance situations, PI3K-AKT-mTOR (Phosphatidyl Inositol 3 Kinase-Protein Kinase B-mTOR) signaling is activated by Insulin-like Growth Factor-I and other growth factors (Nobukuni et al., 2005; Cohen and Hall, 2009). Growth factor signaling phosphorylates phosphatidyl inositol 3 kinase (PI3K) and activates protein kinase B (Akt). Activated Akt phosphorylates and inhibits the mTORC1 inhibitor, tuberous sclerosis 2 and 1 complex (TSC2-TSC1 complex), thereby activating mTORC1 (Laplane and Sabatini, 2013; Bar-Peled and Sabatini, 2014). Under amino acid abundant conditions, mTORC1 activation results in phosphorylation of two downstream effectors, ribosomal protein S6

kinase (S6K1) and eIF4E-binding protein 1 (4E-BP1) to promote translation (Hara et al. 1998; Wang et al. 1998). Phosphorylation of S6K1 activates its substrate ribosomal protein S6 (rpS6) which participates in a crucial step in mRNA translation (Proud, 2009). Phosphorylation of 4E-BP1 also regulates a limiting step in the translation initiation machinery, namely availability of the mRNA cap binding protein eIF4E for eIF4F formation (Kimball and Jefferson, 2005).

Phosphorylation of mTORC1 and its substrates, 4E-BP1 and S6K1, drive changes in translational efficiency and ribosomal capacity in response to amino acid availability (Zoncu et al., 2011; Anthony et al., 2001; Dennis et al., 2011). This is studied in *Gcn2^{-/-}* animals under amino acid deletion conditions, but whether or not ATF4 mediates the GCN2 effect in this pathway is to be elucidated.

Whether the GCN2-eIF2-ATF4 ISR regulates mTORC1 or vice versa is a controversial topic. Ben-Sahra et al. 2016 found that mTORC1 is required to activate ATF4 regardless of the AAR or ER stress situations. In contrast, Ye et al. 2015 discovered that activation of mTORC1 is regulated by the ISR through ATF4 in response to amino acid deficiency. In this regard, our lab established that amino acid deficiency via ASNase inhibits hepatic mTORC1 signaling. However, mTORC1 is activated in the livers of *Gcn2^{-/-}* mice, leading to hyperphosphorylation of S6K1 and 4E-BP1 (Bunpo et al., 2009, Wilson et al., 2013), suggesting that mTORC1 is under GCN2 control. To what extent ATF4 coordinates mTORC1 activity in response to GCN2 activation is unstudied.

Recent studies identify Sestrin2 as an ATF4-regulated inhibitor of mTORC1 during amino acid deprivation (Ye et al., 2015; Kimball et al., 2016, Saxton et al., 2015; Wolfson et al., 2016). Whether or not Sestrin2 is regulated by ATF4 under ASNase is unknown.

ATF4 Is a Master Regulator

Our laboratory established that GCN2 is required for a majority of early signaling and gene expression events to ASNase. These acute events include increased phosphorylation of eIF2 and expression of downstream effectors ASNS, CHOP, 4E-BP1, and fibroblast growth factor (FGF21) to ASNase (Wilson et al., 2013; Wilson et al., 2015). While the canonical AAR places ATF4 upstream of these transcriptional events during ASNase, there are no studies confirming direct regulatory control by ATF4.

ATF4 is a member of the basic leucine zipper protein family of DNA binding proteins (Podust et al., 2001). It is also a CREB protein family member (named CREB2), binding to the CAMP response element (CRE) site in promoter regions of the DNA (Karpinski et al., 1992). ATF4 regulates the transcription of specific genes that have the CRE site with the sequence 5'-GTGACGTACAG-3' as well as the CARE sequence: 5'-TGATGXAAX- 79-3' (Hai et al., 1989). ATF4 is expressed in multiple tissues, and is described as a master regulator of cellular stress responses (B'chir et al., 2013). Protein expression of ATF4 is very low under normal conditions because of its short half-life and its low efficiency of translation (Dey et al., 2010). This transcription factor plays several roles in the

body such as bone formation (Makowski et al., 2014), maintaining memory (Bartsch et al., 2000), and the metabolism of glucose and lipid (Seo et al., 2009). ATF4 is also involved in protein synthesis by increasing cellular amino acids supply through elevating transcription of amino acid transporters and synthetases such as ASNS (Siu et al., 2002; Harding et al., 2003; Malmberg and Adams, 2008).

The role of ATF4 in determining cell fate is unclear. It is reported that ATF4 and CHOP activation increase protein synthesis, oxidative stress, and subsequent cell death in response to ER stress condition (Han et al., 2013). In contrast, other studies find that loss of ATF4 exacerbates ER stress by inducing oxidative stress and cell death (Fusakio et al., 2016). It is suggested that during environmental stress, the cellular choice between adaptation and apoptosis depends on the extent and duration of ATF4 expression and its downstream target CHOP (Fusakio et al., 2016). The role of ATF4 in deciding cell fate during ASNase is unstudied. This dissertation project aims to follow the AAR pathway downstream of GCN2 to determine if the AAR is mediated by ATF4. This will also help me to determine if loss of ATF4 function exacerbates or mitigates hepatotoxicity by ASNase.

Regulation of protein synthesis is under GCN2 and mTORC1 control in response to amino acid status. Some studies suggest an interaction between these kinases, but the exact mechanism is not well defined. Activation of GCN2 by amino acid insufficiency resulted in ATF4 translation (Vattem et al., 2004). The role of ATF4 in regulating the response to amino acid depletion is

increasingly studied especially as transcription factor that regulates the gene expression of amino acid transporters (Lopez et al., 2007) and amino acid synthesis enzymes (Siu et al., 2002). An important question is whether GCN2 regulates mTORC1 via ATF4 or not. It is found that under conditions of serum/glutamine starvation, ATF4 upregulates amino acid transporters leading to increase amino acid uptake by the cells and then activation of mTORC1 (Chen et al., 2014) suggesting that ATF4 is upstream and controlling mTORC1 signaling. However, this stands in contrast with the recent work of Ben-Sahra et al. 2016 which places ATF4 downstream of mTORC1. My dissertation project will attempt to clarify this controversy as it relates to amino acid starvation by ASNase.

ATF4 functions to activate Sestrin2, a stress response protein that is also classified as a mTORC1 inhibitor (Ye et al., 2015; Ding et al., 2016). Sestrin2 is induced under oxidative stress, amino acid starvation, and ER stress by ATF4 (Lee et al., 2012; Ye et al., 2015; Brüning et al., 2013). Sestrin2 inhibits mTORC1 in a manner dependent on AMPK and TSC2 by inhibiting the small GTPase Rheb (Budanov & Karin, 2008; Wullschlegel et al., 2006; Lee et al., 2010; Dann et al., 2007). It is reported that Sestrin2 is a phosphoprotein and that its phosphorylation state is dependent on leucine availability and that there is a relation between the degree of Sestrin2 phosphorylation and the degree of mTORC1 inhibition. Under conditions of leucine deficiency, Sestrin2 becomes highly phosphorylated and interacts with other proteins to inhibit mTORC1 (Kimball et al., 2016). ASNase treatment blocks hepatic mTORC1 signaling in wild type mice (Bunpo et al., 2009; Wilson et al., 2013), but the role of ATF4 is

unknown. This dissertation project seeks to clarify the role of ATF4 and Sestrin2 in mTORC1 signaling in response to ASNase.

Summary

A lack of knowledge about the mechanism of ASNase-induced hepatotoxicity compromises its safety and effective use. Why some patients fail to tolerate the drug while others are able to complete treatment without experiencing adverse metabolic events remains a mystery (Pieters et al., 2011). Gaining an improved understanding of these toxicities at the molecular level may boost treatment options.

This dissertation project follows an approach which utilizes genetic mouse models to examine ASNase molecular mechanism of action in non-tumor tissues. Previous studies using this approach determined that the GCN2 response to ASNase treatment is essential to mitigate hepatotoxicity (Bunpo et al., 2009, Wilson et al., 2013; Wilson et al., 2015). However, a full understanding of the downstream mechanisms underlying ASNase-induced hepatotoxicity alongside ATF4-mediated AAR remains undefined. While the canonical ISR positions ATF4 at a key point in cellular decision making (Harding et al., 2003), little is known concerning the *in vivo* contribution of ATF4 to the GCN2-activated AAR during ASNase.

Our laboratory determined that GCN2 is required to increase phosphorylation of eIF2 (Reinert et al., 2006) and reduce mTORC1 during ASNase (Bunpo et al., 2009; Bunpo et al., 2010; Wilson et al., 2013). Whether eIF2 phosphorylation and mTORC1 signaling is activated or depressed in the absence of ATF4 is unknown. Moreover, recent studies identify Sestrin2 as an inhibitor of mTORC1 during amino acid deprivation that is regulated by ATF4 (Ye

et al., 2015; Kimball et al., 2016, Wolfson et al., 2016). Thus, repression of mTORC1 during ASNase treatment may be under the control of ATF4.

Mice deleted for *Atf4* (*Atf4*^{-/-}) exhibit pleiotropic phenotypes of reduced growth, lack of vision, and defects in hematopoiesis and glucose homeostasis (Tanaka et al., 1998; Masuoka et al., 2002; Yoshizawa et al., 2009). There is little information in the literature on *Atf4* heterozygotes (*Atf4*^{+/-}) but in my experience they appear normal and healthy, similar to *Gcn2*^{-/-} mice. To understand if *Atf4* heterozygosity alters hepatic AAR activation and/or hepatotoxicity to ASNase, I proposed to examine the effects of ASNase on *Atf4*^{+/-} heterozygote mice compared to wild type (WT) and *Atf4*^{-/-} mice.

It is reported that the metabolic effects of ATF4 deletion are entirely due to expression of ATF4 in the osteoblasts (Yoshizawa et al., 2009), but this has not been independently confirmed. In a previous study, we found that livers of *Atf4* whole body and liver specific deletion of *Atf4* behaved similarly regarding ISR activation in response to ER stress inducing drug (Fusakio et al., 2016). Importantly, no studies have examined liver-specific ATF4 deleted animals to ASNase. Thus, there is a need to clarify the hepatic-specific role of ATF4 when the organism is challenged with amino acid depletion by ASNase.

Literature Cited

- Adams C.M. Role of the transcription factor ATF4 in the anabolic actions of insulin and the anti-anabolic actions of glucocorticoids, *J. Biol. Chem.* 282 (2007). 16744–16753.
- Appel IM, Hop WC, van Kessel-Bakvis C, Stigter R, Pieters R. L-ASNase and the effect of age on coagulation and fibrinolysis in childhood acute lymphoblastic leukemia. *Thromb Haemost.* 2008 Aug;100:330-7.
- Aslanian AM, Fletcher BS, Kilberg MS. Asparagine synthetase expression alone is sufficient to induce L-ASNase resistance in MOLT-4 human leukaemia cells. *Biochem J.* 2001 Jul 1;357:321-8.
- Asselin BL, Ryan D, Frantz CN, Bernal SD, Leavitt P, Sallan SE, Cohen HJ. In vitro and in vivo killing of acute lymphoblastic leukemia cells by L-ASNase. *Cancer Res.* 1989 Aug 1;49(15):4363-8.
- Back SH, Scheuner D, Han J, Song B, Ribick M, Wang J, et al. Translation attenuation through eIF2 α phosphorylation prevents oxidative stress and maintains the differentiated state in beta cells. *Cell Metab* 2009; 10:13–26.
- Baird TD, Wek RC. Eukaryotic initiation factor 2 phosphorylation and translational control in metabolism. *Adv Nutr.* 2012 May 1;3(3):307-21. doi: 10.3945/an.112.002113.
- Balasubramanian MN, Butterworth EA, Kilberg MS. Asparagine synthetase: regulation by cell stress and involvement in tumor biology. *Am J Physiol Endocrinol Metab.* 2013 Apr 15;304(8).
- Barczyk K, Kreuter M, Pryjma J et al (2005) Serum cytochrome c indicates in vivo apoptosis and can serve as a prognostic marker during cancer therapy. *J Int Cancer* 116:167–173.
- Bar-Peled L, Sabatini DM. Regulation of mTORC1 by amino acids. *Trends Cell Biol.* 2014;400–6.
- Bartsch D, Ghirardi M, Casadio A, et al. Enhancement of memory-related long-term facilitation by ApAF, a novel transcription factor that acts downstream from both CREB1 and CREB2. *Cell.* 2000; 103: 595–608.
- B'chir W, Maurin AC, Carraro V, Averous J, Jousse C, Muranishi Y, Parry L, Stepien G, Fafournoux P, Bruhat A. The eIF2 α /ATF4 pathway is essential for stress-induced autophagy gene expression. *Nucleic Acids Res.* 2013 Sep;41(16):7683-99. doi: 10.1093/nar/gkt563.

- Ben-Sahra I, Howell JJ, Asara JM, Manning BD. Stimulation of de novo pyrimidine synthesis by growth signaling through mTOR and S6K1. *Science*. 2013 Mar 15;339(6125):1323-8. doi: 10.1126/science.1228792. Epub 2013 Feb 21.
- Ben-Sahra I, Hoxhaj G, Ricoult SJ, Asara JM, Manning BD. mTORC1 induces purine synthesis through control of the mitochondrial tetrahydrofolate cycle. *Science*. 2016 Feb 12;351(6274):728-33. doi: 10.1126/science.aad0489.
- Berlanga JJ, Santoyo J, De Haro C. Characterization of a mammalian homolog of the GCN2 eukaryotic initiation factor 2alpha kinase. *Eur J Biochem*. 1999 Oct;265(2):754-62. PMID: 10504407
- Bromati CR, Lellis-Santos C, Yamanaka TS, Nogueira TC, Leonelli M, Caperuto LC, Gorjão R, Leite AR, Anhê GF, Bordin S. UPR induces transient burst of apoptosis in islets of early lactating rats through reduced AKT phosphorylation via ATF4/CHOP stimulation of TRB3 expression. *Am J Physiol Regul Integr Comp Physiol*. 2011 Jan;300(1):R92-100. doi: 10.1152/ajpregu.00169.2010. Epub 2010 Nov 10.
- Broome JD. Studies on the mechanism of tumor inhibition by L-ASNase. Effects of the enzyme on asparagine levels in the blood, normal tissues, and 6C3HED lymphomas of mice: differences in asparagine formation and utilization in ASNase-sensitive and -resistant lymphoma cells. *J Exp Med*. 1968 Jun 1;127:1055-72.
- Brugarolas J, Lei K, Hurley RL, Manning BD, Reiling JH, Hafen E et al. (2004). Regulation of mTOR function in response to hypoxia by REDD1 and the TSC1/TSC2 tumor suppressor complex. *Genes Dev* 18: 2893–2904.
- Budanov AV, Karin M. p53 target genes sestrin1 and sestrin2 connect genotoxic stress and mTOR signaling. *Cell*. 2008 Aug 8;134(3):451-60. doi: 10.1016/j.cell.2008.06.028. Erratum in: *Cell*. 2009 Jan 23;136(2):378. PMID: 18692468
- Bunpo P, Cundiff JK, Reinert RB, Wek RC, Aldrich CJ, Anthony TG. The eIF2 kinase GCN2 is essential for the murine immune system to adapt to amino acid deprivation by ASNase. *J Nutr*. 2010 Nov;140: 2020-7.
- Bunpo P, Dudley A, Cundiff JK, Cavener DR, Wek RC, Anthony TG. GCN2 protein kinase is required to activate amino acid deprivation responses in mice treated with the anti-cancer agent L-ASNase. *J Biol Chem*. 2009 Nov 20;284(47):32742-9. doi: 10.1074/jbc.M109.047910. Epub 2009 Sep 25.
- Cao SS, Kaufman RJ. Unfolded protein response. *Curr Biol*. 2012 Aug 21;22(16):R622-6. doi: 10.1016/j.cub.2012.07.004. PMID: 22917505.

- Carraro V, Maurin AC, Lambert-Langlais S, Averous J, Chaveroux C, Parry L, Jousse C, Ord D, Ord T, Fafournoux P, Bruhat A. Amino acid availability controls TRB3 transcription in liver through the GCN2/eIF2 α /ATF4 pathway. 2010. PLoS One. 5(12):e15716. doi: 10.1371/journal.pone.0015716
- Chaabane W, User SD, El-Gazzah M, Jaksik R, Sajjadi E, Rzeszowska-Wolny J, Los MJ. Autophagy, apoptosis, mitoptosis and necrosis: interdependence between those pathways and effects on cancer. Arch Immunol Ther Exp (Warsz). 2013; 61(1):43-58.
- Chakrabarti A, Chen AW, Varner JD. A review of the mammalian unfolded protein response. Biotechnol Bioeng. 2011 Dec;108(12):2777-93. doi: 10.1002/bit.23282.
- Chantranupong L, Wolfson RL, Orozco JM, Saxton RA, Scaria SM, Bar-Peled L, Spooner E, Isasa M, Gygi SP, Sabatini DM. The Sestrins interact with GATOR2 to negatively regulate the amino-acid-sensing pathway upstream of mTORC1. Cell Rep. 2014 Oct 9;9(1):1-8. doi: 10.1016/j.celrep.2014.09.014. Epub 2014 Sep 25.
- Chaveroux C, Lambert-Langlais S, Cherasse Y, Averous J, Parry L, Carraro V, Jousse C, Maurin AC, Bruhat A, Fafournoux P. Molecular mechanisms involved in the adaptation to amino acid limitation in mammals. Biochimie. 2010 Jul;92(7):736-45. doi: 10.1016/j.biochi.2010.02.020. Epub 2010 Feb 23.
- Chen JJ, London IM. Regulation of protein synthesis by heme-regulated eIF-2 alpha kinase. Trends Biochem Sci. 1995 Mar;20(3):105-8. PMID: 7709427
- Chen MR, Huang H, Fen CY, Chen JY. A novel EBNA-1 tag system for high level expression and efficient detection of fusion proteins in vitro and in vivo. J Virol Methods. 2000 Mar;85(1-2):35-41. PMID: 10716336
- Chen R, Zou Y, Mao D, Sun D, Gao G, Shi J, Liu X, Zhu C, Yang M, Ye W, Hao Q, Li R, Yu L. J Cell Biol. 2014 Jul 21; 206 (2):173-82. doi: 10.1083/jcb.201403009. The general amino acid control pathway regulates mTOR and autophagy during serum/glutamine starvation. PMID: 25049270.
- Chen X, Shen J, Prywes R. The luminal domain of ATF6 senses endoplasmic reticulum (ER) stress and causes translocation of ATF6 from the er to the Golgi. J Biol Chem. 2002;13045-52.
- Cheng WP, Wang BW, Lo HM, Shyu KG. Mechanical Stretch Induces Apoptosis Regulator TRB3 in Cultured Cardiomyocytes and Volume-Overloaded Heart. PLoS One. 2015 Apr 21;10(4):e0123235.

- Clemens MJ, Elia A. The double-stranded RNA-dependent protein kinase PKR: structure and function. *J Interferon Cytokine Res.* 1997 Sep;17(9):503-24.
- Cohen A, Hall MN. 2009. An amino acid shuffle activates mTORC1. *Cell.* 136:399–400. <http://dx.doi.org/10.1016/j.cell.2009.01.021>
- Cullinan SB, Diehl JA, Coordination of ER and oxidative stress signaling: the PERK/Nrf2 signaling pathway, *Int. J. Biochem. Cell Biol.* 38 (2006) 317–332.
- Cullinan, S. B. et al. Nrf2 is a direct PERK substrate and effector of PERK-dependent cell survival. 2003; *Molecular and cellular biology* 23, 7198–7209.
- De Sousa-Coelho AL, Marrero PF, Haro D. Activating transcription factor 4-dependent induction of FGF21 during amino acid deprivation. *Biochem J.* 2012 Apr 1;443(1):165-71.
- Deniaud A, Sharaf el dein O, Maillier E, Poncet D, Kroemer G, Lemaire C, Brenner C. Endoplasmic reticulum stress induces calcium-dependent permeability transition, mitochondrial outer membrane permeabilization and apoptosis. *Oncogene.* 2008 Jan 10;27(3):285-99. Epub 2007 Aug 13. PMID: 17700538.
- Dennis MD, McGhee NK, Jefferson LS, Kimball SR. Regulated in DNA damage and development 1 (REDD1) promotes cell survival during serum deprivation by sustaining repression of signaling through the mechanistic target of rapamycin in complex 1 (mTORC1). *Cell Signal.* 2013 Dec;25(12):2709-16. doi: 10.1016/j.cellsig.2013.08.038. Epub 2013 Sep 7. PMID:24018049.
- Dey S, T.D. Baird, D. Zhou, L.R. Palam, D.F. Spandau, R.C. Wek, Both transcriptional regulation and translational control of ATF4 are central to the integrated stress response, *J. Biol. Chem.* 285 (2010) 33165–33174.
- DeYoung MP, Horak P, Sofer A, Sgroi D, Ellisen LW. (2008). Hypoxia regulates TSC1/2-mTOR signaling and tumor suppression through REDD1-mediated 14-3-3 shuttling. *Genes Dev* 22: 239–251.
- Ding B, Parmigiani A, Divakaruni AS, Archer K, Murphy AN, Budanov AV. Sestrin2 is induced by glucose starvation via the unfolded protein response and protects cells from non-canonical necroptotic cell death. *Sci Rep.* 2016 Mar 2;6:22538. doi: 10.1038/srep22538.
- Du K, Herzig S, Kulkarni RN, Montminy M. TRB3: a tribbles homolog that inhibits Akt/PKB activation by insulin in liver. *Science.* 2003 Jun 6;300(5625):1574-7.

- Ehren JL, Maher P. Concurrent regulation of the transcription factors Nrf2 and ATF4 mediates the enhancement of glutathione levels by the flavonoid fisetin. *Biochem Pharmacol.* 2013 Jun 15; 85(12):1816-26.
- Ellisen LW, Ramsayer KD, Johannessen CM, Yang A, Beppu H, Minda K et al. (2002). REDD1, a developmentally regulated transcriptional target of p63 and p53, links p63 to regulation of reactive oxygen species. *Mol Cell* 10: 995–1005.
- Elmore S (2007) Apoptosis: a review of programmed cell death. *Toxicol Pathol* 35:495–516.
- Fawcett TW, Martindale JL, Guyton KZ, Hai T, Holbrook NJ. Complexes containing activating transcription factor (ATF)/cAMP-responsive-elementbinding protein (CREB) interact with the CCAAT/enhancer-binding protein (C/EBP)–ATF composite site to regulate Gadd153 expression during the stress response. *Biochem J* 1999; 339:135–141.
- Fels DR, Koumenis C. The PERK/eIF2alpha/ATF4 module of the UPR in hypoxia resistance and tumor growth. *Cancer Biol Ther.* 2006 Jul; 5(7):723-8.
- Fox DK, Ebert SM, Bongers KS, Dyle MC, Bullard SA, Dierdorff JM, Kunkel SD, Adams CM p53 and ATF4 mediate distinct and additive pathways to skeletal muscle atrophy during limb immobilization *Am J Physiol Endocrinol Metab.* 2014 Aug 1;307(3):E245-61. doi: 10.1152/ajpendo.00010.2014.
- Fusakio, M.E., Willy, J.A., Wang, Y., Mirek, E.T., Al Baghdadi, R.J., Adams, C.M., Anthony, T.G., Wek, R.C. (2016). Transcription factor ATF4 directs basal and select induced gene expression in the unfolded protein response and cholesterol metabolism in liver. *Mol. Biol. Cell.* pii: mbc.E16-01-0039.
- Gjymishka A, Su N, Kilberg MS. Transcriptional induction of the human asparagine synthetase gene during the unfolded protein response does not require the ATF6 and IRE1/XBP1 arms of the pathway. *Biochem J.* 2009 Feb 1;417(3):695-703. doi: 10.1042/BJ20081706.
- Guo F, Cavener DR. The GCN2 eIF2alpha kinase regulates fatty-acid homeostasis in the liver during deprivation of an essential amino acid. *Cell Metabolism.* 2007 February;5:1-12.
- Hai TW, F. Liu, W.J. Coukos, M.R. Green, Transcription factor ATF cDNA clones: an 682 extensive family of leucine zipper proteins able to selectively form DNA-binding 683 heterodimers, *Genes Dev.* 3 (1989) 2083–2090.
- Han J, Back SH, Hur J, Lin YH, Gildersleeve R, Shan J, Yuan CL, Krokowski D, Wang S, Hatzoglou M, Kilberg MS, Sartor MA, Kaufman RJ. ER-stress-

- induced transcriptional regulation increases protein synthesis leading to cell death. *Nat Cell Biol* 15: 481–490, 2013.
- Hara K, Yonezawa K, Weng QP, Kozlowski MT, Belham C, Avruch J. 1998. AA sufficiency and mTOR regulate p70 S6 kinase and eIF-4EBP1 through a common effector mechanism. *J Biol Chem* 273:14484–14494.
- Harding HP, Zhang Y, Zeng H, Novoa I, Lu PD, Calton M, Sadri N, Yun C, Popko B, Paules R, Stojdl DF, Bell CJ, Hettmann T, Leiden JM, Ron D. An integrated stress response regulates amino acid metabolism and resistance to oxidative stress, *Mol. Cell* 11 (2003) 619–633.
- Harding HP, Novoa I, Zhang Y, Zeng H, Wek R, Schapira, M, Ron D. Regulated translation initiation controls stress-induced gene expression in mammalian cells, *Mol. Cell* 6 (2000) 1099–1108.
- Harding HP, Zhang Y, Ron D. Protein translation and folding are coupled by an endoplasmic-reticulum-resident kinase. *Nature*. 1999 Jan 21;397(6716):271-4. Erratum in: *Nature* 1999 Mar 4;398(6722):90. PMID: 9930704
- Hetz, C. The unfolded protein response: controlling cell fate decisions under ER stress and beyond. *Nat. Rev. Mol. Cell Biol.* 13, 89–102 (2012).
- Hill JM, Roberts J, Loeb E, Khan A, MacLellan A, Hill RW. L-ASNase therapy for leukemia and other malignant neoplasms. Remission in human leukemia. *Jama*. 1967 Nov 27;202:882-8.
- Hinnebusch AG. Translational regulation of GCN4 and the general amino acid control of yeast. *Annu Rev Microbiol.* 2005;59:407-50.
- Hiraishi H, Oatman J, Haller SL, Blunk L, McGivern B, Morris J, Papadopoulos E, Gutierrez W, Gordon M, Bokhari W, Ikeda Y, Miles D, Fellers J, Asano M, Wagner G, Tazi L, Rothenburg S, Brown SJ, Asano K. Essential role of eIF5-mimic protein in animal development is linked to control of ATF4 expression. *Nucleic Acids Res.* 2014;42(16):10321-30. doi: 10.1093/nar/gku670. Epub 2014 Aug 21.
- Hollien J, Lin JH, Li H, Stevens N, Walter P, Weissman JS. Regulated Ire1-dependent decay of messenger RNAs in mammalian cells. *J Cell Biol.* 2009 Aug 10;186(3):323-31. doi: 10.1083/jcb.200903014. Epub 2009 Aug 3. PMID: 19651891
- Hollien J, Weissman JS. Decay of endoplasmic reticulum-localized mRNAs during the unfolded protein response. *Science*. 2006 Jul 7;313(5783):104-7. PMID: 16825573

- Inoki K, Li Y, Xu T, Guan KL. Rheb GTPase is a direct target of TSC2 GAP activity and regulates mTOR signaling. *Genes Dev.* 2003 Aug 1;17(15):1829-34. Epub 2003 Jul 17. PMID: 12869586
- Jewell JL, Russell RC, Guan KL. 2013. AA signalling upstream of mTOR. *Nat Rev Mol Cell Biol* 14: 133–139.
- Jiang HY, Wek SA, McGrath BC, Lu D, Hai T, Harding HP, et al. Activating transcription factor 3 is integral to the eukaryotic initiation factor 2 kinase stress response. *Mol Cell Biol* 2004;24: 1365–1377.
- Jiang HY, Wek SA, McGrath BC, Lu D, Hai T, Harding HP, et al. Activating transcription factor 3 is integral to the eukaryotic initiation factor 2 kinase stress response. *Mol Cell Biol* 2004;24: 1365–1377.
- Jin HO, Seo SK, Woo SH, Kim ES, Lee HC, Yoo DH, An S, Choe TB, Lee SJ, Hong SI, Rhee CH, Kim JI, Park IC. Activating transcription factor 4 and CCAAT/enhancer-binding protein-beta negatively regulate the mammalian target of rapamycin via Redd1 expression in response to oxidative and endoplasmic reticulum stress. *Free Radic Biol Med.* 2009 Apr 15;46(8):1158-67. doi: 10.1016/j.freeradbiomed.2009.01.015. Epub 2009 Jan 27. PMID: 19439225.
- Kadowaki H, Nishitoh H. Signaling pathways from the endoplasmic reticulum and their roles in disease. *Genes (Basel).* 2013 Jul 1;4(3):306-33. doi: 10.3390/genes4030306.
- Karpinski BA, Morle GD, Huggenvik J, Uhler MD, Leiden JM. Molecular cloning of human CREB-2: an ATF/CREB transcription factor that can negatively regulate transcription from the cAMP response element. *Proceedings of the National Academy of Sciences of the United States of America.* June 1992, 89 (11): 4820–4. doi:10.1073/pnas.89.11.4820. PMC 49179free to read. PMID 1534408
- Kerr J F R, Wyllie A H, Currie, A R (1972). Apoptosis: a basic biological phenomenon with ranging implications in tissue kinetics. *Br. J. Cancer* 26:239–257.
- Kieslich M, Porto L, Lanfermann H, Jacobi G, Schwabe D, Bohles H. Cerebrovascular complications of L-ASNase in the therapy of acute lymphoblastic leukemia. *J Pediatr Hematol Oncol.* 2003 Jun;25:484-7.
- Kilberg MS, Balasubramanian M, Fu L, Shan J The transcription factor network associated with the amino acid response in mammalian cells. *Adv Nutr.* 2012 May 1;3(3):295-306. doi: 10.3945/an.112.001891.
- Kilberg MS, Shan J, Su N. ATF4-dependent transcription mediates signaling of amino acid limitation, *Trends Endocrinol. Metab.* 20 (2009) 436–443.

- Kim DH, Sarbassov DD, Ali SM, King JE, Latek RR, Erdjument-Bromage H, Tempst P, Sabatini DM. mTOR interacts with raptor to form a nutrient-sensitive complex that signals to the cell growth machinery. *Cell*. 2002 Jul 26;110(2):163-75.
- Kim DH, Sarbassov DD, Ali SM, Latek RR, Guntur KV, Erdjument-Bromage H, Tempst P, Sabatini DM. GbetaL, a positive regulator of the rapamycin-sensitive pathway required for the nutrient-sensitive interaction between raptor and mTOR. *Mol Cell*. 2003 Apr;11(4):895-904.
- Kim E, Goraksha-Hicks P, Li L, Neufeld TP, Guan KL. 2008. Regulation of TORC1 by Rag GTPases in nutrient response. *Nat Cell Biol* 10: 935–945.
- Kim J, Kundu M, Viollet B, Guan K L. 2011. AMPK and mTOR regulate autophagy through direct phosphorylation of Ulk1. *Nat Cell Biol* 13: 132–141
- Kim, E J, Lee, YJ, Kang, S, Lim, Y.B. (2014). Ionizing radiation activates PERK/eIF2 α /ATF4 signaling via ER stress-independent pathway in human vascular endothelial cells. *Int. J. Radiat. Biol.* 90(4):306-12.
- Kimball SR, Gordon BS, Moyer JE, Dennis MD, Jefferson LS. Leucine induced dephosphorylation of Sestrin2 promotes mTORC1 activation. *Cell Signal*. 2016 Aug; 28(8):896-906. doi: 10.1016/j.cellsig.2016.03.008. Epub 2016 Mar 21. PMID: 27010498.
- Kimball SR, Jefferson LS. (2005) Role of amino acids in the translational control of protein synthesis in mammals. *Semin Cell Dev Biol*. 16:21–7.
- Kimball SR, Jefferson LS. Induction of REDD1 gene expression in the liver in response to endoplasmic reticulum stress is mediated through a PERK, eIF2 α phosphorylation, ATF4-dependent cascade. *Biochem Biophys Res Commun*. 2012 Oct 26;427(3):485-9. doi: 10.1016/j.bbrc.2012.09.074. Epub 2012 Sep 20. PMID: 23000413.
- Kinnally KW, Peixoto PM, Ryu SY et al (2011) Is mPTP the gatekeeper for necrosis, apoptosis, or both? *Biochim Biophys Acta* 1813:616–622.
- Kitamura M. Biphasic, bidirectional regulation of NF-kappaB by endoplasmic reticulum stress. *Antioxid Redox Signal*. 2009; 11(9):2353–64. Epub 2009/02/04. doi: 10.1089/ARS.2008.2391 PMID: 19187000.
- Knoderer HM, Robarge J, Flockhart DA. Predicting ASNase-associated pancreatitis. *Pediatr Blood Cancer*. 2007 Oct 15;49:634-9.
- Kober L, Zehe C, Bode J. Development of a Novel ER Stress Based Selection System for the Isolation of Highly Productive Clones. 2012;2599–611.

- Krishna M. Vattam and Ronald C. Wek. Reinitiation involving upstream ORFs regulates ATF4 mRNA translation in mammalian cells *Proc Natl Acad Sci U S A*. 2004 Aug 3; 101(31): 11269–11274.
- Landau H, Lamanna N. Clinical manifestations and treatment of newly diagnosed acute lymphoblastic leukemia in adults. *Curr Hematol Malig Rep*. 2006 Sep;1(3):171-9. doi: 10.1007/s11899-996-0005-8.
- Laplanche M, Sabatini DM (2013). Regulation of mTORC1 and its impact on gene expression at a glance. *J Cell Sci*. 15;126(Pt 8):1713-9. doi: 10.1242/jcs.125773.
- Laplanche M, Sabatini DM. 2012. mTOR signaling in growth control and disease. *Cell* 149: 274–293.
- Lee JH, Budanov AV, Park EJ, Birse R, Kim TE, Perkins GA, Ocorr K, Ellisman MH, Bodmer R, Bier E, Karin M. Sestrin as a feedback inhibitor of TOR that prevents age-related pathologies. *Science*. 2010 Mar 5;327(5970):1223-8. doi: 10.1126/science.1182228.
- Lee K, Tirasophon W, Shen X, Michalak M, Prywes R, Okada T, Yoshida H, Mori K, Kaufman RJ. IRE1-mediated unconventional mRNA splicing and S2P-mediated ATF6 cleavage merge to regulate XBP1 in signaling the unfolded protein response. *Genes Dev*. 2002;452–66.
- Lerner AG et al. (2012). IRE1 α induces thioredoxin-interacting protein to activate the NLRP3 inflammasome and promote programmed cell death under irremediable ER stress. *Cell Metab* 16, 250–264.
- Leslie M, Case MC, Hall AG, Coulthard SA. Expression levels of asparagine synthetase in blasts from children and adults with acute lymphoblastic leukaemia. *Br J Haematol*. 2006 Mar;132:740-2.
- Liew, C. W., Bochenski, J., Kawamori, D., Hu, J., Leech, C. A., Wanic, K., Malecki, M., Warram, J. H., Qi, L., Krolewski, A. S., and Kulkarni, R. N. (2010) The pseudokinase tribbles homolog 3 interacts with ATF4 to negatively regulate insulin exocytosis in human and mouse beta cells. *J Clin Invest* 120, 2876–2888.
- Locasale JW. Serine, glycine and one-carbon units: cancer metabolism in full circle. *Nat Rev Cancer*. 2013 Aug;13(8):572-83. doi: 10.1038/nrc3557. Epub 2013 Jul 4.
- Los M, Wesselborg S, Schulze-Osthoff K (1999) The role of caspases in development, immunity, and apoptotic signal transduction: lessons from knockout mice. *Immunity* 10:629–639.

- Lu L, Han AP, Chen JJ. Translation initiation control by heme-regulated eukaryotic initiation factor 2 α kinase in erythroid cells under cytoplasmic stresses. *Mol Cell Biol*. 2001 Dec;21(23):7971-80.
- Lubkowski, J., Palm, G. J., Gilliland, G. L., Derst, C., Röhm, K. H., & Wlodawer, A. (1996). Crystal structure and amino acid sequence of Wolinella succinogenes I-ASNase. *European Journal of Biochemistry*, 241, 201–207.
- Luo JQ, Chen DW, Yu B. Upregulation of amino acid transporter expression induced by L-leucine availability in L6 myotubes is associated with ATF4 signaling through mTORC1-dependent mechanism. *Nutrition*. 2013 Jan;29(1):284-90. doi: 10.1016/j.nut.2012.05.008. Epub 2012 Sep 15. PMID: 22985970
- Ma Y, Brewer JW, Diehl JA, Hendershot LM. Two distinct stress signaling pathways converge upon the CHOP promoter during the mammalian unfolded protein response. *J Mol Biol* 2002; 318:1351–1365.
- Ma Y, Hendershot LM. The role of the unfolded protein response in tumor development: friend or foe? *Nat Rev Cancer* 2004; 4:966-77.
- Makowski AJ, Uppuganti S, Wadeer SA, Whitehead JM, Rowland BJ, Granke M, Mahadevan-Jansen A, Yang X, Nyman JS The loss of activating transcription factor 4 (ATF4) reduces bone toughness and fracture toughness. *Bone*. 2014 May;62:1-9. doi: 10.1016/j.bone.2014.01.021.
- Malhi H, Kaufman RJ. Endoplasmic reticulum stress in liver disease. *J Hepatol*. 2011;54 (4):795-809.
- Malhotra JD, Miao H, Zhang K, Wolfson A, Pennathur S, Pipe SW, et al. Antioxidants reduce endoplasmic reticulum stress and improve protein secretion. *Proc Natl Acad Sci USA* 2008;105: 18525–18530.
- Malmberg SE, Adams CM. Insulin signaling and the general amino acid control response. Two distinct pathways to amino acid synthesis and uptake. *J Biol Chem*. 2008 Jul 11;283(28):19229-34. doi: 10.1074/jbc.M801331200. Epub 2008 May 14.
- Manning BD, Cantley LC. AKT/PKB signaling: navigating downstream. *Cell*. 2007 Jun 29;129(7):1261-74.
- Marciniak SJ, Yun CY, Oyadomari S, Novoa I, Zhang Y, Jungreis R, Nagata K, Harding HP, Ron D. CHOP induces death by promoting protein synthesis and oxidation in the stressed endoplasmic reticulum. *Genes Dev* 18: 3066–3077, 2004.
- Morris DR, Geballe AP. Upstream open reading frames as regulators of mRNA translation. *Mol Cell Biol*. 2000; 20(23):8635-42. PMID: 11073965

- Mungrue IN, Pagnon J, Kohannim O, Gargalovic PS, Lusa AJ.
CHAC1/MGC4504 is a novel proapoptotic component of the unfolded protein response, downstream of the ATF4-ATF3-CHOP cascade. *J Immunol* 2009;182:466–476.
- Mungrue IN, Pagnon J, Kohannim O, Gargalovic PS, Lusa AJ.
CHAC1/MGC4504 is a novel proapoptotic component of the unfolded protein response, downstream of the ATF4-ATF3-CHOP cascade. *J Immunol* 2009;182:466–476.
- Nobukuni, T., M. Joaquin, M. Roccio, S.G. Dann, S.Y. Kim, P. Gulati, M.P. Byfield, J.M. Backer, F. Natt, J.L. Bos, et al. 2005. Amino acids mediate mTOR/raptor signaling through activation of class 3 phosphatidylinositol 3OH-kinase. *Proc. Natl. Acad. Sci. USA*. 102:14238–14243.
<http://dx.doi.org/10.1073/pnas.0506925102>
- Offman MN, Krol M, Patel N, Krishnan S, Liu J, Saha V, Bates PA. Rational engineering of L-ASNase reveals importance of dual activity for cancer cell toxicity. *Blood*. 2011; 5:1614-21.
- Ollenschläger G, Roth E, Linkesch W, Jansen S, Simmel A, Mödder B. ASNase-induced derangements of glutamine metabolism: the pathogenetic basis for some drug-related side-effects. *Eur J Clin Invest*. 1988;512–6.
- Ord, T., Ord, D., Kuuse, S., Plaas, M., Ord, T. (2012). Trib3 is regulated by IL-3 and affects bone marrow-derived mast cell survival and function. *Cell Immunol*. 280(1):68-75.
- Oshiro N, Takahashi R, Yoshino K, Tanimura K, Nakashima A, Eguchi S, Miyamoto T, Hara K, Takehana K, Avruch J, Kikkawa U, Yonezawa K. The proline-rich Akt substrate of 40 kDa (PRAS40) is a physiological substrate of mammalian target of rapamycin complex 1. *J Biol Chem*. 2007 Jul 13;282(28):20329-39. Epub 2007 May 21.
- Osowski CM et al. (2012). Thioredoxin-interacting protein mediates ER stress-induced beta cell death through initiation of the inflammasome. *Cell Metab* 16, 265–273.
- Ozcan U, Ozcan L, Yilmaz E, Düvel K, Sahin M, Manning BD, Hotamisligil GS. Loss of the tuberous sclerosis complex tumor suppressors triggers the unfolded protein response to regulate insulin signaling and apoptosis. *Mol Cell*. 2008 Mar 14;29(5):541-51. doi: 10.1016/j.molcel.2007.12.023.
- Panosyan EH, Grigoryan RS, Avramis IA, Seibel NL, Gaynon PS, Siegel SE, Fingert HJ, Avramis VI. Deamination of glutamine is a prerequisite for optimal asparagine deamination by ASNases in vivo (CCG-1961). *Anticancer Res*. 2004; 2C:1121-5.

- Parmigiani A, Nourbakhsh A, Ding B, Wang W, Kim YC, Akopiants K, Guan KL, Karin M, Budanov AV. Sestrins inhibit mTORC1 kinase activation through the GATOR complex. *Cell Rep*. 2014 Nov 20;9(4):1281-91.
- Parsons SK, Skapek SX, Neufeld EJ, Kuhlman C, Young ML, Donnelly M, Brunzell JD, Otvos JD, Sallan SE, Rifai N. ASNase-associated lipid abnormalities in children with acute lymphoblastic leukemia. *Blood*. 1997 Mar 15;89:1886-95.
- Patil S, Coutsouvelis J, Spencer A. ASNase in the management of adult acute lymphoblastic leukaemia: Is it used appropriately? *Cancer Treat Rev*. 2010 Sep 3.
- Payne JH, Vora AJ. Thrombosis and acute lymphoblastic leukaemia. *Br J Haematol*. 2007 Aug;138:430-45.
- Peng TI, Jou MJ. Oxidative stress caused by mitochondrial calcium overload. *Ann N Y Acad Sci*. 2010 Jul;1201:183-8. doi: 10.1111/j.1749-6632.2010.05634.x. PMID: 20649555.
- Podust LM, Krezel AM, Kim Y. Crystal structure of the CCAAT box/enhancer-binding protein beta activating transcription factor-4 basic leucine zipper heterodimer in the absence of DNA . *J. Biol. Chem*. (2001) 276 (1): 505–13. doi:10.1074/jbc.M005594200. PMID 11018027
- Pratt CB, Johnson WW. Duration and severity of fatty metamorphosis of the liver following L-ASNase therapy. *Cancer*. 1971 Aug;28:361-4.
- Proud CG. (2009) mTORC1 signalling and mRNA translation. *Biochem Soc Trans*. 37(Pt 1):227–31.
- Pui CH, Evans WE. Treatment of acute lymphoblastic leukemia. *N Engl J Med*. 2006 Jan 12;354:166-78.
- Pui CH, Robison LL, Look AT. Acute lymphoblastic leukaemia. *Lancet*. 2008 Mar 22;371:1030-43.
- Qiu H, Dong J, Hu C, Francklyn CS, Hinnebusch AG. The tRNA-binding moiety in GCN2 contains a dimerization domain that interacts with the kinase domain and is required for tRNA binding and kinase activation. *EMBO J*. 2001;1425–38.
- Qiu Q, Zheng Z, Chang L, Zhao YS, Tan C, Dandekar A, et al. Toll-like receptor-mediated IRE1alpha activation as a therapeutic target for inflammatory arthritis. *EMBO J*. 2013; 32(18):2477–90. Epub 2013/08/15. doi: emboj2013183 [pii] doi: 10.1038/emboj.2013.183 PMID: 23942232.

- Raetz EA, Salzer WL. Tolerability and efficacy of L-ASNase therapy in pediatric patients with acute lymphoblastic leukemia. *J Pediatr Hematol Oncol*. 2010 Oct;32:554-63.
- Ramya LN, Doble M, Rekha VPB, Pulicherla KK. L-ASNase as potent anti-leukemic agent and its significance of having reduced glutaminase side activity for better treatment of acute lymphoblastic leukaemia. *Applied Biochemistry and Biotechnology*. 2012; 167(8):2144-59.
- Reinert RB, Oberle LM, Wek SA, Bunpo P, Wang XP, Mileva I, Goodwin LO, Aldrich CJ, Durden DL, McNurlan MA, Wek RC, Anthony TG. Role of glutamine depletion in directing tissue-specific nutrient stress responses to L-ASNase. *J Biol Chem*. 2006 Oct 20; 281(42):31222-33. Epub 2006 Aug 24.
- Rytting ME. Role of L-ASNase in acute lymphoblastic leukemia: focus on adult patients. *Blood and Lymphatic Cancer: Targets and Therapy* 2012;2 117–124
- Rzymiski T, Milani M, Pike L, Buffa F, Mellor HR, Winchester L, Pires I, Hammond E, Ragoussis I, Harris AL. Regulation of autophagy by ATF4 in response to severe hypoxia. *Oncogene*. 2010 Aug 5;29(31):4424-35. doi: 10.1038/onc.2010.191. Epub 2010 May 31.
- Sahoo S, Hart J. Histopathological features of L-ASNase-induced liver disease. *Semin Liver Dis*. 2003 Aug;23:295-9.
- Salgado MC, Metón I, Anemaet IG, Baanante IV. Activating transcription factor 4 mediates up-regulation of alanine aminotransferase 2 gene expression under metabolic stress. *Biochim Biophys Acta*. 2014; 1839 (4):288-96.
- Sancak Y, Bar-Peled L, Zoncu R, Markhard AL, Nada S, Sabatini DM. 2010. Regulator–Rag complex targets mTORC1 to the lysosomal surface and is necessary for its activation by AAs. *Cell* 141: 290–303.
- Sancak Y, Peterson TR, Shaul YD, Lindquist RA, Thoreen CC, Bar-Peled L, Sabatini DM. 2008. The Rag GTPases bind raptor and mediate AA signaling to mTORC1. *Science* 320: 1496–1501.
- Schaap FG, Kremer AE, Lamers WH, et al. Fibroblast growth factor 21 is induced by endoplasmic reticulum stress. *Biochimie*. 2013; 95: 692–9
- Schwarzer R, Dames S, Tondera D, Klippel A, Kaufmann J. TRB3 is a PI 3-kinase dependent indicator for nutrient starvation. *Cell Signal*. 2006;18(6):899-909.
- Seo J, Fortuno ES, Suh JM, et al. Atf4 regulates obesity, glucose homeostasis, and energy expenditure. *Diabetes*. 2009; 58: 2565–73.

- Seo J, Fortuno ES, Suh JM, et al. Atf4 regulates obesity, glucose homeostasis, and energy expenditure. *Diabetes*. 2009; 58: 2565–73.
- Shang L, Chen S, Du F, Li S, Zhao L, Wang X. 2011. Nutrient starvation elicits an acute autophagic response mediated by Ulk1 dephosphorylation and its subsequent dissociation from AMPK. *Proc Natl Acad Sci* 108: 4788–4793.
- She P, Bunpo P, Cundiff JK, Wek RC, Harris RA, Anthony TG. General control nonderepressible 2 (GCN2) kinase protects oligodendrocytes and white matter during branched-chain amino acid deficiency in mice. *J Biol Chem*. 2013 Oct 25;288(43):31250-60. doi: 10.1074/jbc.M113.498469.
- Shen J, Chen X, Hendershot L, Prywes R. ER stress regulation of ATF6 localization by dissociation of BiP/GRP78 binding and unmasking of golgi localization signals. *Dev Cell*. 2002;99–111.
- Shimobayashi M, Hall MN. 2014. Making new contacts: the mTOR network in metabolism and signalling crosstalk. *Nat Rev Mol Cell Biol* 15: 155–162.
- Siu F, Bain PJ, LeBlanc-Chaffin R, Chen H, Kilberg MS. ATF4 is a mediator of the nutrient sensing response pathway that activates the human asparagine synthetase gene. *J Biol Chem*. 2002.
- Sofer A, Lei K, Johannessen CM, Ellisen LW. Regulation of mTOR and cell growth in response to energy stress by REDD1. *Mol Cell Biol*. 2005 Jul;25(14):5834-45.
- Song B, Scheuner D, Ron D, Pennathur S, Kaufman RJ. Chop deletion reduces oxidative stress, improves beta cell function, and promotes cell survival in multiple mouse models of diabetes. *J Clin Invest* 2008; 118:3378–3389.
- Sood R, Porter A, Olsen D, Cavener D, Wek R. A mammalian homologue of GCN2 protein kinase important for translational control by phosphorylation of eukaryotic initiation factor-2a. *Genetics*. 2000a Feb;154:787-801. PMID: 10655230
- Sood R, Porter AC, Ma K, Quilliam LA, Wek RC. Pancreatic eukaryotic initiation factor-2alpha kinase (PEK) homologues in humans, *Drosophila melanogaster* and *Caenorhabditis elegans* that mediate translational control in response to endoplasmic reticulum stress. *Biochem J*. 2000b Mar 1;346 Pt 2:281-93.
- Spinola-Castro AM, Siviero-Miachon AA, Andreoni S, Tosta-Hernandez PD, Macedo CR, Lee ML. Transient hyperglycemia during childhood acute lymphocytic leukemia chemotherapy: an old event revisited. *Clin Adv Hematol Oncol*. 2009 Jul;7:465-72.

- Stipanuk MH. (2007) Leucine and protein synthesis: mTOR and beyond. *Nutr Rev.* 65:122–9.
- Su N, Kilberg MS. C/EBP homology protein (CHOP) interacts with activating transcription factor 4 (ATF4) and negatively regulates the stress-dependent induction of the asparagine synthetase gene. *J Biol Chem.* 2008 Dec 12;283:35106-17.
- Suryawan A, Jeyapalan AS, Orellana RA, Wilson FA, Nguyen HV, Davis TA (2008) Leucine stimulates protein synthesis in skeletal muscle of neonatal pigs by enhancing mTORC1 activation. *Am J Physiol Endocrinol Metab.* 295(4):E868-75. doi: 10.1152/ajpendo.90314.
- Suryawan A, Torrazza RM, Gazzaneo MC, Orellana RA, Fiorotto ML, El-Kadi SW, Srivastava N, Nguyen HV, Davis TA. (2012) Enteral leucine supplementation increases protein synthesis in skeletal and cardiac muscles and visceral tissues of neonatal pigs through mTORC1-dependent pathways. *Pediatr Res.* 71(4 Pt 1):324-31. doi: 10.1038/pr.2011.79
- Szegezdi E, Logue SE, Gorman AM, Samali A. Mediators of endoplasmic reticulum stress-induced apoptosis. *EMBO Rep* 2006;7:880–885.
- Tee AR, Manning BD, Roux PP, Cantley LC, Blenis J. Tuberous sclerosis complex gene products, Tuberin and Hamartin, control mTOR signaling by acting as a GTPase-activating protein complex toward Rheb. *Curr Biol.* 2003 Aug 5;13(15):1259-68. PMID: 12906785.
- Teske BF, Fusakio ME, Zhou D, Shan J, McClintick JN, Kilberg MS, Wek RC. CHOP induces activating transcription factor 5 (ATF5) to trigger apoptosis in response to perturbations in protein homeostasis. *Mol Biol Cell.* 2013; 24(15):2477-90. doi: 10.1091/mbc.E13-01-006.
- Teske, B.F., Wek, S.A., Bunpo, P., Cundiff, J.K., McClintick, J.N., Anthony, T.G., Wek, R.C. (2011). The eIF2 kinase PERK and the integrated stress response facilitate activation of ATF6 during endoplasmic reticulum stress. *Mol. Biol. Cell.* 22(22):4390-405.
- Tirasophon W, Welihinda AA, Kaufman RJ. A stress response pathway from the endoplasmic reticulum to the nucleus requires a novel bifunctional protein kinase/endoribonuclease (Ire1p) in mammalian cells. *Genes Dev.* 1998 Jun 15;12(12):1812-24. PMID: 9637683
- Urano F, Wang X, Bertolotti A, Zhang Y, Chung P, Harding HP, et al. Coupling of stress in the ER to activation of JNK protein kinases by transmembrane protein kinase IRE1. *Science.* 2000; 287 (5453):664–6. Epub 2000/01/29. doi: 8218 [pii]. PMID: 10650002.

- Vattem KM, Wek RC. Reinitiation involving upstream ORFs regulates ATF4 mRNA translation in mammalian cells. *Proc Natl Acad Sci U S A*. 2004;11269–74.
- Visweswaraiah J, Lageix S, Castilho B a., Izotova L, Kinzy TG, Hinnebusch AG, Sattlegger E. Evidence that eukaryotic translation elongation factor 1A (eEF1A) binds the Gcn2 protein C terminus and inhibits Gcn2 activity. *J Biol Chem*. 2011;36568–79.
- Walter P, Ron D. The unfolded protein response: from stress pathway to homeostatic regulation. *Science* 334, 1081–1086 (2011).
- Wang C, Li H, Meng Q, Du Y, Xiao F, Zhang Q, Yu J, Li K, Chen S, Huang Z, Liu B, Guo F. ATF4 deficiency protects hepatocytes from oxidative stress via inhibiting CYP2E1 expression. *J Cell Mol Med*. 2014 Jan; 18(1):80-90. doi: 10.1111/jcmm.12166.
- Wang S, Kaufman RJ. The impact of the unfolded protein response on human disease. *J. Cell Biol*. 197, 857–867 (2012).
- Wang X, Campbell LE, Miller CM, Proud CG. 1998. AA availability regulates p70 S6 kinase and multiple translation factors. *Biochem J* 334(Pt 1): 261–267.
- Wani NA, Kosar T, Pala NA, Qureshi UA. Sagittal sinus thrombosis due to L-ASNase. *J Pediatr Neurosci*. 2010 Jan;5:32-5.
- Wek RC, Jiang H-Y, Anthony TG. Coping with stress: eIF2 kinases and translational control. *Biochem Soc Trans*. 2006;7–11.
- Wek RC, Jiang HY, Anthony TG. Coping with stress: eIF2 kinases and translational control. *Biochem Soc Trans*. 2006 Feb;34(Pt 1):7-11. PMID: 16246168
- Whitney ML, Jefferson LS, Kimball SR ATF4 is necessary and sufficient for ER stress-induced upregulation of REDD1 expression. *Biochem Biophys Res Commun*. 2009 Feb 6;379(2):451-5. doi: 10.1016/j.bbrc.2008.12.079. Epub 2008 Dec 27. PMID: 19114033
- Wilson FA, Suryawan A, Gazzaneo MC, Orellana RA, Nguyen HV, Davis TA (2010) Stimulation of muscle protein synthesis by prolonged parenteral infusion of leucine is dependent on amino acid availability in neonatal pigs. *J Nutr*. 140(2):264-70. doi: 10.3945/jn.109.113621.
- Wilson GJ, Bunpo P, Cundiff JK, Wek RC, Anthony TG. The eukaryotic initiation factor 2 kinase GCN2 protects against hepatotoxicity during ASNase treatment. *Am J Physiol Endocrinol Metab*. 2013 Nov 1;305(9):E1124-33. doi: 10.1152/ajpendo.00080.2013. Epub 2013 Sep 3.

- Wilson GJ, Lennox BA, She P, Mirek ET, Al Baghdadi RJ, Fusakio ME, Dixon JL, Henderson GC, Wek RC, Anthony TG. GCN2 is required to increase fibroblast growth factor 21 and maintain hepatic triglyceride homeostasis during ASNase treatment. *Am J Physiol Endocrinol Metab.* 2015; 308:E283-93.
- Wullschlegel S, Loewith R, Hall MN. TOR signaling in growth and metabolism. *Cell.* 2006 Feb 10;124(3):471-84. Review. PMID: 16469695
- Wullschlegel, S, Loewith R, Hall MN. TOR signaling in growth and metabolism. 2006; *Cell* 124, 471–484.
- Xiao G., T. Zhang, S. Yu, S. Lee, V. Calabuig-Navarro, J. Yamauchi, S. Ringquist, H.H. Dong, ATF4 protein deficiency protects against high fructose-induced hypertriglyceridemia in mice, *J. Biol. Chem.* 288 (2013) 25350–25361.
- Xu J, Lloyd DJ, Hale C, et al. Fibroblast growth factor 21 reverses hepatic steatosis, increases energy expenditure, and improves insulin sensitivity in diet-induced obese mice. *Diabetes.* 2009; 58: 250–9
- Yamaguchi S, Ishihara H, Yamada T, Tamura A, Usui M, Tominaga R, Munakata Y, Satake C, Katagiri H, et al. ATF4-mediated induction of 4E-BP1 contributes to pancreatic beta cell survival under endoplasmic reticulum stress. *Cell Metab.* 2008 Mar;7:269-76.
- Ye J, Palm W, Peng M, King B, Lindsten T, Li MO, Koumenis C, Thompson CB. GCN2 sustains mTORC1 suppression upon amino acid deprivation by inducing Sestrin2. *Genes Dev.* 2015 Nov 15;29(22):2331-6. doi: 10.1101/gad.269324.115.
- Yoshida H, Matsui T, Yamamoto A, Okada T, Mori K. XBP1 mRNA is induced by ATF6 and spliced by IRE1 in response to ER stress to produce a highly active transcription factor. *Cell.* 2001;881–91.
- Yoshizawa T, Hinoi E, Jung DY, Kajimura D, Ferron M, Seo J, Graff JM, Kim JK, Karsenty G. The transcription factor ATF4 regulates glucose metabolism in mice through its expression in osteoblasts. *J Clin Invest.* 2009 Sep;119(9):2807-17. doi: 10.1172/JCI39366. Epub 2009 Aug 10. PMID: 19726872
- Zhang K, Kaufman RJ. From endoplasmic-reticulum stress to the inflammatory response. *Nature.* 2008 Jul 24;454(7203):455-62. doi: 10.1038/nature07203. PMID: 18650916.
- Zhang P, McGrath BC, Reinert J, Olsen DS, Lei L, Gill S, Wek SA, Vatter KM, Wek RC, Kimball SR, Jefferson LS, Cavener DR. The GCN2 eIF2alpha kinase is required for adaptation to amino acid deprivation in mice. *Mol Cell Biol.* 2002 Oct;22(19):6681-8.

COMMON ABBREVIATIONS

4E-BP1 - eIF4E Binding Protein 1

AAR - Amino Acid Response

Akt - Protein Kinase B

ALL - Acute Lymphoblastic Leukemia

ANOVA - Analysis of Variance

ASNS - Asparagine Synthetase

ATF3 - Activating Transcription Factor 3

ATF4 - Activating Transcription Factor 4

ATF5 - Activating Transcription Factor 5

ATF6 - Activating Transcription Factor 6

B6J - C57 Black 6 Jackson

BiP - B cell immunoglobulin protein

BW - Body weight

CHAC1- cation transport regulator-like protein 1

CHOP/GADD153 - C/EBP Homologous Protein

Ddit4 - DNA Damage Inducible Transcript 4

eIF2 - Eukaryotic Initiation Factor 2

EIF2AK - eukaryotic initiation factor 2-alpha kinase

eIF4E - eukaryotic initiation factor 4E

ER - Endoplasmic Reticulum

FGF21 - Fibroblast growth factor 21

GADD34 - Growth arrest and DNA damage-inducible protein

GCN2 - General Control Nonderepressible 2

Grp78 - Glucose regulatory protein 78

HRI - Heme regulated inhibitor

i.p. - intraperitoneal

IRE1 - Inositol requiring 1

ISR - Integrated Stress Response

IU - International Units

KO - Knock out

MEF - mouse embryonic fibroblast

mTORC1 - Mammalian Target of Rapamycin Complex 1

NRF2 - Nuclear factor, erythroid derived 2, like 2

P70S6K - Ribosomal p70 S6 Kinase

PBS – Phosphate buffered saline

p-eIF2 - Phosphorylated eIF2

PERK - PKR-like ER-resident Kinase

PI3K - Phosphoinositide 3 Kinase

PKR - RNA dependent protein kinase

PPARG - Peroxisome proliferator activated receptor gamma

PVDF - Polyvinylidene difluoride

REDD1 - Regulated in development and DNA damage responses 1

RT-qPCR – Reverse Transcriptase-quantitative Polymerase Chain Reaction

sXBP1 - Spliced X-Box Binding Protein 1

TSC1 - Tuberous Sclerosis 1

TSC2 - Tuberous Sclerosis 2

TUNEL - Terminal deoxynucleotidyl transferase (TdT) dUTP Nick-End Labeling

UPR - Unfolded Protein Response

uXBP1 - unspliced X-Box Binding Protein 1

WT - Wild-type

XBP1 - X Box Binding Protein 1

Figures

Figure 1. The ISR. In mammals, Eif2 is phosphorylated by four different kinases in response to various environmental stresses.

Figure 2. Hypothesized model of amino acid response (AAR) pathway activated by ASNase in liver. ASNase induces eIF2 phosphorylation and subsequent activation of the AAR. These events correspond with hepatic adaptive recovery in intact GCN2 mice. Mice lacking *Atf4* fails to activate the homeostatic AAR and this corresponds with ASNase-induced hepatotoxicity.

Figures

Fig. 1

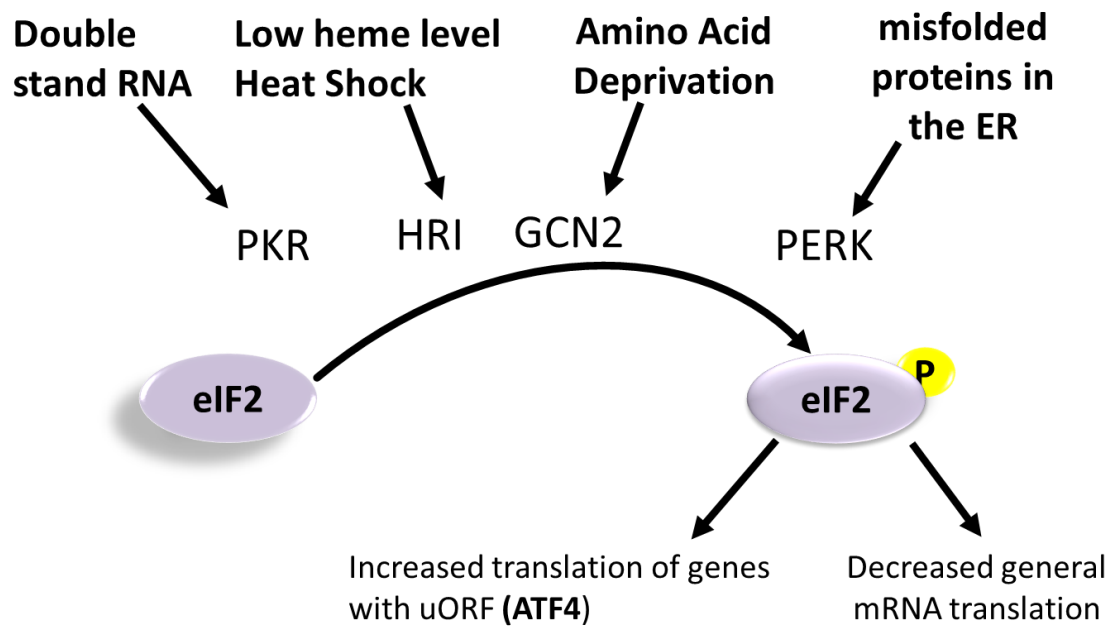
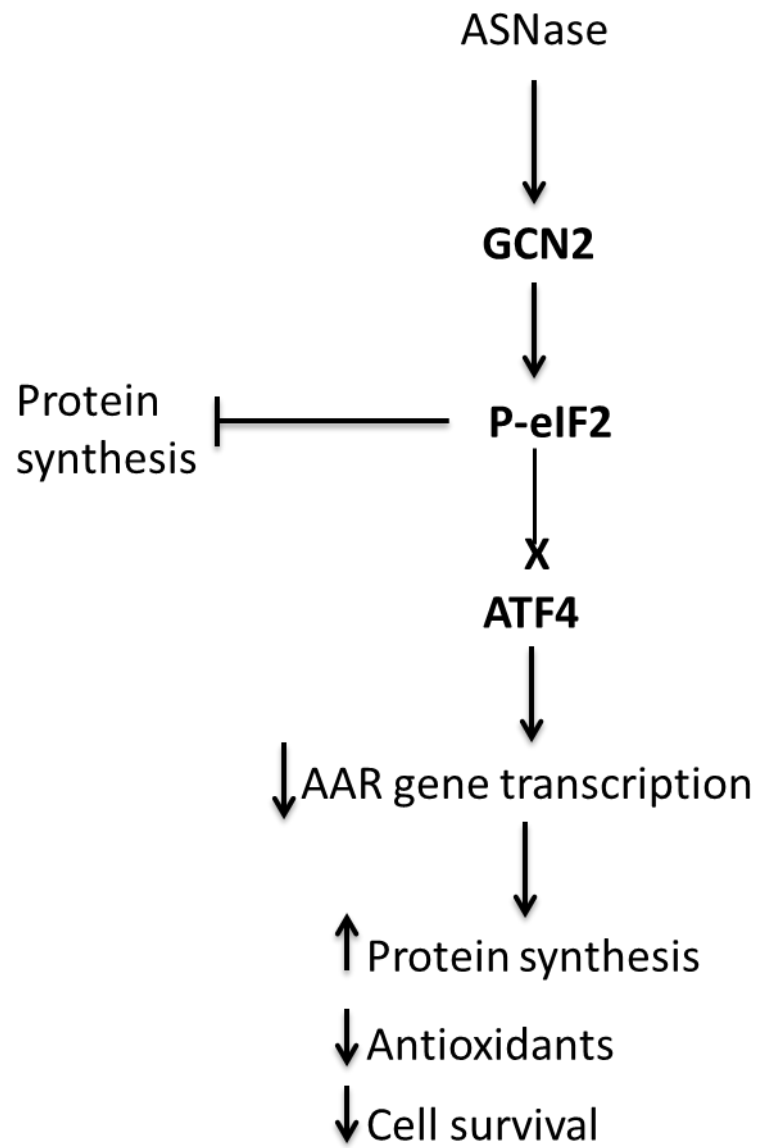


Fig. 2



Research Objectives and Hypotheses

Global Dissertation Object: To investigate the role of ATF4 in guiding the liver response to amino acid depletion by ASNase.

Aim 1. Describe the liver response to ASNase in mice deleted for *Atf4* versus *Gcn2*.

Hypothesis for Aim 1: ATF4 deficiency augments hepatotoxicity to ASNase similar to loss of GCN2.

Rationale for Aim 1: Based on our previous work with *Gcn2*^{-/-} mice treated with ASNase, I reason that ASNase toxicity mechanisms might be completely or partially driven by its downstream effector, ATF4.

Aim 2. Determine if *Atf4* heterozygosity alters the hepatic response to ASNase.

Hypothesis for Aim 2: ATF4 heterozygosity alters hepatic AAR activation and augments hepatotoxicity to ASNase.

Rationale for Aim 2: Similar to *Gcn2*^{-/-} mice, *Atf4*^{+/-} mice appear normal and healthy. However, *Gcn2*^{-/-} mice fail to activate the AAR in response to ASNase, intensifying hepatotoxicity. Based on this, I reason that loss

of one *Atf4* allele will alter induction of the AAR and aggravate ASNase-induced hepatotoxicity.

Aim 3. Examine the hepatic response to ASNase in mice with a liver-specific deletion of *Atf4*.

Hypothesis for Aim 3: Loss of *Atf4* in the liver alters hepatic AAR activation and augments hepatotoxicity to ASNase.

Rationale for Aim 3: Some studies suggest that ATF4 regulates metabolism via extrahepatic endocrine functions but other studies describe metabolic roles for ATF4 in liver during ER stress. To what extent ASNase hepatotoxicity is due to liver deletion of *Atf4* versus extrahepatic deletion is unknown. Based on available data, I reason that ATF4 regulates the AAR in liver directly and so loss of hepatic expression will alter the AAR and compromise liver health during ASNase.

CHAPTER TWO: Roles of ATF4 in the Murine Response to ASNase in Liver.

ABSTRACT

Hepatotoxicity is a major cause of treatment failure in leukemia patients receiving ASNase. In liver, ASNase activates the AAR via increased expression of ATF4 following phosphorylation of eukaryotic initiation factor 2 (p-eIF2) by GCN2 kinase. GCN2 deletion blocks induction of the homeostatic AAR gene expression program and amplifies mTORC1 signaling, augmenting hepatotoxicity. The aim of this study was twofold: 1) describe the liver response to ASNase in mice deleted for *Atf4*, and 2) determine if *Atf4* heterozygosity alters the hepatic response to ASNase. I compared global gene expression patterns and selected cell responses in livers from wildtype, *Gcn2*^{-/-}, and *Atf4*^{-/-} mice treated with ASNase or excipient. These analyses revealed that ATF4 controls a hepatic gene expression profile that overlaps with GCN2 and serves to limit AAR activation and maintain cellular metabolism via multiple cytoplasmic nuclear factors. *Atf4*^{-/-} or *Atf4*^{+/-} mice displayed amplification of the AAR and exhibited ER stress. Furthermore, downregulation of mTORC1 activity during ASNase was unaffected by ATF4 deletion. *Conclusions*: ATF4 serves to self-contain the AAR and is not required for downregulation of mTORC1 activity during amino acid depletion by ASNase.

Introduction

ASNase is a chemotherapy agent used to treat acute lymphoblastic leukemia, the most common childhood cancer (Ribeiro and Pui, 2005).

Hepatotoxicity by ASNase causes metabolic complications that correspond with inhibition of liver protein synthesis (Reinert et al., 2006), but the molecular basis for this relationship is unclear. Furthermore, why some patients fail to tolerate the drug while others are able to complete treatment without experiencing adverse metabolic events remains a mystery (Pieters et al., 2011).

ASNase induces remission by depleting blood levels of asparagine and glutamine, starving leukemic lymphoblasts of substrates essential for tumor growth (Panosyan et al., 2004; Offman et al., 2011). In liver and other tissues, amino acid depletion by ASNase increases p-eIF2 by GCN2 (EIF2AK4) (Reinert et al., 2006; Bunpo et al., 2009). This phosphorylation event alters gene-specific translation, promoting synthesis of basic-region leucine zipper DNA binding proteins such as ATF4 (CREB2). The binding of ATF4 to CARE/AARE in DNA activates a homeostatic transcriptional program called the AAR (Kilberg et al., 2012). Activation of the AAR regulates nutrient uptake and metabolism, energy and redox homeostasis, and cell cycle control (Harding et al., 2003; Cullinan and Diehl, 2006; Kilberg et al., 2009; Adams, 2007; Xiao et al., 2013, Balasubramanian et al., 2013). Animals lacking GCN2 fail to activate the AAR in response to ASNase, and this failure corresponds with hepatotoxicity, pancreatitis and immunosuppression (Reinert et al., 2006; Phillipson-Weiner et al., 2016; Bunpo et al., 2010). GCN2 functions to prevent and/or mitigate adverse

metabolic events to ASNase; however, to what extent these outcomes are attributed to the central AAR regulator ATF4 is unknown.

A family of eIF2 kinases catalyzes p-eIF2 under diverse stress conditions. The integration of this information at the level of p-eIF2 (first described as the ISR by Harding et al., 2003) results in ATF4 synthesis. ATF4 in combination with other basic-region leucine zipper DNA binding proteins then promotes a program of gene expression specifically tailored to each environmental stress. For example, during ER stress, p-eIF2 by PERK (EIF2AK3) leads to ATF4 synthesis (Fusakio et al., 2016) which in combination with the ER transmembrane proteins ATF6 and IRE1 reduce the client load and increase chaperone mediated recovery processes as part of the UPR (Yoshida et al., 2001). In the case of irrecoverable stress, ATF4 and its transcriptional target, CHOP (DDIT3/GADD153), promote programmed cell death pathways (Su and Kilberg., 2008; Han et al., 2013). It is suggested that during environmental stress, the cellular choice between adaptation and apoptosis depends on the extent and duration of ATF4 expression and its downstream target CHOP (Fusakio et al., 2016). While the canonical AAR places ATF4 at a key point in cellular decision making (Harding et al., 2003), little is known concerning the *in vivo* contribution of ATF4 to the GCN2-activated AAR during ASNase or any form of amino acid stress.

A second sensor of amino acid availability is mTORC1 (Zoncu et al., 2011). Phosphorylation of mTORC1 and its substrates, S6K1 and 4E-BP1, drive changes in translational efficiency and ribosomal capacity in response to amino

acid availability (Zoncu et al., 2011; Anthony et al., 2001, Dennis et al., 2011).

Amino acid deficiency via ASNase treatment inhibits hepatic mTORC1 signaling; however, mTORC1 is activated in the livers of *Gcn2*^{-/-} mice, leading to hyperphosphorylation of S6K1 and 4E-BP1. Recent studies identify Sestrin2 as an inhibitor of mTORC1 during amino acid deprivation that is regulated by ATF4 (Ye et al., 2015; Kimball et al., 2016). Thus, repression of mTORC1 during ASNase treatment may also be under the control of ATF4.

In this study, I hypothesized that the GCN2-eIF2-ATF4-AAR serves to protect the liver during ASNase treatment. With this in mind, my objective was to determine if loss of ATF4 precluded AAR activation by ASNase and in turn, aggravated hepatotoxicity similar to loss of GCN2. To address this objective, I crafted two Aims: 1) Describe the liver response to ASNase in mice deleted for *Atf4*, and 2) Determine if *Atf4* heterozygosity alters the hepatic response to ASNase. In this study, I administered ASNase to mice lacking *Gcn2* or *Atf4* and performed RNA sequencing (RNA-Seq) to examine global gene expression and pathway analysis. Selected hepatic responses to ASNase were further evaluated in these mice plus mice with heterozygous *Atf4* deletion to assess intermediate phenotypes. These analyses reveal that in liver: 1) ATF4 controls a gene expression profile that controls cellular metabolism via cytoplasmic nuclear receptor activation, 2) total or partial loss of ATF4 amplifies the AAR, leading to induction of a broader cell stress afflicting the ER, 3) GCN2, but not ATF4, influences mTORC1 activity during amino acid depletion by ASNase and 4) ASNase-induced increases in Sestrin2 expression and phosphorylation do not

require GCN2 or ATF4. These findings substantially advance our understanding of the mechanisms by which ASNase produces adverse metabolic events and the processes by which the AAR is controlled in liver.

Materials and Methods

Animals.

Animals and Genotyping: Male and female C57BL/6J mice (≥ 8 generations), (age 8-12 weeks) carrying a homozygous deletion of *Gcn2* (*Gcn2*^{-/-}) or *Atf4* (*Atf4*^{-/-}) (Jackson Laboratories, Bar Harbor, ME) were used alongside wildtype controls (WT) in these experiments. All mice were individually housed in clear plastic cages with corncob bedding in a room with a 12:12-hour light-dark cycle. Mice were freely provided commercial rodent chow (5001 Laboratory Rodent Diet, LabDiet) and tap water. All animal protocols were approved by the Institutional Animal Care and Use Committee at Rutgers (IACUC), The State University of New Jersey. Animals were bred and maintained at the Rutgers Bartlett animal care facility.

Genotyping.

Animals were genotyped by Polymerase Chain Reaction (PCR) analysis of ear DNA using standard PCR methods. Ear snips were digested using digest solution. The following primers were utilized for PCR methods: GTT TCT ACA

GCT TCC TCC ACT CTT, common to *ATF4*^{+/+} and *ATF4*^{-/-} mice. *ATF4*^{+/+} Forward CAT ACT GGC TTT GTG CCA GA, and *ATF4* Mutant Forward ATT AAG GGC CAG CTC ATT CC. These primers amplify a 465 base pairs (bp) band in the *ATF4*^{+/+} mice, and a 354 bp band in *ATF4*^{-/-} mice, as described by Jackson laboratory (<http://jaxmice.jax.org/strain/013072.html>). *Gcn2* primers are 5' to exon12 (5'-GGTCTGAAGTAGAAGGATGTCAAGTTC-3'), 3' to exon12 (5'-TCCATCAGTTTGCTTCTCTC-3'), and pPNT5 (5'-TACTGTGGTTTCCAAATGTGTCAGTTT-3'). These primers amplify a 550 bp band in *Gcn2*^{+/+}, and 890 bp band in the *Gcn2*^{-/-} (Zhang et al., 2002).

Experimental Design.

Mice were administered once-daily intraperitoneal (i.p.) injections of native *E. coli* L-ASNase (Elspar®, Deerfield, Illinois) in phosphate buffered saline (PBS) at 0 or 3.0 international units per gram body weight (IU/g BW) after the start of the light cycle as previously detailed (Wilson et al., 2015). The doses are based on our previous work as described in (Reinert et al., 2006) and enzyme activity was determined prior to injection by the Nesslerization technique by detecting the level of ammonia as was described (Reinert et al., 2006, Bunpo et al. 2010). Briefly, the production of ammonia by ASNase over time was measured and compared with known ammonia standards. Resulting values represented the activity of the enzyme in international units (IU), where one IU equaled the amount of enzyme that catalyzed the formation of 1 μmol of ammonia/min.

Body weight was recorded daily and at the point of euthanasia.

Body composition.

Body composition of live mice prior first injection and before euthanasia was determined by magnetic resonance using an EchoMRI instrument (Echo Medical Systems, Houston, TX).

Sample collection.

Mice from all treatment groups were euthanized by decapitation ~8 h after the eighth daily injection. Trunk blood collected to obtain serum and tissues were rapidly dissected and rinsed in ice-cold PBS, blotted and weighed. One portion of each liver was snap-frozen in liquid nitrogen for RNA isolation while a second portion was used to determine triglyceride concentrations and a third portion was used for protein expression analysis. Frozen samples were stored at -80°C until analysis. A final portion was fixed in 4% paraformaldehyde as previously described (Wilson et al., 2015).

RNA-Sequencing.

Frozen liver samples were processed to obtain high quality RNA for RNA-Sequencing (RNA-Seq). Total RNA was extracted from frozen livers using NucleoSpin® RNA Kit (Macherey-Nagel, Newmann-Neander, Germany) followed by DNase treatment. The A260/280 and 260/230 absorbance ratios were identified using NanoDrop1000 (Thermo Fisher Scientific, Wilmington, DE) and RNA Integrity Number (RIN) was determined using an Agilent Bioanalyzer 2100 (Agilent Technologies, Waldbronn, Germany). RNA-Seq was performed at the JP

Sulzberger Columbia Genome Center (Columbia University, NY, NY). Poly-A purified RNA was used with the TruSeq RNA Sample Prep Kit v2 from total RNA having a RIN ≥ 8.0 . Libraries were sequenced on an Illumina HiSeq 2500 with a read depth of 30 million, 100 bp single-end reads. The resulting fastq files were subject to the following bioinformatics pipeline. The reads were mapped to the mouse genome (mm10) with Tophat v2.0 (<http://ccb.jhu.edu/software.shtml>) then differences in gene expression were determined using Cuffdiff and evaluated according to drug treatment and genetic strain.

RNA-Seq Data quality and differential gene expression.

The quality control plotting methods Principle Component Analysis (PCA) and Volcano plot were conducted using R (Pumpkin Helmet v3.2.2). PCA as a dimensionality reduction strategy was used to explore the relationship between the different treatment groups and strains comparing two directions (PC1 and PC2) to identify which direction the data have the most spread (Trapnell et al., 2012). Volcano plot was carried out to visualize the relationship between the fold change and the significance by comparing \log_2 (Fold Change) to \log_{10} (statistical relevance) (Trapnell et al., 2012). Differences in gene expression were evaluated according to drug treatment and genetic strain. Fastq files were aligned to the mouse genome (mm10) using TopHat (v2.1.0) and Bowtie (v1.1.2) (<http://ccb.jhu.edu/software.shtml>) and mapped reads were submitted to Cufflinks (v2.2.1) using the default settings. The assembled transcript files were quantified by Cuffdiff and then indexed and visualized using CummeRbund (v2.12.0). To

initiate the Venn diagrams, differentially expressed gene lists were put into Venny 2.0.2 (<http://bioinfoqp.cnb.csic.es/tools/venny/>) that created the gene categories A-G in Figure 2.

Pathway Analyses.

Resulting gene lists from the Venn categories (A-G) were analyzed for biological relevance by Ingenuity Pathway Analysis (IPA). In addition, differentially expressed gene lists were evaluated for gene ontology and KEGG pathway enrichment analysis using DAVID (v6.7) (Huang et al., 2009). In both approaches, statistical significance of gene enrichment was $p < 0.05$.

Integrated Genome Viewer (IGV) (v2.3) was used to confirm the deletion of the *Gcn2* and *Atf4* genes (<https://www.broadinstitute.org/igv/v1.2>).

Heat maps.

Heat maps (Fig 2C-D) show the level of significance of pathways across multiple gene sets. The $-\log_{10}$ of P values represent the statistical significance values were color-indexed (white for no significance to dark red for the highest significance) (Han et al., 2013). Heat map (Fig 2E, Fig 3B) were generated in R using cummeRbund for the purpose of visualizing differentially expressed genes (Trapnell et al., 2012).

Hepatic mRNA expression levels by Reverse Transcriptase Quantitative PCR.

Total RNA was extracted as described above. 1µg of purified RNA was reverse transcribed using the High-Capacity cDNA Reverse Transcription Kit (Applied Biosystems, Foster City, CA). Relative mRNA expression levels were determined by quantitative PCR using TaqMan reagents and the StepOnePlus Real-Time PCR System (Applied Biosystems, Foster, CA). Each mRNA from a single biological sample was measured in triplicate and normalized to 18S ribosomal RNA. Results were obtained by the comparative Ct (cycle threshold) method and are expressed as fold change with respect to the experimental control as previously detailed (Wilson et al., 2013).

Immunoblot Analysis.

Tissue lysates were prepared as previously described (Wilson et al., 2015; Bunpo et al., 2009). The following primary antibodies were purchased from Cell Signaling Technology (Beverly, MA): phospho-eIF2α (#3597); phospho-Akt Thr308 (#9275); total AKT (#9272); phospho-P70S6K Thr389 (#9205); total P70S6K (#9202); phospho-PERK Thr980 (#3179); total PERK (#3192); and GAPDH (#2118). Other primary antibodies included: total eIF2α (#sc11386, Santa Cruz Biotechnology, Dallas, TX); 4EBP1 (#A300-501A, Bethyl Laboratories, Montgomery, TX); and SESN2 (#10082-224, ProteinTech, Rosemont, IL). Immunoblot membranes were processed and developed using enhanced chemiluminescence (Amersham Biosciences, Pittsburgh, PA). Chemiluminescence signal intensities were digitally captured using a FluorChem

M multiplex imager (Protein Simple) and band densities were quantitated using Carestream Molecular Imaging Software (version 5.0).

Histology.

A portion of each fixed liver sample was paraffin-embedded and sections (5 μ M) were stained with hematoxylin, counterstained with eosin, dehydrated and mounted for light microscopy observation and also evaluated for DNA fragmentation by TUNEL assay as described (Bunpo et al., 2010). Frozen sections from fixed liver were stained with Oil Red O to visualize neutral lipid content (Wilson et al., 2013). Liver triglycerides were also measured biochemically using a commercially available kit (Biovision).

Statistical Analysis.

Global transcriptome analyses (n=3 per group) were conducted in R using cummeRbund. Differentially expressed genes were considered to be statistically significant when the q value (or False Discovery Rate, FDR) was < 0.1 (unadjusted $p < 0.017$). All other measurements utilized 4-8 animals per group and are reported as means \pm SEM. Differences between treatment groups were analyzed by two-way ANOVA, with strain and drug as independent variables and a level of significance, $p < 0.05$ (STATISTICA; StatSoft, Tulsa, OK). When an overall significance was detected, differences among individual means were evaluated using Tukey's post-hoc test.

Results

Atf4^{-/-} and Gcn2^{-/-} mice share somatic but not tissue-specific responses to ASNase.

I sought to understand the role of ATF4 relative to GCN2 in liver adaptation to ASNase treatment. To accomplish this, I injected ASNase at 3 international units per gram body weight (3 IU/g BW) into WT, *Gcn2^{-/-}*, and *Atf4^{-/-}* mice once daily for 8 days using phosphate buffered saline (PBS) as a control. Before treatment commenced, *Atf4^{-/-}* mice had significantly less fat mass than WT and *Gcn2^{-/-}* mice (Fig. 1A), that is consistent with its reported lean phenotype (Seo et al., 2009). Following ASNase treatment, WT mice experienced minimal change in body weight (Fig. 1B) and body composition (Fig. 1C-D) but *Atf4^{-/-}* and *Gcn2^{-/-}* mice both lost substantial amounts of body weight and body fat without altering lean mass. Compared to WT mice, ASNase also increased liver and pancreas mass and reduced spleen mass in *Gcn2^{-/-}* mice (Fig. 1E) in accordance with previous observations (Phillipson-Weiner et al., 2016; Bunpo et al., 2010; Wilson et al., 2015). However, none of the ASNase-induced effects were observed in *Atf4^{-/-}* mice and organ/tissue masses resembled WT.

ATF4 and GCN2 control overlapping patterns of hepatic gene expression during ASNase.

I performed transcriptional profiling of poly-A mRNA via massively parallel sequencing of cDNA (RNA-seq) to further define the role of ATF4 and GCN2 in liver in response to ASNase. To accomplish this, total RNA was extracted from

liver of WT, *Gcn2*^{-/-} and *Atf4*^{-/-} mice treated with ASNase or PBS excipient. After RNA-Seq, I examined data quality by examining the percentages of mapped reads and evaluated fragments per kilobase of transcript per million mapped reads (FPKM) values for isoforms, transcripts and annotated genes. Next, I confirmed the *Gcn2*^{-/-} and *Atf4*^{-/-} deletions at the genome level (Fig. 2A-C). I also assessed the degree of global changes in gene expression among the samples visualized as cross-comparison Volcano plots (Fig. 2D). Furthermore, Principle Component Analysis indicated that livers from ASNase-treated *Atf4*^{-/-} and *Gcn2*^{-/-} mice were quite different from the other samples indicating ASNase caused a considerable change in gene expression (Fig. 2E).

A comparative examination of PBS-injected mice by Venn analysis showed many hepatic genes required *Gcn2* and/or *Atf4* for basal expression (Fig 2F). I found 545 genes were dependent (either directly or indirectly) on GCN2 while 408 genes required ATF4 relative to WT PBS-treated controls with 263 shared between *Gcn2*^{-/-} and *Atf4*^{-/-} (category B). Pathway analyses of genes within the three categories indicated that many of the effected biological processes were shared; among them were stellate cell activation of hepatic fibrosis, complement cascades, activation of cytoplasmic nuclear binding proteins, calcium signaling, glycolysis and gluconeogenesis (Fig. 2G). Several pathways such as epithelial nitric oxide synthase signaling, the coagulation system, phagosome formation, and adipogenesis were predominantly associated with GCN2 whereas ATF4 was exclusively associated with processes including cholesterol biosynthesis, ketogenesis and the oxidative branch of the pentose

phosphate pathway. Thus, while the global influence of GCN2 in the non-stressed liver was largely mediated by ATF4, several key biological processes were unique to each protein. These findings indicate that both GCN2 and ATF4 function to regulate gene expression in the absence of apparent stress and that these key ISR regulators can serve partially in separate signaling pathways.

I also examined the effect of ASNase on hepatic gene expression by Venn analysis (ASNase versus PBS in each genetic strain) (Fig. 2H). In WT mice, ASNase altered expression of 525 genes compared to PBS; of these, 61% changed independent of GCN2 and ATF4 (category D). ASNase altered 2,508 genes in *Gcn2*^{-/-} mice whereas ASNase altered 3,786 genes in *Atf4*^{-/-} mice. Of these, 36% were common to loss of *Gcn2* or *Atf4* but not shared with WT (category F) while 36% of genes altered in *Gcn2*^{-/-} mice were not shared with *Atf4*^{-/-} or WT (category E) and 57% of genes altered in *Atf4*^{-/-} were not shared with *Gcn2*^{-/-} or WT (category G). Pathway analyses were performed on these specified gene categories to explore biological processes affected (Fig. 2I). These analyses identified signaling via peroxisome proliferator-activated receptor, p53, and AMPK and oxidative phosphorylation as altered by *Gcn2* status whereas loss of *Atf4* influenced signaling via eIF2, eIF4, p70S6K, ER stress and the UPR and tRNA charging were altered in the absence of ATF4. I also found that a variety of metabolic processes were misaligned in the absence of GCN2 or ATF4. For example, genes implicated in acute phase response, hepatic fibrosis, xenobiotic metabolism, mitochondrial dysfunction, nuclear factor

2 (NRF2)-mediated oxidative stress response, and cholesterol biosynthesis were altered in both *Gcn2*^{-/-} and *Atf4*^{-/-} mice.

An important cellular process altered by loss of *Gcn2* or *Atf4* independent of ASNase was nuclear receptor activation. Nuclear receptors control organismal development, metabolism and homeostasis by regulating the expression of specific genes (Kliwer et al., 2002; Kliwer et al., 2002b; Dossa et al., 2016). Gene ontology analysis revealed that pathways associated with retinoid x receptor (RXR), liver X receptor (LXR), pregnane x receptor (PXR) and vitamin D receptor (VDR) were altered by loss of GCN2 or ATF4. The relative expression changes of the nuclear receptor genes in WT, *Gcn2*^{-/-} and *Atf4*^{-/-}, with and without ASNase, is documented in the Heat map (Fig 2J). These findings indicate that defects in the GCN2-ATF4 AAR compromise expression of cytoplasmic nuclear receptors, especially during amino acid deprivation.

ATF4 and GCN2 differentially regulate the AAR in response to ASNase.

GCN2 is critical for activation of the AAR by ASNase in liver (Bunpo et al., 2009; Wilson et al., 2015; Wilson et al., 2013) but the role of its downstream effector ATF4 in the implementation of this pathway is unknown. To address this question, I first measured p-eIF2 and found that in contrast to loss of *Gcn2*, loss of *Atf4* amplified basal p-eIF2 and did not block induction of p-eIF2 by ASNase (Fig. 3A). A global view of the AAR was then crafted by creating a heat map of hepatic gene expression (Fig. 3B) (Shan et al., 2010). Clustering these data revealed three major AAR response patterns: 1) ASNase-induced elevations in

both *Gcn2*^{-/-} and *Atf4*^{-/-}, 2) ASNase-induced elevations in *Atf4*^{-/-} but not *Gcn2*^{-/-} and 3) ASNase-induced elevations in WT that were lost in both mutants *Gcn2*^{-/-} and *Atf4*^{-/-}. I used RT-qPCR to confirm individual genes within the three clusters of the AAR; *Sesn2* belonging to pattern 1 (Fig. 3C), *Asns* belonging to pattern 2 (Fig. 3D) and *Fgf21* belonging to pattern 3 (Fig. 3E). This gene cluster analysis indicates that the GCN2-activated AAR is mediated only partially through ATF4 and that ATF4 functions to limit activation of the AAR by ASNase.

Deletion of Atf4 promotes ER stress to ASNase.

Amplification of the AAR in ASNase-treated *Atf4*^{-/-} mice and ingenuity pathway analysis revealed that components of the ER stress pathway were highly enriched. To test this premise further, I measured phosphorylation of PERK and found no change by strain or drug, suggesting robust p-eIF2 by GCN2 in the *Atf4*^{-/-} animals (Fig 4A). However, another important measure of ER stress, Xbp1 mRNA splicing, was greatly elevated in ASNase-treated *Atf4*^{-/-} mice (Fig. 4B). Several other measures of ER stress, such as *Atf6* (Fig 4C) along with *Ddit3* (encoding CHOP) (Fig. 4D), were significantly increased, indicating partial engagement of the UPR.

GCN2 regulates mTORC1 independent of ATF4.

Mice lacking *Gcn2* show hyperactivation of mTORC1 in liver during ASNase alongside elevations in circulating branched chain amino acids (BCAA) leucine, isoleucine and valine (Bunpo et al., 2009; Wilson et al., 2013). I first

examined the phosphorylation state of S6K1 and 4E-BP1, which are downstream of mTORC1 to explore the connection among GCN2, ATF4, mTORC1 and BCAA in response to ASNase. Consistent with our previously published findings, phosphorylation levels of S6K1 and 4E-BP1 in liver were stable or even reduced by ASNase in WT but amplified in *Gcn2*^{-/-} mice (Fig. 5A-B, 5E). Recently, several reports attributed GCN2 regulation of mTORC1 to ATF4 (Ye et al., 2015; Wolfson et al., 2016; Ding et al., 2016). In contrast with this idea, mTORC1 signaling was repressed in *Atf4*^{-/-} similar to WT. To understand the underlying mechanism, I measured signaling via the upstream protein kinase B/Akt (p-Thr308). ASNase treatment reduced Akt phosphorylation levels in both *Gcn2*^{-/-} and *Atf4*^{-/-} whereas WT remained relatively constant (Fig. 5C, 5E), indicating that this was not a determining effector. I also examined Sestrin2 phosphorylation that inversely correlates with mTORC1 activity during leucine deprivation (Kimball et al., 2016). Consistent with this idea, ASNase increased Sestrin2 phosphorylation in liver of WT mice; however, Sestrin2 phosphorylation also increased in ASNase-treated *Gcn2*^{-/-} and to an even larger extent in ASNase-treated *Atf4*^{-/-} mice (Fig. 5D-E). These results suggest that neither Sestrin2 phosphorylation nor ATF4 are required for hepatic mTORC1 inhibition to amino acid deprivation by ASNase. Accordingly I conclude that in response to ASNase, GCN2 regulates mTORC1 independent of ATF4.

Heterozygous loss of ATF4 promotes hepatic ER stress and apoptosis to ASNase.

Atf4^{-/-} mice exhibit pleiotropic phenotypes of reduced growth, lack of vision, and defects in hematopoiesis and glucose homeostasis (Tanaka et al., 1998; Masuoka et al., 2002; Yoshizawa et al., 2009). In contrast, *Atf4* heterozygotes (*Atf4*^{+/-}) appear normal and healthy. I examined the effects of ASNase on *Atf4*^{+/-} mice compared to WT and *Atf4*^{-/-} to understand if ATF4 heterozygosity altered hepatic AAR activation and/or hepatotoxicity to ASNase. Prior to treatment, *Atf4*^{-/-} but not *Atf4*^{+/-} mice were leaner than *Atf4*^{+/+} mice (Fig. 6A). ASNase reduced body weight in all strains, with *Atf4*^{+/-} mice displaying body weights that were intermediate between *Atf4*^{+/+} and *Atf4*^{-/-} mice (Fig. 6D). *Atf4*^{+/-} mice were similar to *Atf4*^{+/+} in body composition following PBS or ASNase injections (Fig. 6B-C). Only *Atf4*^{-/-} mice displayed reduced body fat following ASNase. ASNase did not significantly alter liver or pancreas mass but reduced spleen weight in *Atf4*^{+/+}, *Atf4*^{+/-} and *Atf4*^{-/-} mice (Fig. 6E).

ASNase elevated liver triglycerides in all strains but the increase in *Atf4*^{-/-} mice was reduced relative to *Atf4*^{+/+} and *Atf4*^{+/-} mice (Fig. 6F-G). Liver sections from *Atf4*^{+/-} mice showed a high level of DNA fragmentation that was intermediate between *Atf4*^{+/+} and *Atf4*^{-/-} mice, indicating greater hepatic stress both basally and following ASNase (Fig. 6H-I). Consistent with this idea, basal p-eIF2 levels in *Atf4*^{+/-} livers were elevated relative to *Atf4*^{+/+} and ASNase further increased p-eIF2 to levels equivalent to *Atf4*^{-/-} mice (Fig. 6J). In addition, livers from *Atf4*^{+/-} mice treated with ASNase expressed *Atf4*, *Ppp1r15a*, and *4ebp1* greater than *Atf4*^{+/+} while *Atf5* was expressed equal to that measured in *Atf4*^{-/-} mice, reflecting aggravated, maladaptive AAR induction (Fig. 6K-L). In contrast, livers from *Atf4*^{+/-}

mice treated with ASNase expressed *Fgf21* similar to livers from *Atf4*^{+/-} mice indicating that one *Atf4* allele was sufficient to fully rescue loss of *Fgf21* expression. Nonetheless, the overall amplified AAR induction in livers from *Atf4*^{+/-} mice treated with ASNase corresponded with elevated ER stress. Similar to the *Atf4*^{-/-}, ASNase-treated *Atf4*^{+/-} mice showed increased *Ddit3* and *Atf6* mRNA expression, along with *Xbp1* mRNA splicing compared with its own PBS controls and increased *Hspa5* mRNA expression as compared to *Atf4*^{+/-} PBS (Fig. 7A-C). Gene expression of *Nrf2*, a marker of oxidative stress that is also identified as an ATF4 interacting protein (He et al., 2001), was also elevated in ASNase-treated *Atf4*^{+/-} livers above ASNase-treated *Atf4*^{+/-} livers (Fig. 7D), indicating that heterozygosity of ATF4 is partially alleviated by an increase in *Atf4* expression, but there remains an altered AAR and greater hepatic stress.

Discussion

Liver dysfunction as a result of oxidative stress and hepatic steatosis is an ASNase-associated adverse event that complicates remission induction and reduces treatment success (Bunpo et al., 2009, 2010, Wilson et al., 2013, 2015). A maladaptive GCN2-eIF2-AAR was previously described by our laboratory as a molecular basis for metabolic complications by ASNase (Reinert et al., 2006; Bunpo et al., 2009; Seo et al., 2009; Wilson et al., 2013) but the role of ATF4 in this process is unknown. Herein I present a global view of how loss of GCN2 or ATF4 alters the liver transcriptome basally and during ASNase treatment. I identify cytoplasmic nuclear receptors linked to the regulation of cellular

metabolism as novel targets of the GCN2-ATF4 pathway. I find that coordination of mTORC1 signaling by GCN2 does not require ATF4 or Sestrin2. Finally, I also find that both total and partial loss of *Atf4* expression is unable to self-limit the adaptive AAR to ASNase, resulting in ER stress and greater cell death. These findings challenge prevailing ideas on ATF4 function and add new mechanistic insight into how the liver adapts to AA deprivation.

ATF4 is a master regulator of metabolism and thermogenesis in ways that are for the most part mysterious. Global deletion of *Atf4* increases energy expenditure, resulting in a lean phenotype, and compromises eye and bone development (Seo et al., 2009; Tanaka et al., 1998; Masuoka et al., 2002; Wang et al., 2012). At least one report attributes metabolic control by ATF4 to its expression in osteocytes (Yoshizawa et al., 2009) but other studies using mice harboring a liver-specific deletion of ATF4 show that its expression in liver plays important roles in regulating cholesterol and lipid metabolism as well as oxidative stress responses (Li et al., 2016). This study provides the first global view of the hepatic transcriptome on the background of *Atf4* deletion and a first comparison to deletion of *Gcn2*.

The novel identification of nuclear receptors as ATF4 regulated gene products provides a mechanistic basis for how ATF4 regulates metabolism during AA deprivation. Among the noted differences, the identification of cytoplasmic nuclear receptor families, especially RXR, PXR and LXR, provides an important molecular clue explaining the downregulation of many metabolic pathways in *Gcn2*^{-/-} and *Atf4*^{-/-} mice. Biomolecular data mining using EVEX (evexdb.org)

indicates that ATF4 binds LXR, PXR and RXR and coregulates multiple gene families; many of these encode transcriptional and translational responses to ER and oxidative stress in addition to cellular metabolism. PXR/RXR activation is important in xenobiotic metabolism, lipid metabolism and cholesterol homeostasis (Kliwer et al., 2002a). This pathway in combination with short homologue partner (SHP; gene name Nr0b2) determines the rate of bile acid synthesis (Watanabe et al., 2004; Beuers et al., 2015). A previous transcriptional profiling analysis reported that downregulation of nuclear receptors that regulate xenobiotic and cellular metabolism is an underlying cause of hepatotoxicity to methapyrilene-induced liver injury (Auman et al., 2007). The prevailing data suggest ASNase-associated hepatotoxicity is related to AAR-driven expression of key cytoplasmic nuclear receptors that function to support hepatic metabolism and detoxification during AA stress.

Mice lacking *Gcn2* do not show evidence of hepatic ER stress to ASNase (Reinert et al., 2006; Seo et al., 2009; Wilson et al., 2013). In contrast, ER stress is significantly upregulated in the liver of *Atf4*^{-/-} mice. These results suggest that ATF4 is necessary to limit the AAR and prevent activation of ER stress responses. Recently, we reported that in the absence of *Atf4*, ATF6 and CHOP assume auxiliary functions during pharmacological ER stress, driving the cell toward a maladaptive cell fate (Fusakio et al., 2016). These findings suggest that a maladaptive AAR in the cytosol can trigger select branches of the UPR. It is important to note that the PERK arm was not induced during this ER stress. Given that there is heightened p-eIF2 by GCN2 in ASNase-treated *Atf4*^{-/-} livers, this

finding may indicate that there are feedback systems that sense that can selectively thwart induction of PERK despite ER stress. This idea is consistent with a previous report showing that GCN2 kinase induces p-eIF2 in response to the ER stress inducer, hypoxia, in *Perk*^{-/-} cells (Liu et al., 2010). Furthermore, GCN2 serves as a redundant kinase in the absence of PERK activation to increase p-eIF2 under UPR conditions (Hamanaka et al., 2005). Our current results support these findings and define the need to more fully understand how the binding partners of ATF4 determine cellular outcome. This is especially important because loss of one *Atf4* allele aggravates ER stress by ASNase.

Hyperactivation of mTORC1 signaling is reported in *Gcn2* null mice upon AA deprivation (Bunpo et al., 2009; Wilson et al., 2013), leading to the hypothesis that GCN2 or another player in the ATF4-AAR coordinates amino acid sensing with mTORC1 signaling. One candidate is the phosphoprotein Sestrin2, an mTORC1 inhibitor regulated by ATF4 under conditions of AA deprivation or ER stress (Ye et al., 2015; Kimball et al., 2016; Ding et al., 2016). Under conditions of amino acid deficiency, Sestrin2 becomes highly phosphorylated, promoting its interaction with a complex that subsequently blocks lysosomal localization of mTORC1 (Bar-Peled et al., 2013). According to in vitro studies the phosphorylation of Sestrin2 is selectively induced by leucine deficiency, but not other essential amino acids and that there is a relation between the degree of Sestrin2 phosphorylation and the degree of mTORC1 inhibition (Kimball et al., 2016). Others report that methionine, and to a lesser extent isoleucine and valine also bind directly to Sestrin2 (Wolfson et al., 2016; Saxton et al., 2016).

Furthermore, glutamine deprivation activates Sestrin2 inhibitory effect toward mTORC1 in mouse embryonic fibroblasts (Ye et al., 2015). These studies in total suggest Sestrin2 serves as a regulator of the mTORC1 pathway by sensing the availability of specific amino acids (Wolfson et al., 2016). Our findings extend these published results by showing that in liver an increase in Sestrin2 phosphorylation by itself does not ensure mTORC1 inhibition and does not require GCN2 or ATF4.

In conclusion, the multifactored RNA-seq presented here is the first comprehensive dataset that explores the role of *Gcn2* and *Atf4* in genome-wide transcriptional control in liver of mice; both basally and under stress conditions as a model to understand the molecular basis of treatment failure in response to ASNase. Future areas of investigation include comparing the global transcriptional response in liver to other profiling modalities (i.e. proteomic or metabolic, and in normal tissues and/or cancer cell lines) and using this information to discover novel treatments or therapies to prevent metabolic toxicities to ASNase.

Literature Cited

- Adams, CM. Role of the transcription factor ATF4 in the anabolic actions of insulin and the anti-anabolic actions of glucocorticoids. *J Biol Chem.* 2007;282(23):16744-53.
- Averous, J., Lambert-Langlais, S., Mesclon, F., Carraro, V., Parry, L., Jousse, C., Bruhat, A., Maurin, A.-C., Pierre, P., Proud, C.G., et al. (2016). GCN2 contributes to mTORC1 inhibition by leucine deprivation through an ATF4 independent mechanism. *Sci. Rep.* 6, 27698.
- Anthony TG, Reiter AK, Anthony JC, Kimball SR, Jefferson LS. Deficiency of dietary EAA preferentially inhibits mRNA translation of ribosomal proteins in liver of meal-fed rats. *Am J Physiol Endocrinol Metab* 2001 Sep;281(3):E430-9. PMID: 11500297
- Auman JT, Chou J, Gerrish K, Huang Q, Jayadev S, Blanchard K, et al. Identification of genes implicated in methapyrilene-induced hepatotoxicity by comparing differential gene expression in target and nontarget tissue. *Environ Health Perspect* 2007;4:572- 8.
- Balasubramanian MN, Butterworth EA, Kilberg MS. Asparagine synthetase: regulation by cell stress and involvement in tumor biology. *Am J Physiol Endocrinol Metab.* 2013 Apr 15;304(8):E789-99.
- Bar-Peled L, Chantranupong L, Cherniack AD, Chen WW, Ottina KA, Grabiner BC, et al. A Tumor suppressor complex with GAP activity for the Rag GTPases that signal amino acid sufficiency to mTORC1. *Science.* 2013 May 31;340(6136):1100-6. doi: 10.1126/science.1232044. PMID: 23723238.
- Beuers U, Trauner M, Jansen P, Poupon R. New paradigms in the treatment of hepatic cholestasis: from UDCA to FXR, PXR and beyond. *Journal of Hepatology*, 62(1), pp.S25–S37. Available at: <http://linkinghub.elsevier.com/retrieve/pii/S0168827815001336>.
- Bunpo P, Cundiff JK, Reinert RB, Wek RC, Aldrich CJ, Anthony TG. The eIF2 kinase GCN2 is essential for the murine immune system to adapt to amino acid deprivation by ASNase. *J Nutr.* 2010 Nov;140(11):2020-7.
- Bunpo P, Dudley A, Cundiff JK, Cavener DR, Wek RC, Anthony TG. GCN2 protein kinase is required to activate amino acid deprivation responses in mice treated with the anti-cancer agent L-ASNase. *J Biol Chem.* 2009 Nov 20;284(47):32742-9

- Chen R, Zou Y, Mao D, Sun D, Gao G, Shi J, et al. The general amino acid control pathway regulates mTOR and autophagy during serum/glutamine starvation. *J Cell Biol.* 2014 Jul 21; 206 (2):173-82. doi: 10.1083/jcb.201403009.PMID: 25049270.
- Cullinan SB, Diehl JA. Coordination of ER and oxidative stress signaling: the PERK/Nrf2 signaling pathway. *Int J Biochem Cell Biol.* 2006 Mar;38(3):317-32.
- Dennis MD, Baum JI, Kimball SR, Jefferson LS. Mechanisms involved in the coordinate regulation of mTORC1 by insulin and amino acids. *J Biol Chem.* 2011 Mar 11;286(10):8287-96.
- Ding B, Parmigiani A, Divakaruni AS, Archer K, Murphy AN, Budanov AV. Sestrin2 is induced by glucose starvation via the unfolded protein response and protects cells from non-canonical necroptotic cell death. *Sci Rep.* 2016 Mar 2;6:22538.
- Dossa AY, Escobar O, Golden J, Frey MR, Ford HR, Gayer CP. Bile acids regulate intestinal cell proliferation by modulating EGFR and FXR signaling. *Am J Physiol Gastrointest Liver Physiol* 2016;2:G81- 92.
- Fusakio ME, Willy JA, Wang Y, Mirek ET, Al Baghdadi RJ, Adams CM, et al. Transcription factor ATF4 directs basal and stress-induced gene expression in the unfolded protein response and cholesterol metabolism in the liver. *Mol Biol Cell.* 2016 May 1;27(9):1536-51.
- Hamanaka RB, Bennett BS, Cullinan SB, Diehl JA. PERK and GCN2 contribute to eIF2alpha phosphorylation and cell cycle arrest after activation of the unfolded protein response pathway. *Mol Biol Cell* 2005;12:5493- 501.
- Han J, Back SH, Hur J, Lin YH, Gildersleeve R, Shan J, et al. ER-stress-induced transcriptional regulation increases protein synthesis leading to cell death. *Nat Cell Biol.* 2013 May;15(5):481-90.
- Harding HP, Zhang Y, Zeng H, Novoa I, Lu PD, Calfon M, et al. An integrated stress response regulates amino acid metabolism and resistance to oxidative stress. *Mol Cell.* 2003 Mar;11(3):619-33.
- He CH, Gong P, Hu B, Stewart D, Choi ME, Choi AM, et al. Identification of activating transcription factor 4 (ATF4) as an Nrf2-interacting protein. Implication for heme oxygenase-1 gene regulation. *J Biol Chem* 2001;24:20858- 65.

- Howlader N, Noone AM, Krapcho M: SEER Cancer Statistics Review (CSR) 1975-2013. Bethesda, Md: National Cancer Institute, 2015. Available online. Last accessed July 11, 2016.
- Huang da W, Sherman BT, Lempicki RA. Systematic and integrative analysis of large gene lists using DAVID bioinformatics resources. *Nat Protoc*. 2009;4(1):44-57.
- Kilberg MS, Balasubramanian M, Fu L, Shan J. The transcription factor network associated with the amino acid response in mammalian cells. *Adv Nutr*. 2012 May 1;3(3):295-306.
- Kilberg MS, Shan J, Su N. ATF4-dependent transcription mediates signaling of amino acid limitation. *Trends Endocrinol Metab*. 2009 Nov;20(9):436-43.
- Kimball SR, Gordon BS, Moyer JE, Dennis MD, Jefferson LS. Leucine induced dephosphorylation of Sestrin2 promotes mTORC1 activation. *Cell Signal*. 2016 Aug;28(8):896-906. doi: 10.1016/j.cellsig.2016.03.008. Epub 2016 Mar 21. PMID: 27010498.
- Kliewer SA, Goodwin B, Willson TM. The nuclear pregnane X receptor: a key regulator of xenobiotic metabolism. *Endocr Rev* 2002a;5:687- 702.
- Kliewer SA, Willson TM. Regulation of xenobiotic and bile acid metabolism by the nuclear pregnane X receptor. *J Lipid Res* 2002b;3:359- 64.
- Li K, Xiao Y, Yu J, Xia T, Liu B, Guo Y, et al. Liver specific gene inactivation of the transcription factor ATF4 alleviates alcoholic liver steatosis in mice. *J Biol Chem* 2016; pii: jbc.M116.726836. [Epub ahead of print].
- Liu Y, László C, Liu Y, Liu W, Chen X, Evans SC, et al. Regulation of G(1) arrest and apoptosis in hypoxia by PERK and GCN2-mediated eIF2alpha phosphorylation. *Neoplasia* 2010;1:61- 8.
- Masuoka HC, Townes TM. Targeted disruption of the activating transcription factor 4 gene results in severe fetal anemia in mice. *Blood*. 2002; 99(3):736-45.
- Offman MN, Krol M, Patel N, Krishnan S, Liu J, Saha V, Bates PA. Rational engineering of L-ASNase reveals importance of dual activity for cancer cell toxicity. *Blood* 2011;5:1614- 21.
- Panosyan EH, Grigoryan RS, Avramis IA, Seibel NL, Gaynon PS, Siegel SE, et al. Deamination of glutamine is a prerequisite for optimal asparagine deamination by ASNases in vivo (CCG-1961). *Anticancer Res*. 2004 Mar-Apr;24(2C):1121-5. PMID: 15154634

- Phillipson-Weiner L, Mirek ET, Wang Y, McAuliffe WG, Wek RC, Anthony TG. General control nonderepressible 2 deletion predisposes to ASNase-associated pancreatitis in mice. *Am J Physiol Gastrointest Liver Physiol*. 2016 Jun 1;310(11):G1061-70.
- Pieters R, Hunger SP, Boos J, Rizzari C, Silverman L, Baruchel A, et al. L-ASNase treatment in acute lymphoblastic leukemia: a focus on Erwinia ASNase. *Cancer*, 2011 Jan 15;117(2):238-49. doi: 10.1002/cncr.25489. Epub 2010 Sep 7. Review. PMID: 20824725
- Reinert RB, Oberle LM, Wek SA, Bunpo P, Wang XP, Mileva I, et al. Role of glutamine depletion in directing tissue-specific nutrient stress responses to L-ASNase. *Journal of Biological Chemistry*, 281(42), pp.31222–31233.
- Ribeiro RC, Pui CH. Saving the children--improving childhood cancer treatment in developing countries. *The New England journal of medicine*, 352(21), pp.2158–2160.
- Saxton RA, Knockenhauer KE, Wolfson RL, Chantranupong L, Pacold ME, Wang T, Schwartz TU, Sabatini DM. Structural basis for leucine sensing by the Sestrin2-mTORC1 pathway. *Science*. 2016 Jan 1;351(6268):53-8. doi: 10.1126/science.aad2087. Epub 2015 Nov 19.
- Seo J, Fortuno ES 3rd, Suh JM, Stenesen D, Tang W, Parks EJ, et al. Atf4 regulates obesity, glucose homeostasis, and energy expenditure. *Diabetes* 2009;11:2565-73.
- Shan J, Lopez MC, Baker HV, Kilberg MS. Expression profiling after activation of amino acid deprivation response in HepG2 human hepatoma cells. *Physiol Genomics*. 2010 May;41(3):315-27.
- Su N, Kilberg MS. C/EBP homology protein (CHOP) interacts with activating transcription factor 4 (ATF4) and negatively regulates the stress-dependent induction of the asparagine synthetase gene. *J Biol Chem*. 2008 Dec 12;283(50):35106-17.
- Tanaka T, Tsujimura T, Takeda K, Sugihara A, Maekawa A, Terada N, et al. Targeted disruption of ATF4 discloses its essential role in the formation of eye lens fibers. *Genes Cells*. 1998 Dec; 3 (12):801-10.
- Trapnell C, Roberts A, Goff L, Pertea G, Kim D, Kelley DR, Pimentel H, Salzberg SL, Rinn JL, Pachter L. Differential gene and transcript expression analysis of RNA-seq experiments with TopHat and Cufflinks. *Nat Protoc*. 2012 Mar 1;7(3):562-78.

- Wang W, Lian N, Ma Y, Li L, Gallant RC, Elefteriou F, et al. Chondrocytic Atf4 regulates osteoblast differentiation and function via Ihh. *Development* 2012; 3:601-11.
- Watanabe M, Houten SM, Wang L, Moschetta A, Mangelsdorf DJ, Heyman RA, et al. Bile acids lower triglyceride levels via a pathway involving FXR, SHP, and SREBP-1c. *J Clin Invest* 2004;10:1408- 18.
- Wilson GJ, Bunpo P, Cundiff JK, Wek RC, Anthony TG. The eukaryotic initiation factor 2 kinase GCN2 protects against hepatotoxicity during ASNase treatment. *Am J Physiol Endocrinol Metab* 2013 Nov 1;305(9):E1124-33.
- Wilson GJ, Lennox BA, She P, Mirek ET, Al Baghdadi RJ, Fusakio ME, et al. GCN2 is required to increase fibroblast growth factor 21 and maintain hepatic triglyceride homeostasis during ASNase treatment. *Am J Physiol Endocrinol Metab*. 2015 Feb 15;308(4):E283-93.
- Wolfson RL, Chantranupong L, Saxton RA, Shen K, Scaria SM, Cantor JR, et al. Sestrin2 is a leucine sensor for the mTORC1 pathway. *Science*. 2016 Jan 1;351(6268):43-8.
- Xiao G, Zhang T, Yu S, Lee S, Calabuig-Navarro V, Yamauchi J, et al. ATF4 protein deficiency protects against high fructose-induced hypertriglyceridemia in mice. *J Biol Chem*. 2013 Aug 30;288(35):25350-61.
- Ye J, Palm W, Peng M, King B, Lindsten T, Li MO, Koumenis C, Thompson CB. GCN2 sustains mTORC1 suppression upon amino acid deprivation by inducing Sestrin2. *Genes Dev*. 2015 Nov 15;29(22):2331-6.
- Yoshida H, Matsui T, Yamamoto A, Okada T, Mori K. XBP1 mRNA is induced by ATF6 and spliced by IRE1 in response to ER stress to produce a highly active transcription factor. *Cell*. 2001 Dec 28;107(7):881-91.
- Yoshizawa T, Hinoi E, Jung DY, Kajimura D, Ferron M, Seo J, et al. The transcription factor ATF4 regulates glucose metabolism in mice through its expression in osteoblasts. *J Clin Invest*. 2009 Sep;119(9):2807-17.
- Zhang P, McGrath BC, Reinert J, Olsen DS, Lei L, Gill S, Wek SA, Vatter KM, Wek RC, Kimball SR, Jefferson LS, Cavener DR. The GCN2 eIF2alpha kinase is required for adaptation to amino acid deprivation in mice. *Mol Cell Biol*. 2002 Oct;22(19):6681-8 .
- Zoncu R, Efeyan A, Sabatini DM. mTOR: from growth signal integration to cancer, diabetes and ageing. *Nat Rev Mol Cell Biol*. 2011 Jan;12(1):21-35.

Figure Captions

Figure 1. Whole body and tissue responses to ASNase. (A) Percent of body fat mass and percent of body lean mass was measured by EchoMRI before the treatment (day 0) in wildtype (WT), *Gcn2*^{-/-} and *Atf4*^{-/-} mice. (B) Percent of body fat mass change after 8 d of i.p. injection of PBS or ASNase. (C) Percent of body lean mass change after 8 d of i.p. injection of PBS or ASNase. (D) Percent body weight (BW) change in wildtype (WT), *Gcn2*^{-/-} and *Atf4*^{-/-} mice treated with 8 daily i.p. injections of PBS or ASNase (3 IU/g BW) and euthanized 8 h after the last injection. (E) Percent weight change of liver, pancreas, and spleen relative to BW. Data were analyzed by two-factor ANOVA, n=4-6 animals per group. Means without a common letter are statistically different (P<0.05).

Figure 2. Transcriptional profiling of livers from WT, *Gcn2*^{-/-} and *Atf4*^{-/-} mice treated with PBS or ASNase. Deletion of *Gcn2* and *Atf4* genes in mice. (A, B) Integrity Genome Viewer (IGV) plots show the absence of *Gcn2* and *Atf4* exons in *Gcn2*^{-/-} and *Atf4*^{-/-} mice respectively after being aligned to the mouse genome mm10. (C) Gene expression of *Atf4* measured by using RT-qPCR. Data represent n=3 per group. *Atf4* gene expression was analyzed by two-factor ANOVA, Means not sharing a common letter are different, P<0.05. (D) Volcano plot shows the genes that differ significantly (highlighted in red) among PBS and ASNase treatment conditions in wildtype (WT), *Gcn2*^{-/-} and *Atf4*^{-/-} mice treated with 8 daily intraperitoneal injections of PBS or ASNase (3 IU/g BW) and

euthanized 8 h after the last injection ($P < 0.05$). X-axis represents Log2 (fold change) and Y axis represents the $-\log(P\text{-value})$. (E) Principle Component Analysis (PCA) plot with X-axis represents PC1, the first component points in the direction of highest variance. The Y-axis represents PC2, the second component points in the direction of highest variance. (F) Venn diagram showing altered basal gene expression divided into three categories: unique to *Gcn2* deletion [A], unique to *Atf4* deletion [C] or common to deletion of either [B]. (G) Venn diagram showing categories of gene expression altered by ASNase including gene changes independent of the GCN2-ATF4-AAR [D]; those unique to *Gcn2*^{-/-} [E]; those unique to *Atf4*^{-/-} [G]; and those common to *Gcn2*^{-/-} and *Atf4*^{-/-} [F]. (H) IPA of basal gene expression categories A-C in above Venn diagram. (I) IPA of ASNase-induced gene expression categories D-G in the above Venn diagram. (J) Heat map of nuclear receptor gene expression. Data represent n=3 per group. All differentially expressed genes shown were statistically significant (q value or FDR < 0.1; unadjusted p < 0.017).

Figure 3. Loss of *Gcn2* or *Atf4* differentially alters the hepatic AAR to ASNase.

(A) Phosphorylation of eIF2 in liver by immunoblot analysis. (B) RNA-Seq expression data presented in a heat map clusters the hepatic AAR to ASNase into three categories: stable or increased gene expression in both *Gcn2*^{-/-} and *Atf4*^{-/-}, represented by *Sesn2* (C), elevated gene expression in *Atf4*^{-/-} but not in *Gcn2*^{-/-}, represented by *Asns* (D), and reduced expression in both *Gcn2*^{-/-} and *Atf4*^{-/-}, represented by *Fgf21* (E) Color scale shows genes with increased

expression (dark brown range) and decreased expression (light yellow range).

Gene expression in C-E was measured by RT-qPCR. Data were analyzed by two-factor ANOVA, $n=3$ per group. Means without a common letter are different, $P<0.05$.

Figure 4. Whole body deletion of *Atf4* induces genetic markers of hepatic ER stress following 8 d ASNase. (A) Phosphorylation of PERK in liver by immunoblot analysis. (B) Gene expression of spliced (*sXbp1*) and unspliced (*uXbp1*) Xbp1 measured by RT-qPCR. (C) Gene expression of *Atf6* measured by RT-qPCR. (D) Gene expression of *Ddit3* measured by RT-qPCR. Data were analyzed by two-factor ANOVA, $n=3$ per group. Means without a common letter are different, $P<0.05$.

Figure 5. Hepatic mTORC1 signaling is hyperactivated in response to ASNase in *Gcn2*^{-/-} but not *Atf4*^{-/-} mice. Densitometry of immunoblots for (A) Phospho-S6K1 at threonine 389 B) Phospho-4E-BP1 C) Phospho Akt at threonine 308 and D) Phospho Sestrin2. E) Representative immunoblots for panels A-D.

Figure 6. Heterozygous deletion of *Atf4* alters hepatic AAR and promotes cell death in response to ASNase. (A) Percentage of body fat and lean mass before the treatment (day 0) in wildtype (*Atf4*^{+/+}), *Atf4*^{+/-} and *Atf4*^{-/-} mice as measures by EchoMRI. (B) Percent of body fat mass change after 8 d of i.p. injection of PBS or ASNase. (C) Percent of body lean mass change after 8 d of intraperitoneal

injection of PBS or ASNase (D) Percent body weight (BW) change in *Atf4*^{+/+}, *Atf4*^{+/-} and *Atf4*^{-/-} mice treated with PBS or ASNase (daily i.p. injections of 3 IU/g BW for 8 days) and sacrificed 8 h after the last injection. (E) Percent weight change of liver, pancreas, and spleen relative to body weight. (F) Oil Red O stained liver sections (5μm) show neutral lipid accumulations, red dots. (G) Triglyceride concentrations in the livers of *Atf4*^{+/+}, *Atf4*^{+/-} and *Atf4*^{-/-} mice as measured by Triglyceride Quantification Colorimetric/Fluorometric assay. (H) Fragmented DNA visualization using TUNEL assay in liver sections (10μm). Images show visual features determined in 3-5 mice per group using X 20 objective in *Atf4*^{+/+}, *Atf4*^{+/-} and *Atf4*^{-/-} mice. (I) Apoptosis was ascertained by manual counting of TUNEL-positive nuclei using Image J software. (J) Phospho-eIF2 was measure by immunoblot analysis and quantified relative to total eIF2. (K) Gene expression of *Atf4* in liver as measured by RT-qPCR. (L) Gene expression of AAR genes *Asns*, *Atf3*, *Atf5*, *Fgf21*, *Eif4ebp1*, *Ppp1r15a* in *Atf4*^{+/+}, *Atf4*^{+/-} and *Atf4*^{-/-} mice. Data were analyzed by two-factor ANOVA, n=4-8 per group. Means not sharing a common letter are different, P<0.05.

Figure 7. Heterozygous loss of *Atf4* predisposes mice to ER stress when treated with ASNase. Expression of ER stress genes A) *Ddit3* (*Chop*) B) *Xbp1* splicing C) *Hspa5* and *Atf6* in liver was measured by RT-qPCR. D) Expression of oxidative stress marker *Nrf2* in liver was measured by RT-qPCR. Data were analyzed by two-factor ANOVA, n=4-8 per group. Means not sharing a common letter are different, P<0.05.

Figures

Figure 1

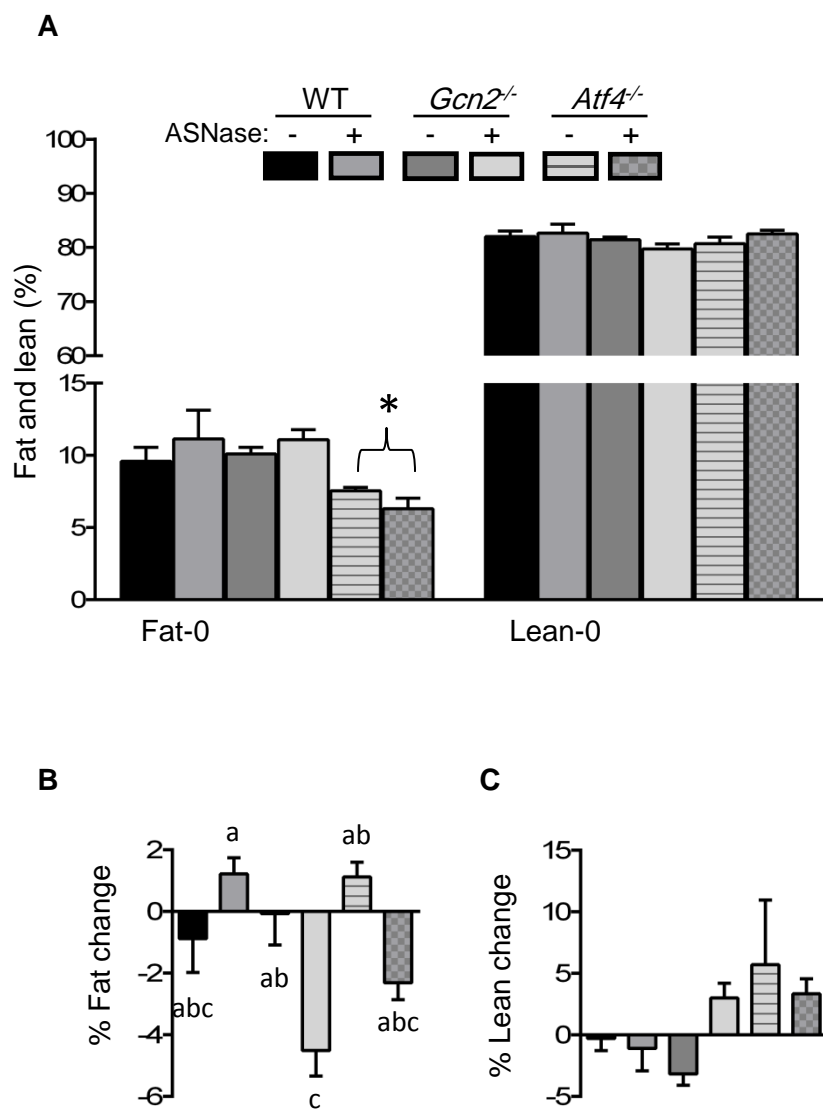
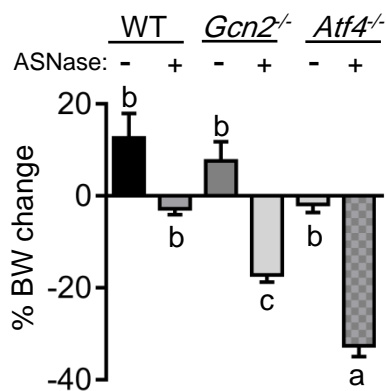


Figure 1

D



E

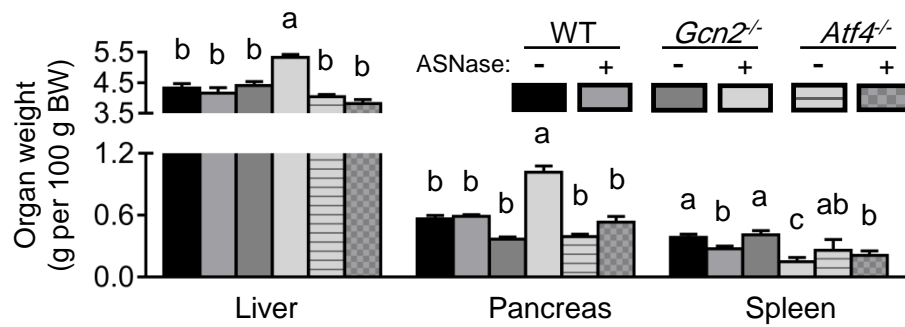
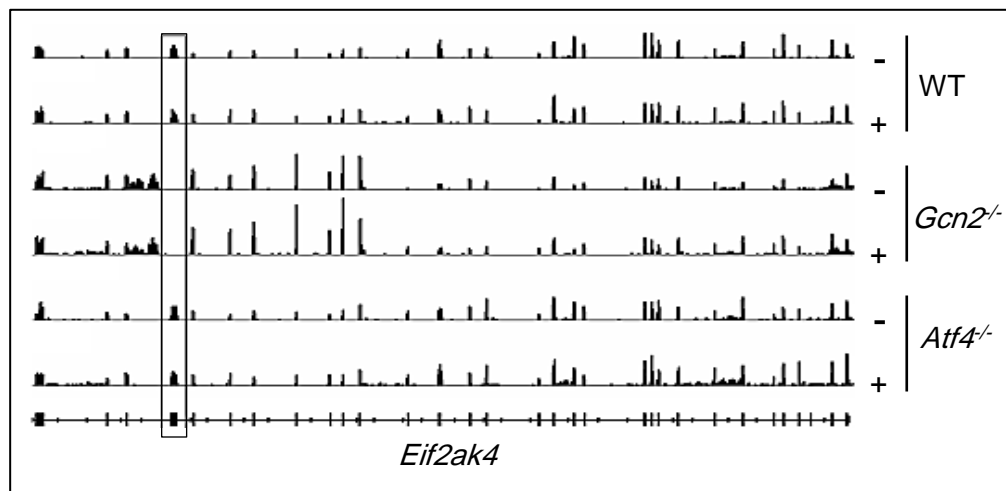
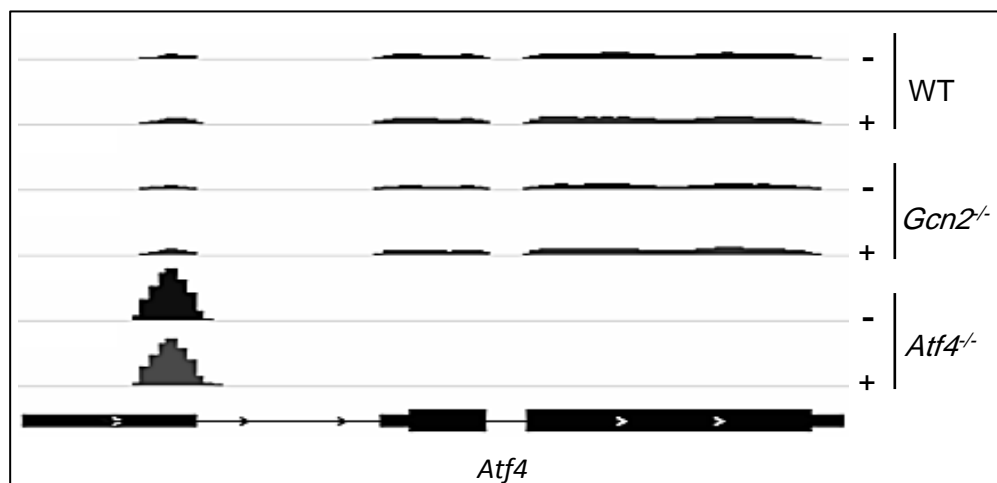


Figure 2

A



B



C

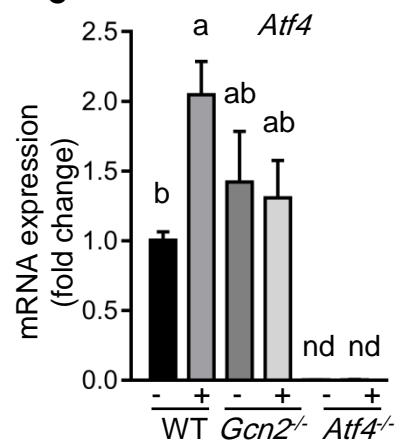


Figure 2

D

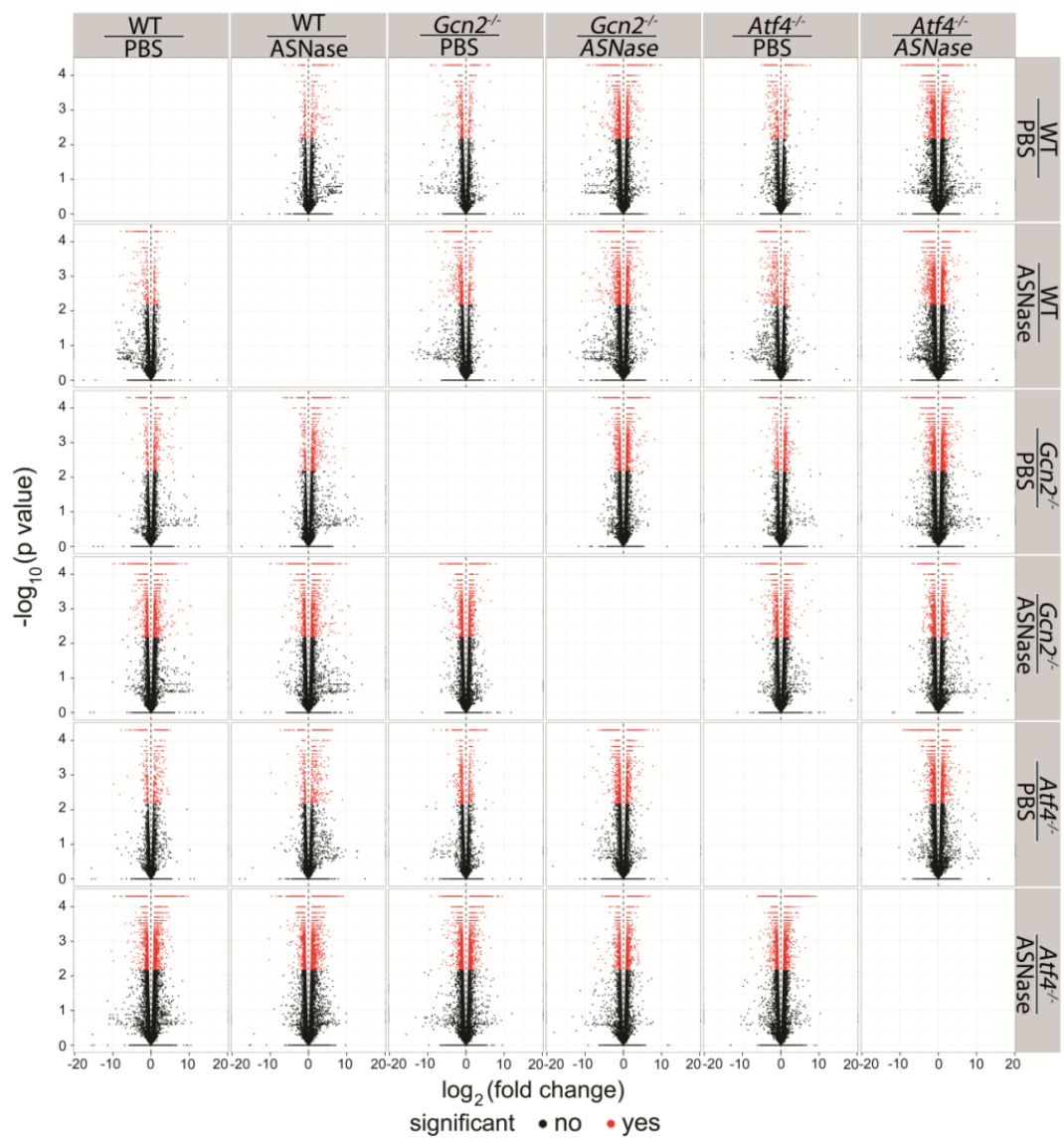
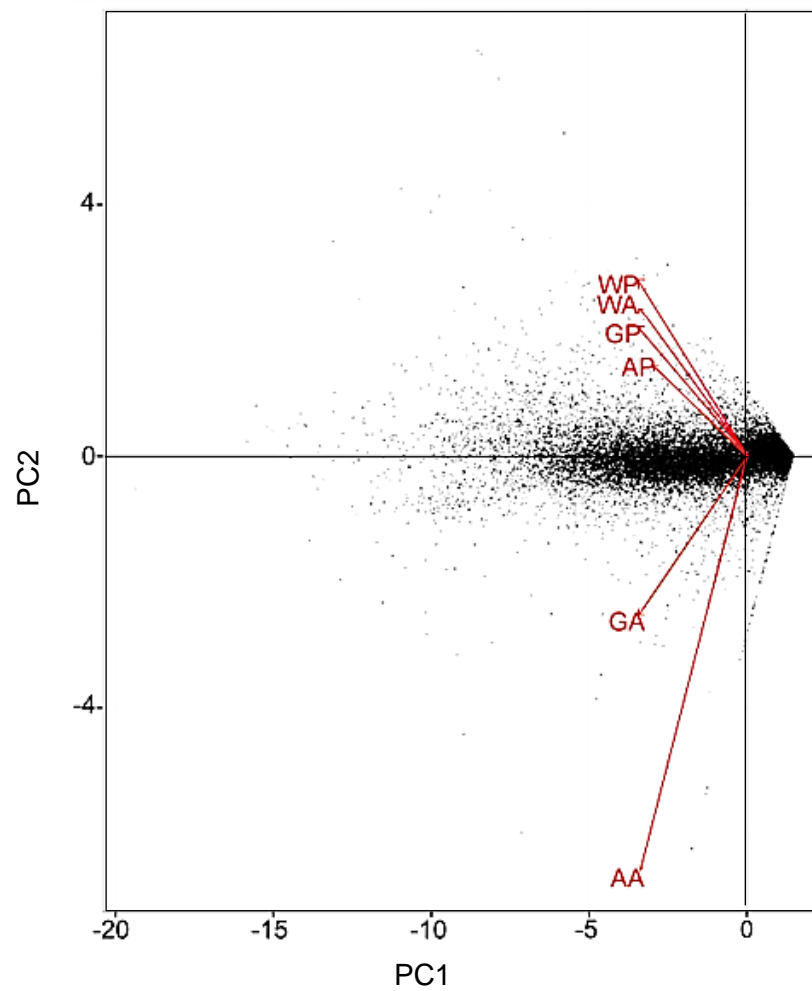


Figure 2

E



WP = WT mice treated with PBS

WA = WT mice treated with ASNase

GP = *Gcn2*^{-/-} mice treated with PBS

GA = *Gcn2*^{-/-} mice treated with ASNase

AP = *Atf4*^{-/-} mice treated with PBS

AA = *Atf4*^{-/-} mice treated with ASNase

Figure 2

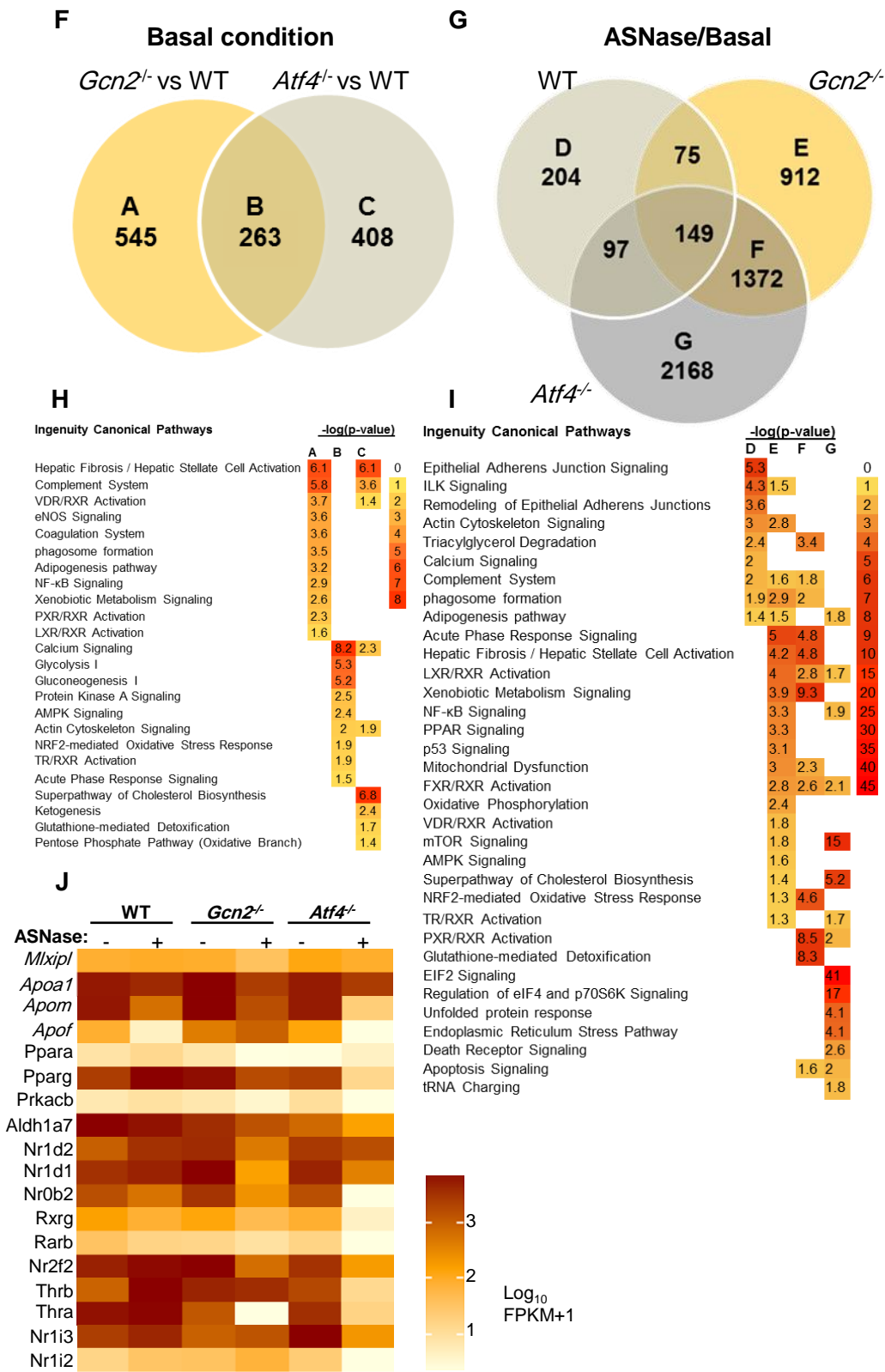


Figure 3

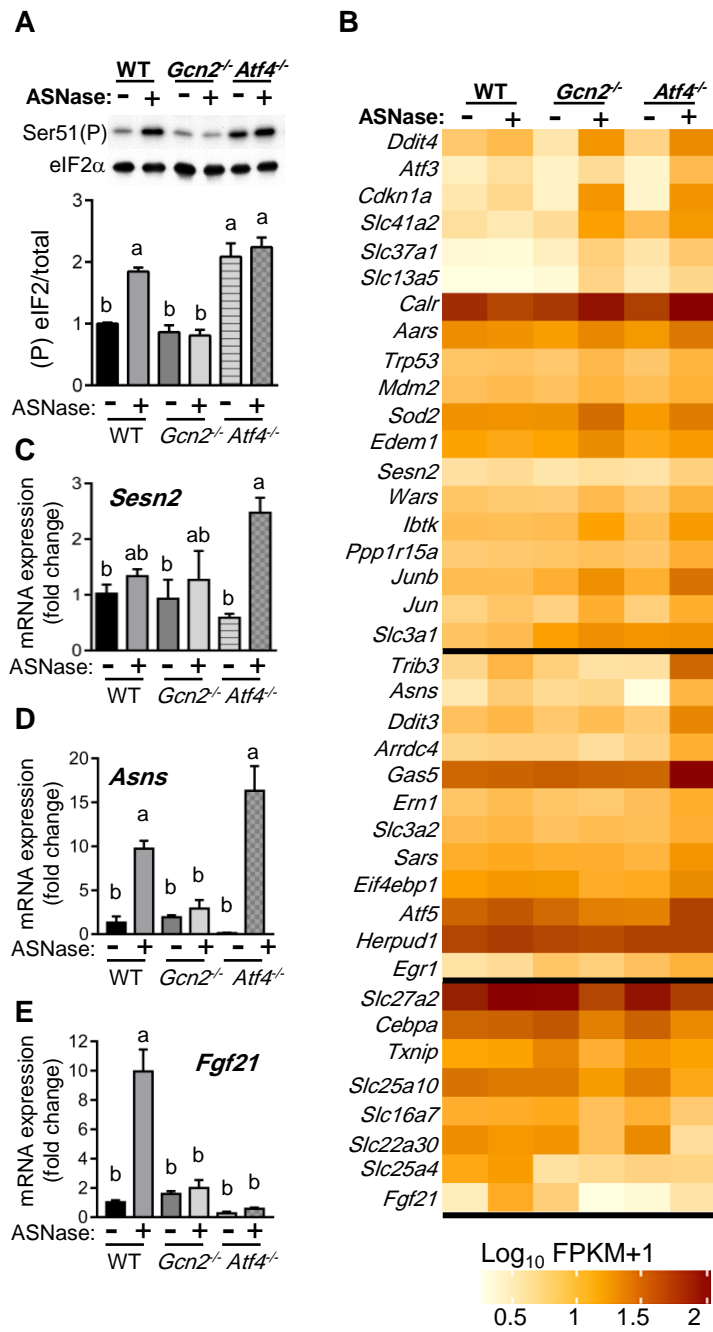


Figure 4

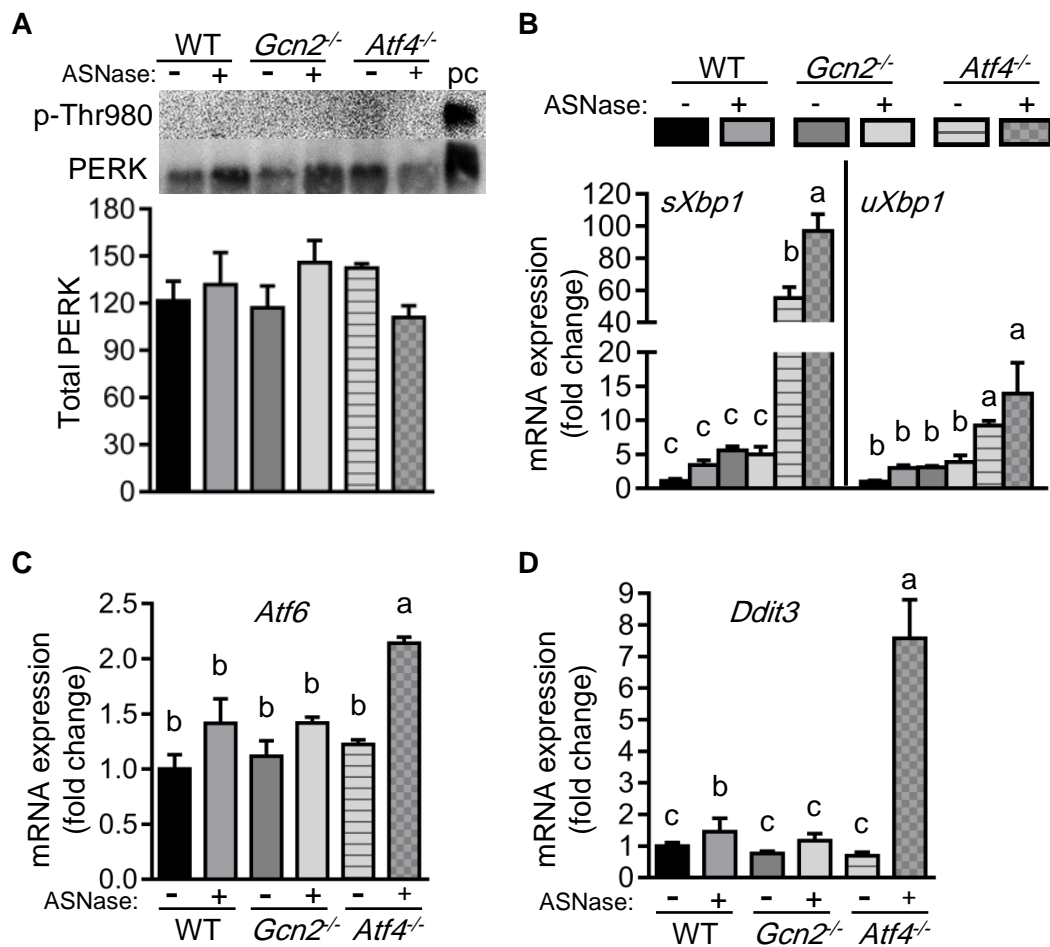


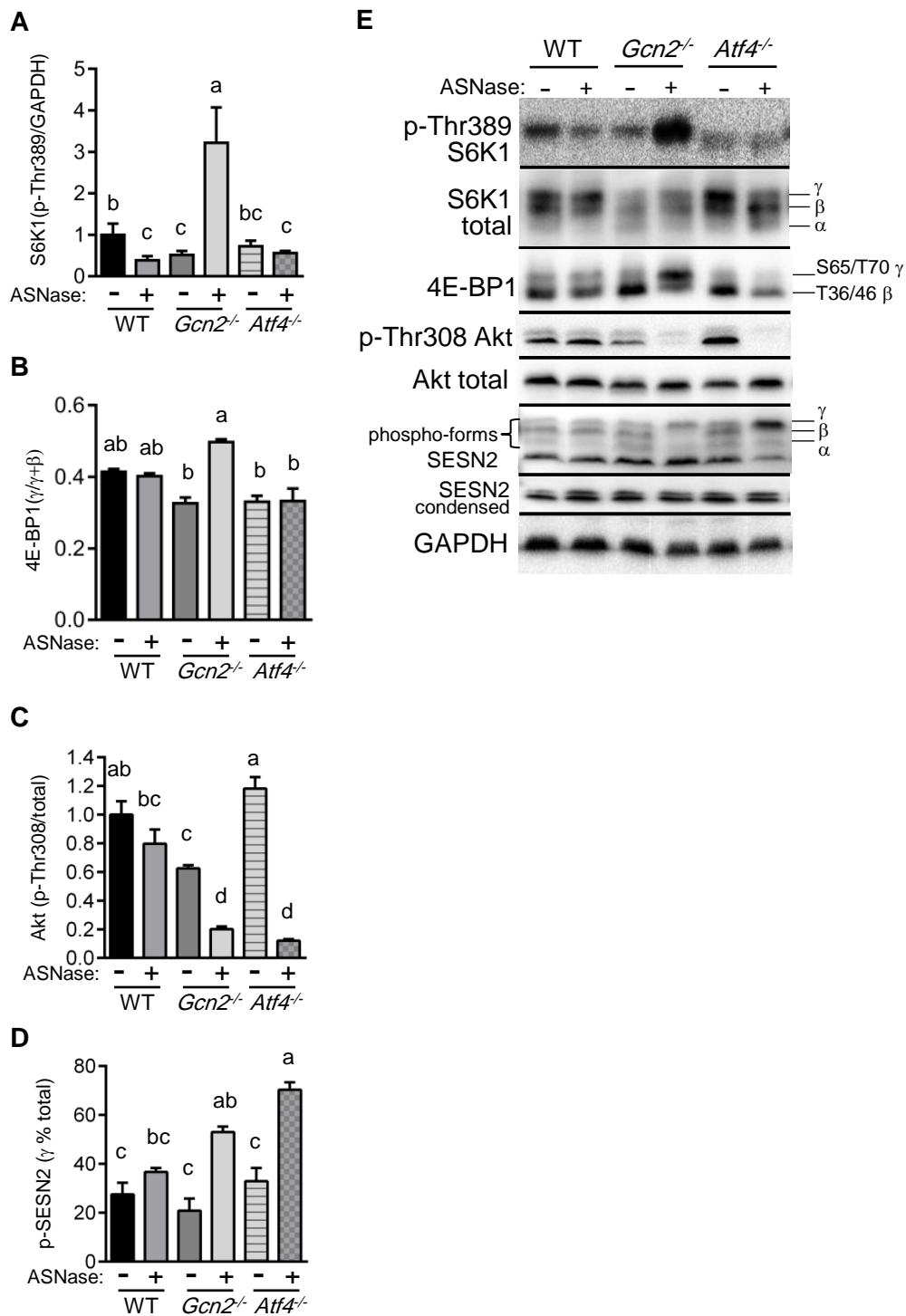
Figure 5

Figure 6

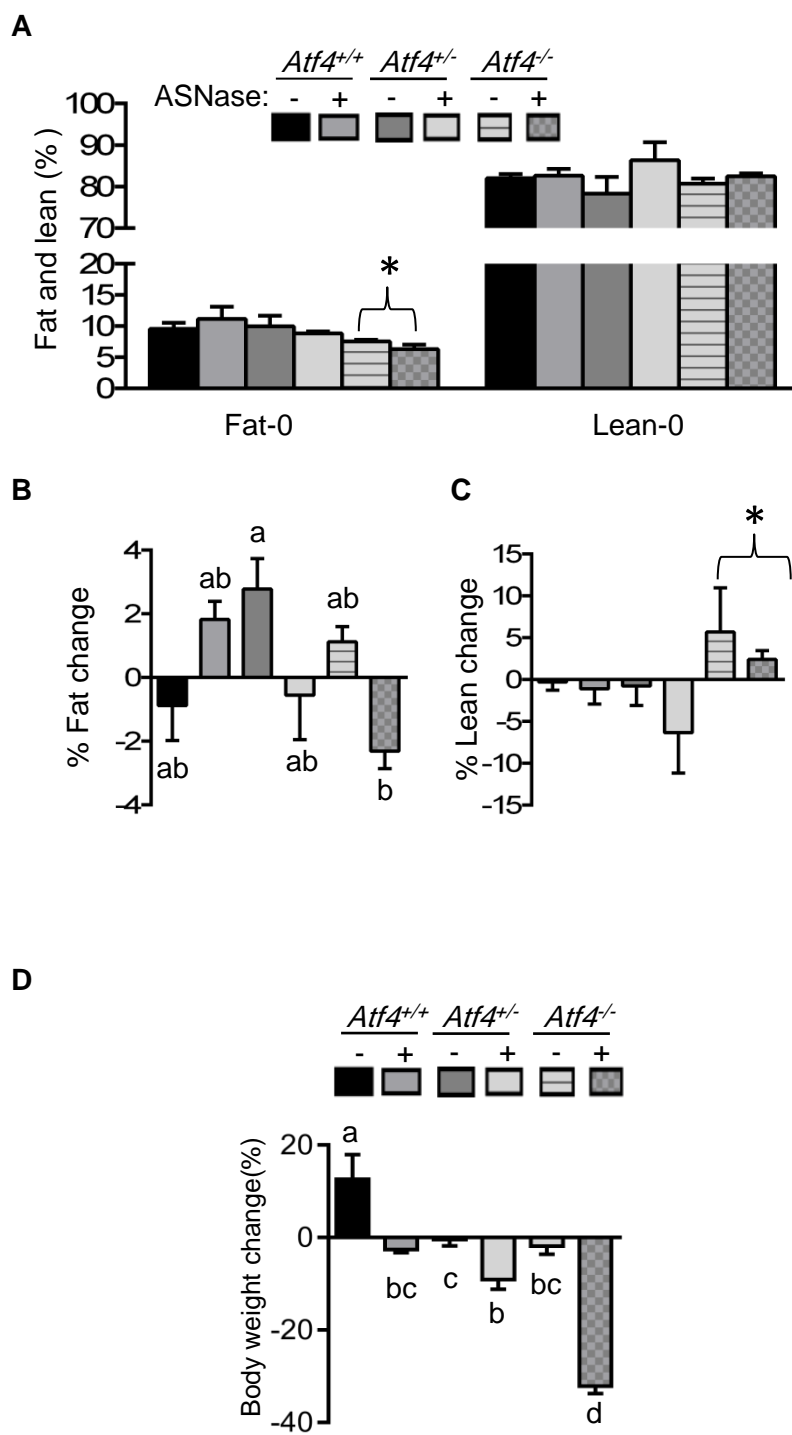


Figure 6

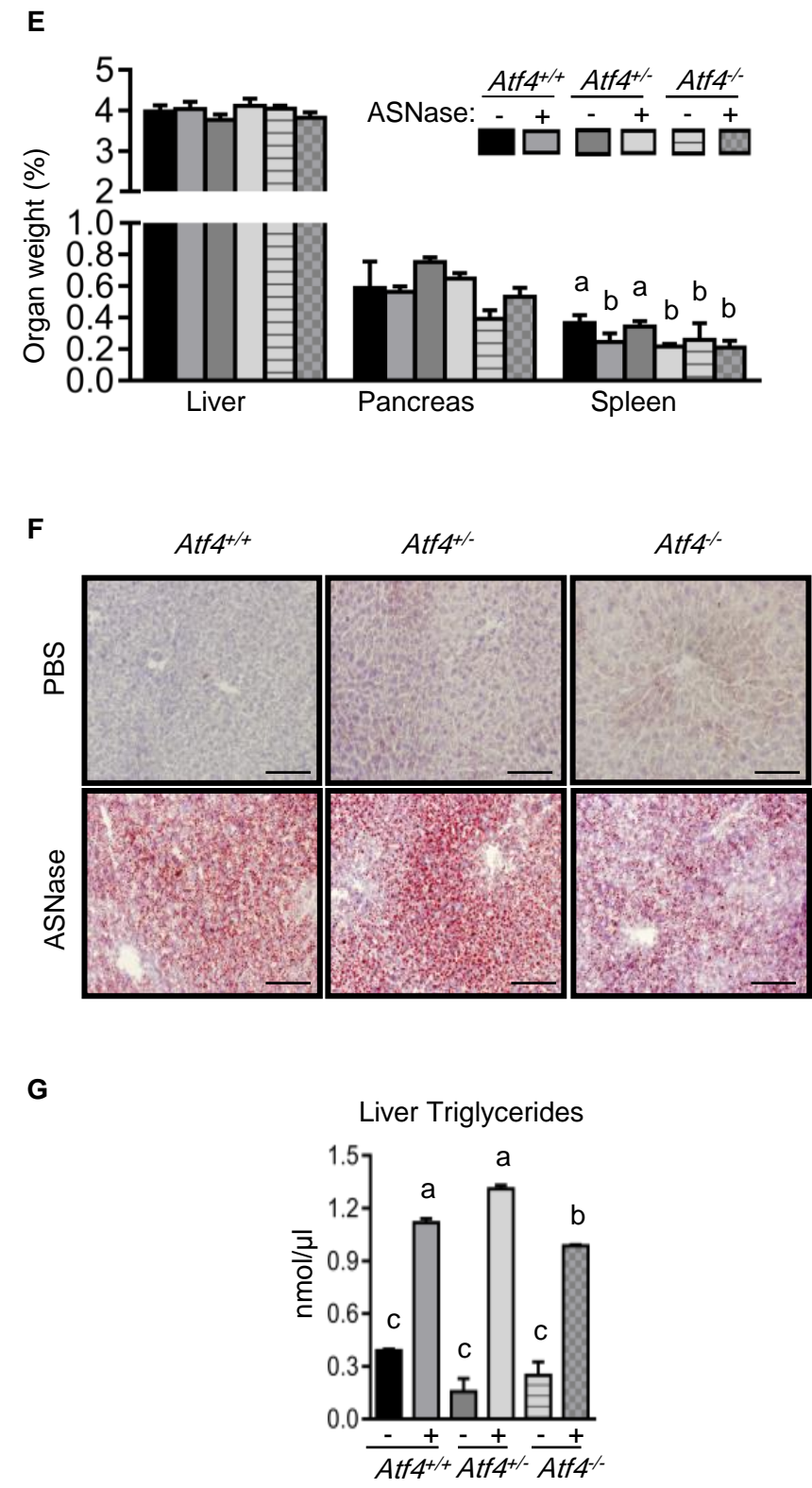
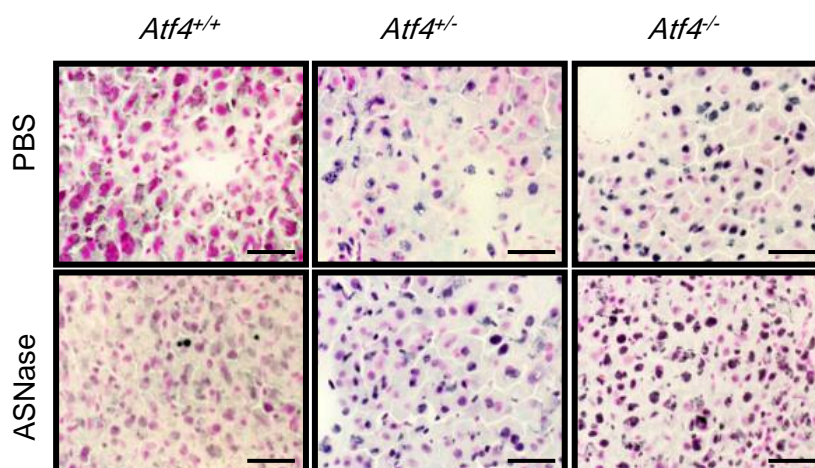


Figure 6

H



I

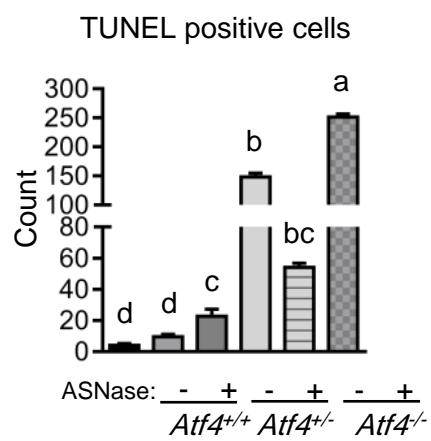


Figure 6

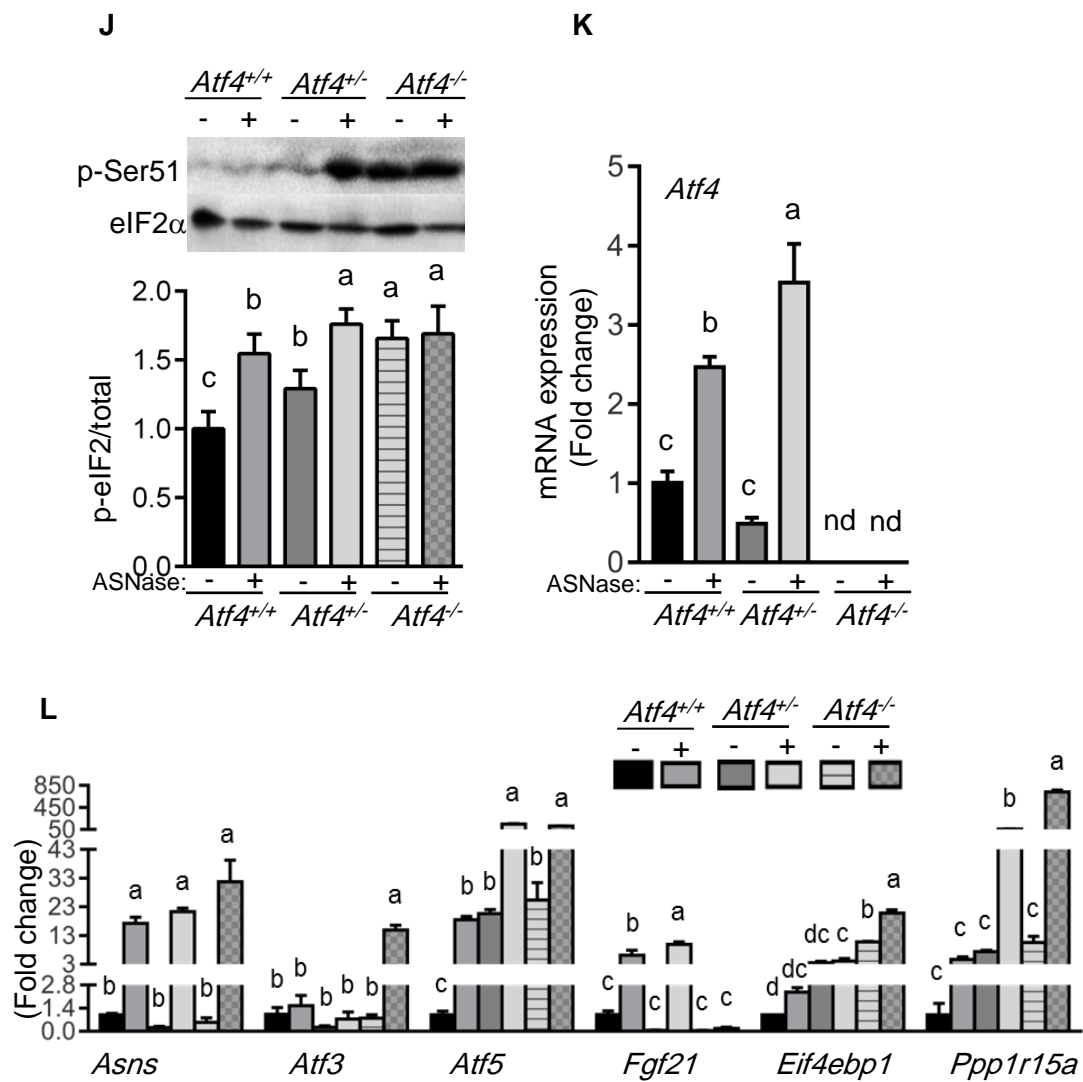
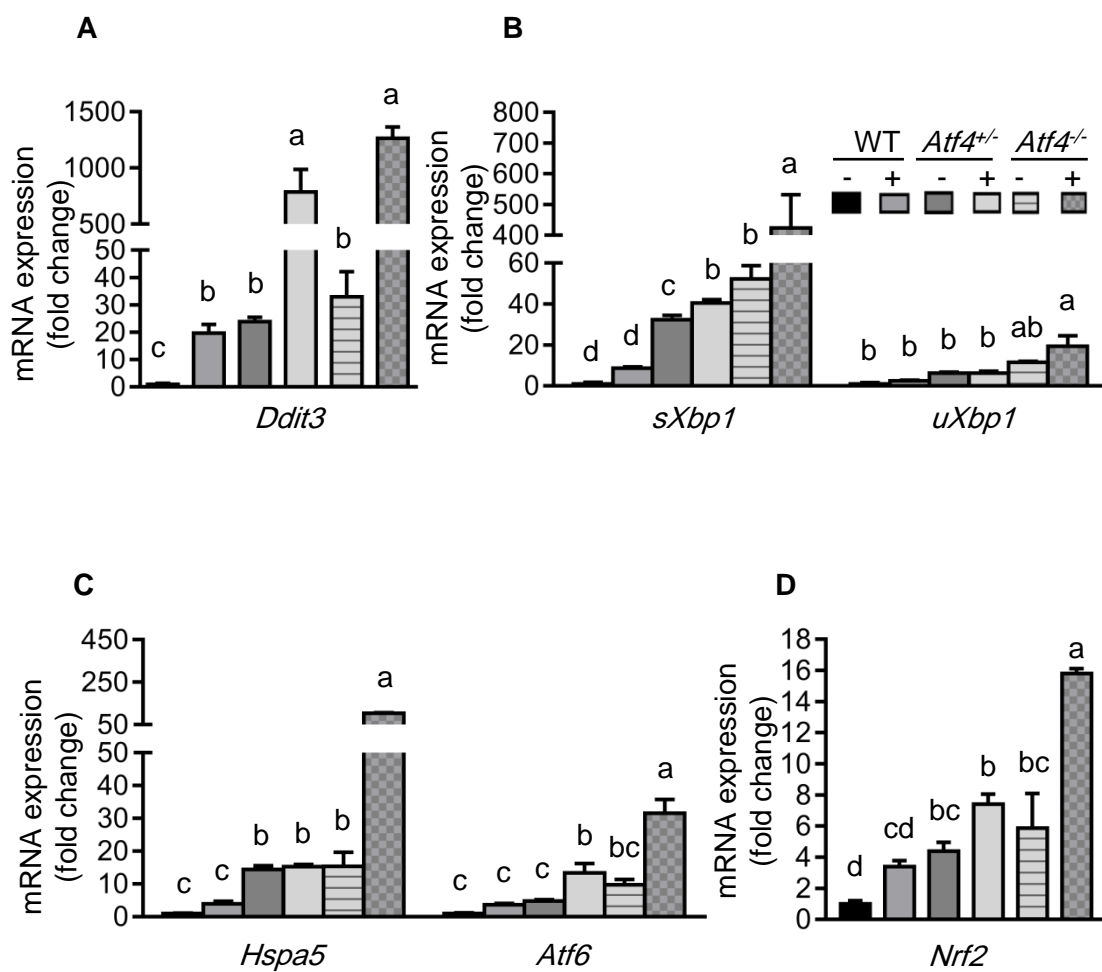


Figure 7

CHAPTER THREE: **Hepatic ATF4 Regulates Stress Response to ASNase in Mice.**

ABSTRACT

ASNase activates the AAR, increasing gene-specific translation of the transcription factor ATF4 to regain homeostasis via altered gene expression. In this study I examine the role of hepatic *Atf4* in liver of mice treated with ASNase. To accomplish this, I treated eight week old liver-specific *Atf4* homozygous null mice as well as their homozygous wild type littermates with ASNase for eight days and compared the hepatic AAR alongside a broader assessment of liver health using a combination of biochemical and histological approaches. Further I compared the global transcriptomic analyses of vehicle-treated/nonstressed whole body *Atf4*^{-/-} versus liver-specific *Atf4* homozygous null mice to address the hepatic role of ATF4 in controlling basal gene expression. RNA-seq analyses show that only a small portion (71/1039) of gene changes were shared, but gene ontology and pathway analyses revealed that most of the cellular processes altered in liver-specific *Atf4* homozygous null mice were either shared or partially overlapped with those being altered in *Atf4*^{-/-} mice, supporting a direct role for liver-derived ATF4 in regulating liver metabolism. The results also indicate that hepatic loss of *Atf4* augments the AAR to ASNase. The amplified AAR corresponded with induction of genetic markers of ER stress and increased cell death, indicating that loss of *Atf4* results in maladaptive outcomes. Furthermore, I found that ATF4 expression in the liver is dispensable for hepatic mTORC1 activity during amino acid depletion by ASNase. The results of this study reveal

that *Atf4* deletion in the liver promotes a maladaptive AAR and activates ER stress to amino acid deficiency. In addition, mTORC1 activation in the liver is not dependent on ATF4.

Introduction

ALL is the most common type of cancer in children and adolescents, and it is a frequent cause of death in those under age 20. ASNase is one of the chemotherapies used to treat ALL (Ribeiro et al., 2005; Pui et al., 2008; Patil et al., 2010; Raetz and Salzer, 2010), and it is widely recommended as it improves remission induction rate (Hill et al., 1967; Landau and Lamanna, 2006). Nevertheless, ASNase has many deleterious side effects that include liver failure and metabolic complications secondary to liver dysfunction that lead to treatment abandonment (Appel et al., 2008). Importantly, the exact mechanisms underlying ASNase-induced hepatotoxicity remain incompletely understood. Acquiring an improved understanding of the mechanism of these toxicities may improve treatment options.

ASNase depletes circulating levels of asparagine and glutamine and in liver activates the eIF2 kinase GCN2 (Reinert et al., 2006; Bunpo et al., 2009; Wilson et al., 2013). Phosphorylation of eIF2 by GCN2 dampens global protein synthesis rates while simultaneously promoting gene-specific translation of protein factors such as ATF4. ATF4 facilitates expression of a set of genes to cope with the stress by binding to response elements called CARE or AARE. This adaptive mechanism is known as the AAR (Kilberg et al., 2012). GCN2 is necessary for hepatic adaptation to ASNase through activating the GCN2-eIF2-ATF4-AAR (Bunpo et al., 2009). Lack of GCN2 function precludes AAR induction and exacerbates hepatotoxicity (Wilson et al., 2013; Wilson et al., 2015; Chapter 2).

GCN2 kinase is the primary responder to amino acid deficiency by ASNase in liver of mice. However, my work in Chapter 2 shows that treatment of mice deleted for *Atf4* with ASNase induces hepatic ER stress and specifically the XBP1 and ATF6 arms of the UPR. To what extent loss of hepatic ATF4 versus extra-hepatic ATF4 led to a maladaptive AAR and ER stress is unclear. My recent published work shows that in the absence of ATF4, ATF6 and CHOP assume auxiliary maladaptive response to ER stress-induced drug which correspond with compromised cholesterol and bile acid homeostasis (Fusakio et al., 2016).

The objective of this study was to evaluate the role of hepatic ATF4 in liver responses to ASNase and compare whole body versus liver-specific loss of *Atf4* on the liver transcriptome under non-stressed or basal conditions (Aim 3). Based on my results in Chapter 2, I hypothesize that loss of hepatic *Atf4* induces a maladaptive AAR which leads to greater ER stress and hepatotoxicity during ASNase.

In Chapter 2, I confirmed that mTORC1 activity is elevated in *Gcn2*^{-/-} treated with ASNase, similar to our previous published findings (Bunpo et al., 2009; Wilson et al., 2013). I then extended these findings by discovering that loss of *Atf4* did not unleash mTORC1 activity during ASNase. This finding conflicts with the recent report implicating ATF4 in mTORC1 downregulation by amino acid deprivation via Sestrin2 (Ye et al., 2015; Wolfson et al., 2016; Ding et al., 2016). However, at least one report supports my findings that *Gcn2* but not ATF4 regulates mTORC1 under amino acid deprivation (Averous et al. 2016).

Based on this report and my results in Chapter 2, I hypothesized that loss of hepatic ATF4 would not disrupt mTORC1 inhibition during ASNase.

In this study I addressed Aim 3 by first performing RNA sequencing (RNA-Seq) to examine global gene expression and pathway analyses in livers of whole body versus liver-specific *Atf4* deletion in non-stressed conditions. In addition, I administered ASNase to mice lacking *Atf4* from the liver only to assess the AAR, ER stress, and mTORC1 signaling. Collectively, these analyses indicated that in liver: 1) loss of hepatic *Atf4* in the nonstressed state alters a gene expression profile that partially overlaps with livers from mice with whole body deletion of *Atf4*, 2) Hepatic loss of *Atf4* alters the AAR to ASNase and induces ER stress to ASNase, 4) Hepatic *Atf4* does not regulate mTORC1 activity in the liver by ASNase, and 5) Sestrin2 phosphorylation in liver does not require hepatic ATF4. These findings fundamentally expand basic knowledge of the importance of hepatic ATF4 basally and in guiding the AAR, ER stress, and mTORC1 mechanisms by ASNase.

Materials and methods

Animals.

All animal protocols were approved by the Institutional Animal Care and Use Committee at Rutgers, The State University of New Jersey. In this study, male and female liver-specific *Atf4* null mice (*lsAtf4*^{-/-}, or also known as Cre+ mice) were generated by crossing mice homozygous for a floxed *Atf4* allele (*Atf4*^{f/f}) with mice expressing Cre recombinase driven by the albumin promoter

(Alb-Cre). In these studies, control mice are *Atf4^{fl/fl}* littermates that lack the Alb-Cre transgene (*lsAtf4^{+/+}* or also known as Cre-). Generation of the conditional *Atf4* knockout targeting construct is previously described (Ebert *et al.*, 2012). Animals were genotyped by PCR analysis of ear DNA using standard methods. The following primers were utilized for PCR: *Atf4* Flox Forward GCAGACGTTCTGGGTTAGA and *Atf4* Flox Reverse GCTTCCTGCCTACATTGCTC. These primers amplify 345 bp in Cre- mice and 465 bp in Cre+ mice (Ebert *et al.*, 2012). All mice were individually housed in clear plastic cages with corn cob bedding in a temperature and humidity controlled room with a 12:12 h light:dark cycle. Mice were freely provided commercial rodent chow (5001 Laboratory Rodent Diet, LabDiet) and tap water throughout the experiment.

Experimental Design.

In a first experiment, differential global gene expression analyses were conducted on liver RNA samples from untreated WT, *Atf4^{-/-}*, Cre- and Cre+ mice that were subjected to RNA-Seq. In a second experiment, Cre- and Cre+ mice were assigned by body weight to receive either 8 daily intraperitoneal (i.p.) injections of native *E. coli* L-ASNase (Elspar®) in phosphate buffered saline (PBS) at 0 or 3.0 international units per gram body weight (IU/g BW) once daily as previously detailed (Wilson *et al.*, 2015). The treatment groups in this second experiment were: Cre- / PBS, Cre- / ASNase, Cr+/PBS, and Cre+/ ASNase. Mice from all treatment groups were euthanized by decapitation ~8 hours after the final

injection. Tissues (e.g., liver, pancreas, spleen, blood) were collected. Dissected livers were rinsed in ice-cold PBS, blotted and weighed. One portion was then snap-frozen in liquid nitrogen before storage at -80°C while another portion was fixed in 4% paraformaldehyde. Body composition of live mice was measured prior to the first injection and before euthanasia by magnetic resonance using an EchoMRI instrument (Echo Medical Systems, Houston, TX).

RNA-Sequencing.

Frozen liver samples were processed to obtain high quality RNA for cDNA synthesis to conduct RNA-Seq analysis. Total RNA was extracted from frozen livers followed by DNase treatment using NucleoSpin® RNA Kit (Macherey-Nagel, GmbH & Co. KG, Newmann-Neander, Germany). The A260/280 and 260/230 absorbance ratios were and the RNA Integrity Number (RIN) were measured to validate the high quality of RNA samples (RIN \geq 8.0) (Agilent Bioanalyzer 2100). RNA from liver samples of whole body *Atf4*^{-/-} and Cre+ non-stressed mice were submitted to Columbia Genome Center (Columbia University, NY) as described in Chapter 2.

Bioinformatics.

As described in Chapter 2, global gene expression changes were analyzed using the TUXEDO bioinformatics pipeline. Differentially expressed genes were considered statistically significant with a FDR of < 0.1 (unadjusted p

< 0.03). Quality control plotting methods such as Principle Component Analysis (PCA) and Volcano plot were conducted in R (v3.2.2).

Differential gene expression and pathway analyses

A Venn diagram was generated using Venny 2.0.2 (<http://bioinfogp.cnb.csic.es/tools/venny/>). To create the Venn diagram; a list of differentially expressed genes (DEG) for Cre⁺ mice versus Cre⁻ mice under nonstressed conditions was compared with a DEG list from nonstressed whole body *Atf4*^{-/-} mice versus WT using a cutoff of FDR<0.1 to create A-C categories.

Gene lists in each category was submitted to Ingenuity Pathway Analysis (IPA) (<http://www.ingenuity.com/products/ipa>) to identify biological processes and pathways reflected in the gene lists. Significance cutoff used was $p < 0.05$.

Heat map

Genes reflecting specific biological processes were further illustrated by Heat map to display the negative log₁₀ (P value), (white for no significance to dark red for the highest significance) (Han et al., 2013).

Immunoblot analysis.

Frozen livers were weighed and immediately homogenized on ice to prepare tissue lysates to evaluate protein expression as described in Chapter 2 and previous laboratory publications (Bunpo *et al.*, 2009; Wilson *et al.*, 2015). Blots were developed using enhanced chemiluminescence (Amersham

Biosciences). Protein expression was analyzed using a FluorChem M multiplex imager (Protein Simple) and band density was quantitated using Carestream Molecular Imaging Software (version 5.0).

Reverse Transcription-Quantitative Polymerase Chain Reaction.

Total RNA was extracted from frozen livers using TriReagent (Molecular Research Center, Cincinnati, OH) as detailed (Wilson et al., 2015). 1 µg of the purified RNA solutions was used for reverse transcription using the High-Capacity cDNA Reverse Transcription Kit (Applied Biosystems, Foster City, CA). Gene expression levels were determined by quantitative PCR using TaqMan reagents and detected by StepOnePlus Real-Time PCR System (Applied Biosystems). Comparative Ct method was utilized to obtain results normalized to the Cre- PBS treated.

Histology.

Liver samples from each group were sectioned (10 µM) and stained to evaluate DNA fragmentation by Terminal deoxynucleotidyl transferase dUTP nick end labeling (TUNEL) assay as described (Bunpo et al., 2010).

RESULTS

Cre+ phenotypic features to ASNase.

Mice with a liver-specific deletion of *Atf4* were created by mating mice that expressed the *Atf4* gene as homozygous floxed to mice expressing Cre recombinase driven by the albumin promoter (Adams, 2007). In his study, Cre⁺ represents liver-specific *Atf4* knockouts whereas Cre⁻ mice are *Atf4* floxed mice which serve as wildtype controls. To evaluate the liver response to ASNase in Cre⁺ mice, I i.p.-injected ASNase (3 IU/g) into Cre⁻ and Cre⁺ mice once daily for 8 days using PBS as a vehicle solution. Prior to the beginning of the first injection, all mice had similar lean and fat mass (Fig. 1A). In response to ASNase, Cre⁻ mice experienced minimal change in body weight, whereas Cre⁺ mice lost a substantial amount (-2.35% versus -5.23%) of body weight (Fig. 1D). All mice except the Cre⁻ treated with PBS lost significant amounts of lean mass (Fig. 1B) and gained significant amounts of fat regardless of treatment (Fig. 1C). ASNase did not induce change in liver or pancreas weights, whereas spleen weight decreased following ASNase in both strains compared to Cre⁻ mice treated with PBS (Fig. 1E).

Hepatic-only deletion of Atf4 alters basal gene expression.

To further investigate the role of ATF4 basally in liver, I performed RNA-Seq analysis of liver *Atf4*^{-/-} (Cre⁺) versus whole body *Atf4*^{-/-}. RTqPCR confirmed significant reduction (~80%) of *Atf4* gene expression in Cre⁺ mice (Fig. 2A) in agreement with our previous results showing ATF4 loss at both gene and protein levels in Cre⁺ mice (Fusakio et al., 2016). Second, I crafted a Volcano plot to visualize the relationship between the fold change and the significance by

comparing \log_2 (Fold Change) to \log_{10} (statistical relevance) (Fig. 2B). Volcano plot indicated that hepatic gene expression that was altered to the loss of the *Atf4* from the liver only is significantly different from that was changed to the loss of *Atf4* from the whole body. Principle Component Analysis indicated that livers from Cre+ were quite different from whole body *Atf4*^{-/-} mice (Fig. 2C).

Venny analysis of a comparative examination showed that many hepatic genes required *Atf4* for basal expression. Using a FDR<0.1, I found 368 genes were altered by reduced hepatic expression of *Atf4* whereas 600 genes were altered by whole body deletion of *Atf4*. While only 71 genes were altered by both (Fig. 2D), GO term and pathway analyses of gene categories (A-C) showed that either deletion altered many shared biological processes including degradation of nicotine III, II, melatonin I, acetone, superoxide radicals, isoleucine I, glutaryl-CoA, valine I, and tryptophan III, FXR/RXR, PXR/RXR, LXR/RXR, and hepatic fibrosis / hepatic stellate cell, NRF2-mediated oxidative stress response, xenobiotic metabolism, LPS/IL-1 mediated inhibition of RXR function, UPR, fatty acid β -oxidation III, p38 MAPK signaling, ER stress, ATM signaling, ILK signaling, actin cytoskeleton signaling, ERK/MAPK signaling, signaling by Rho family GTPases, and AMPK signaling (Fig. 2E). On the other hand, livers from Cre+ mice demonstrated altered inositol pyrophosphates biosynthesis, acyl-CoA hydrolysis, VEGF signaling, Stat3 Pathway, VEGF Family Ligand-Receptor Interactions, eNOS signaling, p53 signaling, VDR/RXR activation, mTOR signaling, phospholipases, thrombin signaling, Myc mediated apoptosis signaling, cell cycle: G1/S checkpoint regulation, stearate biosynthesis I, integrin signaling,

and NF- κ B signaling. *Atf4* loss from the whole body altered calcium signaling, glutathione-mediated detoxification, superpathway of cholesterol biosynthesis, epithelial adherence junction signaling, complement system, glycolysis I, gluconeogenesis I, acute phase response signaling, retinol biosynthesis, retinoate biosynthesis I, cell cycle: G2/M DNA damage checkpoint regulation, intrinsic prothrombin activation pathway, TR/RXR activation, PPAR α /RXR α activation, and ketogenesis (Fig. 2E).

Hepatic loss of Atf4 amplified cell death and AAR to ASNase.

I injected Cre- and Cre+ mice with either PBS or ASNase for 8 d to explore the effect of hepatic deletion of *Atf4* on the liver health and AAR to ASNase. The results of apoptosis analysis by TUNEL assay showed significant increases in fragmented DNA levels in ASNase-treated Cre+ livers compared to livers from Cre- mice (Fig. 3A). Livers from Cre+ mice also showed significant increases in phosphorylation of eIF2 α at Ser51 following saline and ASNase as compared to Cre- treated with PBS (Fig. 3B). Hepatic *Asns*, *Eif4ebp1*, *Atf5*, and *Ppp1r15a* gene expression increased in ASNase treated Cre+ mice to levels equal to or greater than ASNase-treated Cre- livers (Fig. 3D). In contrast with whole body *Atf4*^{-/-} mice which precluded hepatic *Fgf21* expression to ASNase (Chapter 2, Figure 6F), *Fgf21* gene expression was elevated in the livers of Cre+ mice upon ASNase, suggesting an extrahepatic signal contributed to hepatic *Fgf21* expression. (Fig. 3D).

Hepatic Atf4 loss predisposed mice to ER stress during ASNase.

I evaluated genetic markers induced by ER stress to investigate the hepatic UPR to ASNase in Cre⁺ mice. *Ddit3* (encoding CHOP protein) mRNA expression increased in Cre⁺ livers to ASNase (Fig. 4A). Similarly, ASNase increased *Xbp1* mRNA splicing and *Hspa5* and *Atf6* hepatic gene expression, in Cre⁺ livers (Fig. 4B) compared to PBS treated Cre⁻ mice (Fig. 4C). The oxidative stress marker, *Nrf2* gene expression also showed induction in Cre⁺ compared to the Cre⁻ control (Fig. 4D).

Hepatic loss of Atf4 elevated mTORC1 signaling basally but did not interfere with downregulation by ASNase.

I conducted immunoblot analyses of target proteins to assess phosphorylation state and expression levels to examine the mTORC1 pathway response to ASNase. In accordance with my findings in Chapter 2 (Figure 5A-B), S6K1 and 4E-BP1 phosphorylation levels were significantly reduced by ASNase in Cre⁺ mice (Fig. 5A-B). To further understand the mTORC1 inhibition mechanism, I analyzed the phosphorylation of Akt (p-Thr308) and found it was reduced in all ASNase treated mice regardless of genotype (Fig 5C). Furthermore, I found that ASNase increased the phosphorylation of Sestrin2 and this effect was greater in Cre⁺ mice compared with the corresponding Cre⁻ mice (Fig. 5D).

Discussion

ASNase induces hepatotoxicity that interferes with treatment success and risks drug abandonment (Pieters et al., 2011). Therefore, it is critical to gain an improved understanding of these toxicities at the molecular level to improve remission rates. This study is the first to examine the impact of *Atf4* deletion in liver both on basal gene expression and on the AAR to ASNase. The study is also unique in that it compares genetic loss of *Atf4* in the liver versus the whole body under nonstressed conditions, revealing the critical role that ATF4 serves in regulating the liver transcriptome basally. Further, I discovered that liver deletion of *Atf4* induces ER stress to ASNase similar to the whole body deletion. Finally, my work reveals that hepatic ATF4 is not required to increase Sestrin2 phosphorylation or inhibit mTORC1 in response to ASNase.

At least one report attributes metabolic control by ATF4 to its expression in osteocytes (Yoshizawa et al., 2009) but other studies using mice harboring a liver-specific deletion of ATF4 show that its expression in liver plays important roles in regulating cholesterol and lipid metabolism as well as oxidative stress responses (Li et al., 2016). This study provides the first global view of the hepatic transcriptome of liver specific deletion of *Atf4* and a first comparison to deletion of *Atf4* from the whole body. The nuclear receptors that were found to be regulated by ATF4 in Chapter 2 were also indicated to be altered in liver specific *Atf4* null mice. This suggested that this process might be a mechanistic basis for how hepatic and extrahepatic ATF4 regulate metabolism during amino acid deficiency without treatment.

Mice lacking *Atf4* in liver show evidence of hepatic ER stress to ASNase similar to *Atf4*^{-/-} mice as shown in chapter 2. This is also consistent with what I published recently that in the absence of *Atf4*, ATF6 and CHOP function to drive the cell toward a maladaptive cell fate in response to ER stress (Fusakio et al., 2016). These findings also indicate that maladaptive AAR in the cytosol can trigger the UPR in response to ASNase.

My results in chapter 2 indicated that ATF4 is not required to direct the GCN2 effect on Sestrin 2 or mTORC1 signaling. These findings conflict with recent reports which claim that Sestrin2 is regulated by ATF4 under conditions of AA deprivation or ER stress (Ye et al., 2015; Kimball et al., 2016; Ding et al., 2016). These studies in total suggest Sestrin2 serves as a regulator of the mTORC1 pathway by sensing the availability of specific amino acids (Wolfson et al., 2016; Bar-Peled et al., 2013; Saxton et al., 2016; Ye et al., 2015; Kimball et al., 2016; Ding et al., 2016). Our findings extend these published results by showing that in liver an increase in Sestrin2 phosphorylation correlates with but does not cause mTORC1 inhibition and does not require GCN2 or ATF4.

In conclusion, globally hepatic ATF4 is required to regulate gene expression basally. Hepatic deletion of *Atf4* augments liver toxicity to ASNase similar to the whole body deletion. Alongside that hepatic ATF4 limits AAR amplification and ER stress induction to ASNase. Our findings also showed that Gcn2 regulates mTORC1 signaling in ATF4 independent manner.

Literature Cited

- Appel IM, Hop WC, van Kessel-Bakvis C, Stigter R, Pieters R. L-ASNase and the effect of age on coagulation and fibrinolysis in childhood acute lymphoblastic leukemia. *Thromb Haemost.* 2008 Aug;100:330-7.
- Averous, J., Lambert-Langlais, S., Mesclon, F., Carraro, V., Parry, L., Jousse, C., Bruhat, A., Maurin, A.-C., Pierre, P., Proud, C.G., et al. (2016). GCN2 contributes to mTORC1 inhibition by leucine deprivation through an ATF4 independent mechanism. *Sci. Rep.* 6, 27698.
- Bar-Peled L, Chantranupong L, Cherniack AD, Chen WW, Ottina KA, Grabiner BC, Spear ED, Carter SL, Meyerson M, Sabatini DM. A Tumor suppressor complex with GAP activity for the Rag GTPases that signal amino acid sufficiency to mTORC1. *Science.* 2013 May 31;340(6136):1100-6. doi: 10.1126/science.1232044. PMID: 2372323
- Bertolotti A, Zhang Y, Hendershot LM, Harding HP, Ron D. Dynamic interaction of BiP and ER stress transducers in the unfolded-protein response. *Nat Cell Biol* 2000;2:326–332.
- Brüning A, Rahmeh M, Friese K. Nelfinavir and bortezomib inhibit mTOR activity via ATF4-mediated sestrin-2 regulation. *Mol Oncol.* 2013 Dec;7(6):1012-8. doi: 10.1016/j.molonc.2013.07.010. Epub 2013 Jul 20.
- Bunpo P, Cundiff JK, Reinert RB, Wek RC, Aldrich CJ, Anthony TG. The eIF2 kinase GCN2 is essential for the murine immune system to adapt to amino acid deprivation by ASNase. *J Nutr.* 2010 Nov;140: 2020-7.
- Bunpo P, Dudley A, Cundiff JK, Cavener DR, Wek RC, Anthony TG. GCN2 protein kinase is required to activate amino acid deprivation responses in mice treated with the anti-cancer agent L-ASNase. *J Biol Chem.* 2009 Nov 20;284(47):32742-9. doi: 10.1074/jbc.M109.047910. Epub 2009 Sep 25.
- Ebert SM, Dyle MC, Kunkel SD, Bullard SA, Bongers KS, Fox DK, Dierdorff JM, Foster ED, Adams CM. Stress-induced skeletal muscle Gadd45a expression reprograms myonuclei and causes muscle atrophy. *J Biol Chem.* 2012 Aug 10;287(33):27290-301.
- Fusakio ME, Willy JA, Wang Y, Mirek ET, Al Baghdadi RJ, Adams CM, Anthony TG, Wek RC. Transcription factor ATF4 directs basal and stress-induced gene expression in the unfolded protein response and cholesterol metabolism in the liver. *Mol Biol Cell.* 2016 May 1;27(9):1536-51.
- Han J, Back SH, Hur J, Lin YH, Gildersleeve R, Shan J, Yuan CL, Krokowski D, Wang S, Hatzoglou M, Kilberg MS, Sartor MA, Kaufman RJ. ER-stress-

induced transcriptional regulation increases protein synthesis leading to cell death. *Nat Cell Biol.* 2013 May;15(5):481-90. doi: 10.1038/ncb2738. Epub 2013 Apr 28. PMID: 23624402

Harding HP, Zhang Y, Zeng H, Novoa I, Lu PD, Calton M, Sadri N, Yun C, Popko B, Paules R, Stojdl DF, Bell CJ, Hettmann T, Leiden JM, Ron D, An integrated stress response regulates amino acid metabolism and resistance to oxidative stress, *Mol. Cell* 11 (2003) 619–633.

Hill JM, Roberts J, Loeb E, Khan A, MacLellan A, Hill RW. L-ASNase therapy for leukemia and other malignant neoplasms. Remission in human leukemia. *Jama.* 1967 Nov 27;202:882-8.

Jewell JL, Russell RC, Guan KL. Amino acid signalling upstream of mTOR. *Nat Rev Mol Cell Biol.* 2013 Mar;14(3):133-9. doi: 10.1038/nrm3522. Epub 2013 Jan 30. Review. PMID: 23361334

Kilberg MS, Balasubramanian M, Fu L, Shan J The transcription factor network associated with the amino acid response in mammalian cells. *Adv Nutr.* 2012 May 1;3(3):295-306. doi: 10.3945/an.112.001891.

Landau H, Lamanna N. Clinical manifestations and treatment of newly diagnosed acute lymphoblastic leukemia in adults. *Curr Hematol Malig Rep.* 2006 Sep;1(3):171-9. doi: 10.1007/s11899-996-0005-8.

Laplanche M, Sabatini DM. mTOR signaling in growth control and disease. *Cell.* 2012 Apr 13;149(2):274-93. doi: 10.1016/j.cell.2012a.03.017. Review. PMID: 22500797

Laplanche M, Sabatini DM. mTOR Signaling. *Cold Spring Harb Perspect Biol.* 2012b Feb 1;4(2). pii: a011593. doi: 10.1101/cshperspect.a011593. Review. PMID: 22129599

Malhi H, Kaufman RJ. Endoplasmic reticulum stress in liver disease. *J Hepatol.* 2011;54 (4):795-809.

Oikawa D, Kimata Y, Kohno K, Iwawaki T. Activation of mammalian IRE1alpha upon ER stress depends on dissociation of BiP rather than on direct interaction with unfolded proteins. *Exp Cell Res* 2009;315:2496–2504.

Park HW, Park H, Ro SH, Jang I, Semple IA, Kim DN, Kim M, Nam M, Zhang D, Yin L, Lee JH. Hepatoprotective role of Sestrin2 against chronic ER stress. *Nat Commun.* 2014 Jun 20;5:4233. doi: 10.1038/ncomms5233. PMID: 24947615

- Patil S, Coutsouvelis J, Spencer A. ASNase in the management of adult acute lymphoblastic leukaemia: Is it used appropriately? *Cancer Treat Rev*. 2010 Sep 3.
- Phillipson-Weiner L, Mirek ET, Wang Y, McAuliffe WG, Wek RC, Anthony TG. General control nonderepressible 2 deletion predisposes to ASNase-associated pancreatitis in mice. *Am J Physiol Gastrointest Liver Physiol*. 2016 Jun 1;310(11):G1061-70. doi: 10.1152/ajpgi.00052.2016. Epub 2016 Mar 11. PMID: 26968207
- Pui CH, Robison LL, Look AT. Acute lymphoblastic leukaemia. *Lancet*. 2008 Mar 22;371:1030-43.
- Raetz EA, Salzer WL. Tolerability and efficacy of L-ASNase therapy in pediatric patients with acute lymphoblastic leukemia. *J Pediatr Hematol Oncol*. 2010 Oct;32:554-63.
- Reinert RB, Oberle LM, Wek SA, Bunpo P, Wang XP, Mileva I, Goodwin LO, Aldrich CJ, Durden DL, McNurlan MA, Wek RC, Anthony TG. Role of glutamine depletion in directing tissue-specific nutrient stress responses to L-ASNase. *J Biol Chem*. 2006 Oct 20; 281(42):31222-33. Epub 2006 Aug 24.
- Shimobayashi M, Hall MN. Making new contacts: the mTOR network in metabolism and signalling crosstalk. *Nat Rev Mol Cell Biol*. 2014 Mar;15(3):155-62. doi: 10.1038/nrm3757. Review. PMID: 24556838
- Szegezdi E, Logue SE, Gorman AM, Samali A. Mediators of endoplasmic reticulum stress-induced apoptosis. *EMBO Rep* 2006;7:880–885.
- Wilson GJ, Bunpo P, Cundiff JK, Wek RC, Anthony TG. The eukaryotic initiation factor 2 kinase GCN2 protects against hepatotoxicity during ASNase treatment. *Am J Physiol Endocrinol Metab*. 2013 Nov 1;305(9):E1124-33. doi: 10.1152/ajpendo.00080.2013. Epub 2013 Sep 3.
- Wilson GJ, Lennox BA, She P, Mirek ET, Al Baghdadi RJ, Fusakio ME, Dixon JL, Henderson GC, Wek RC, Anthony TG. GCN2 is required to increase fibroblast growth factor 21 and maintain hepatic triglyceride homeostasis during ASNase treatment. *Am J Physiol Endocrinol Metab* 308: E283-93, 2015.
- Wong MK, Nicholson CJ, Holloway AC, Hardy DB. Maternal nicotine exposure leads to impaired disulfide bond formation and augmented endoplasmic reticulum stress in the rat placenta. *PLoS One*. 2015 Mar 26;10(3):e0122295. doi: 10.1371/journal.pone.0122295. eCollection 2015. PMID: 25811377

Ye J, Palm W, Peng M, King B, Lindsten T, Li MO, Koumenis C, Thompson CB.
GCN2 sustains mTORC1 suppression upon amino acid deprivation by
inducing Sestrin2. *Genes Dev.* 2015 Nov 15;29(22):2331-6.

Figure Captions

Figure 1. Body and tissue responses to ASNase in mice with Cre recombinase-mediated deletion of *Atf4* in liver. (A-C) Body fat mass and percent of body lean mass was measured by EchoMRI before the treatment (day 0) in Cre- and Cre+ mice. (D) Percent body weight (BW) change in Cre- (*Atf4^{flox/flox}*), and Alb-Cre+ (liver-specific *Atf4^{-/-}*) mice treated with 8 daily i.p. injections of ASNase (3 IU/g BW) or saline excipient and killed 8 h after the last injection. (E) Percent weight change of liver, pancreas, and spleen relative to body weight. Data were analyzed by two-factor ANOVA, n=6-8 animals per group. Means not sharing a common letter are different, P<0.05.

Figure 2. Global discovery of genes altered by *lsAtf4^{-/-}* (Cre+) mice basally. (A) *Atf4* gene expression by RT-qPCR. (B) Volcano plot shows the genes that differ significantly (highlighted in red) between 2 conditions (P<0.05). X-axis represents Log2 (fold change) and Y axis represents the negative log(P value). (C) Principle Component Analysis (PCA) plot was conducted to explore the relationship between the two strains, with X-axis represents PC1, the first component points in the direction of highest variance. The Y-axis represents PC2, the second component points in the direction of highest variance. Cre-, Cre+, WT, whole body *Atf4^{-/-}* mice, n=3 per group (P<0.03, FDR<0.1). (D) Venn diagram shows number of genes altered basally can be divided into three categories, unique to Cre+ deletion [A], unique to whole body *Atf4* deletion [C] or

common to deletion of either [B]. (E) IPA of biological changes in gene expression as categorized above within the Venn diagram. Samples went through RNA-Seq analyses are livers of Cre⁻, Cre⁺, WT and whole body *Atf4*^{-/-} mice FDR<0.1, n=3 per group. Means not sharing a common letter are different, P<0.05.

Figure 3. Hepatic deletion of *Atf4* alters AAR and promotes cell death in response to ASNase. (A) Fragmented DNA evaluation as a marker of apoptosis level was measured by TUNEL staining of liver sections (10µm), and ascertained by manual counting of the staining-positive nuclei using Image J software. n=3 per group. (B) Phospho-eIF2 was measure by immunoblot analysis and quantified relative to total eIF2. (C) Gene expression of AAR genes *Asns*, *Atf3*, *Atf5*, *Fgf21*, *Elf4ebp1*, and *Ppp1r15a* in Cre⁻ and Cre⁺ mice. Data were analyzed by two-factor ANOVA, n=6-8 per group. Means not sharing a common letter are different, P<0.05.

Figure 4. Hepatic *Atf4* deletion promotes ER stress to ASNase. Gene expression of (A) *Ddit3*, (B) spliced (s*Xbp1*) and unspliced (u*Xbp1*) *Xbp1*, (C) *Hspa5* and *Atf6*, (D) *Nrf2* measured by RT-PCR. Data were analyzed by two-factor ANOVA, n=6-8 per group. Means not sharing a common letter are different, P<0.05.

Figure 5. Nonstressed Cre⁺ mice demonstrate elevated mTORC1 signaling that is downregulated in response to ASNase independent of Akt phosphorylation and Sestrin2 phosphorylation. (A) Phospho-S6K1 at threonine 389, (B) Phospho-4E-BP1, and (C) Phospho-Akt at threonine 308 was assessed by immunoblot analysis while (D) Phospho-Sestrin2 was assessed by electrophoretic mobility shift. (Data were analyzed by two-factor ANOVA, n=6-8 per group. Means not sharing a common letter are different, $P < 0.05$).

Figures

Figure 1

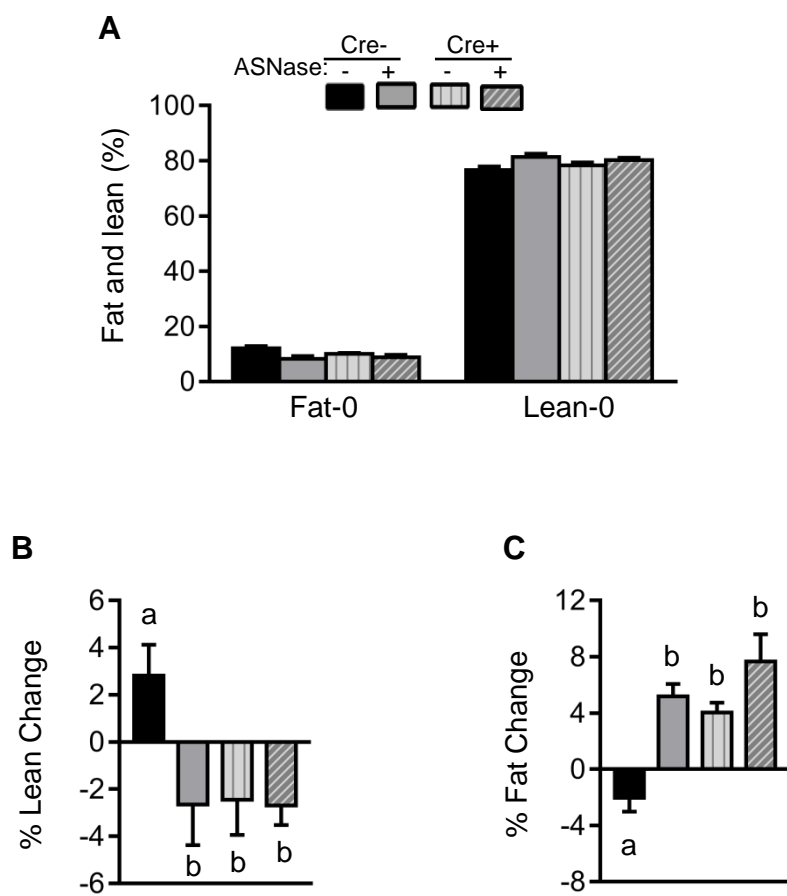
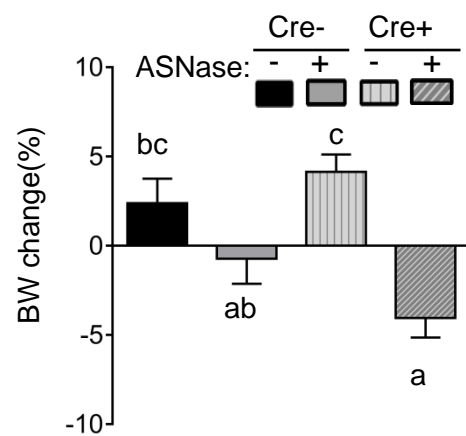


Figure 1

D



E

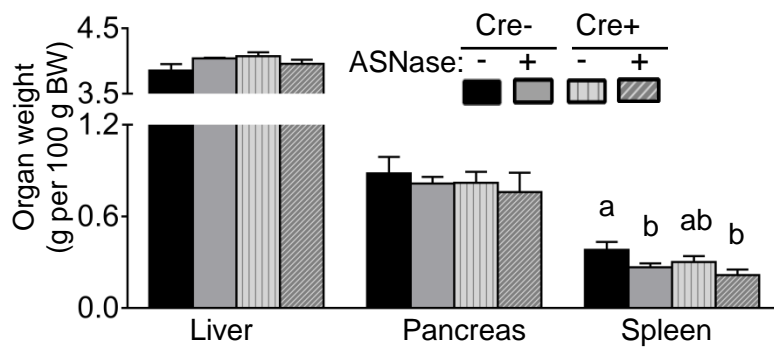


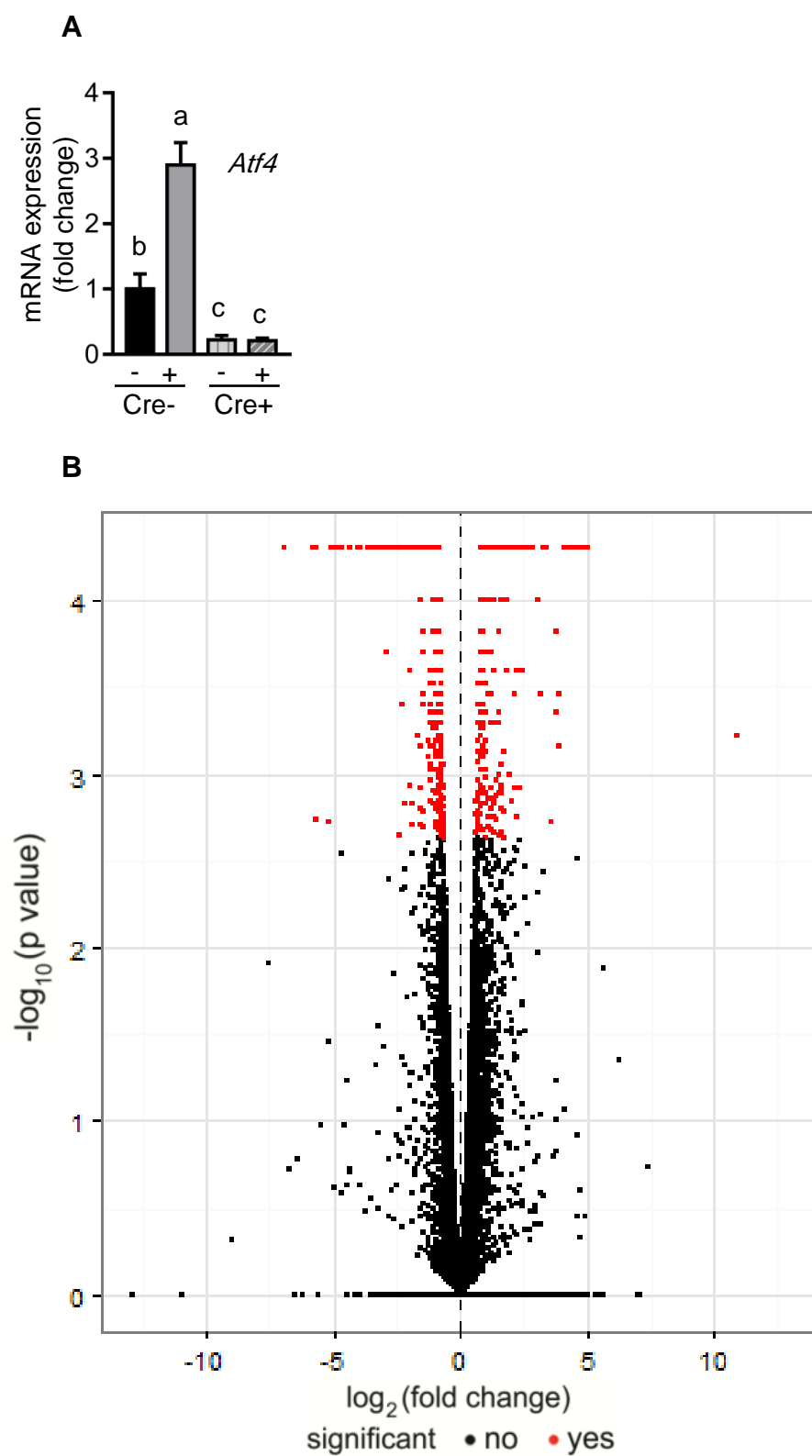
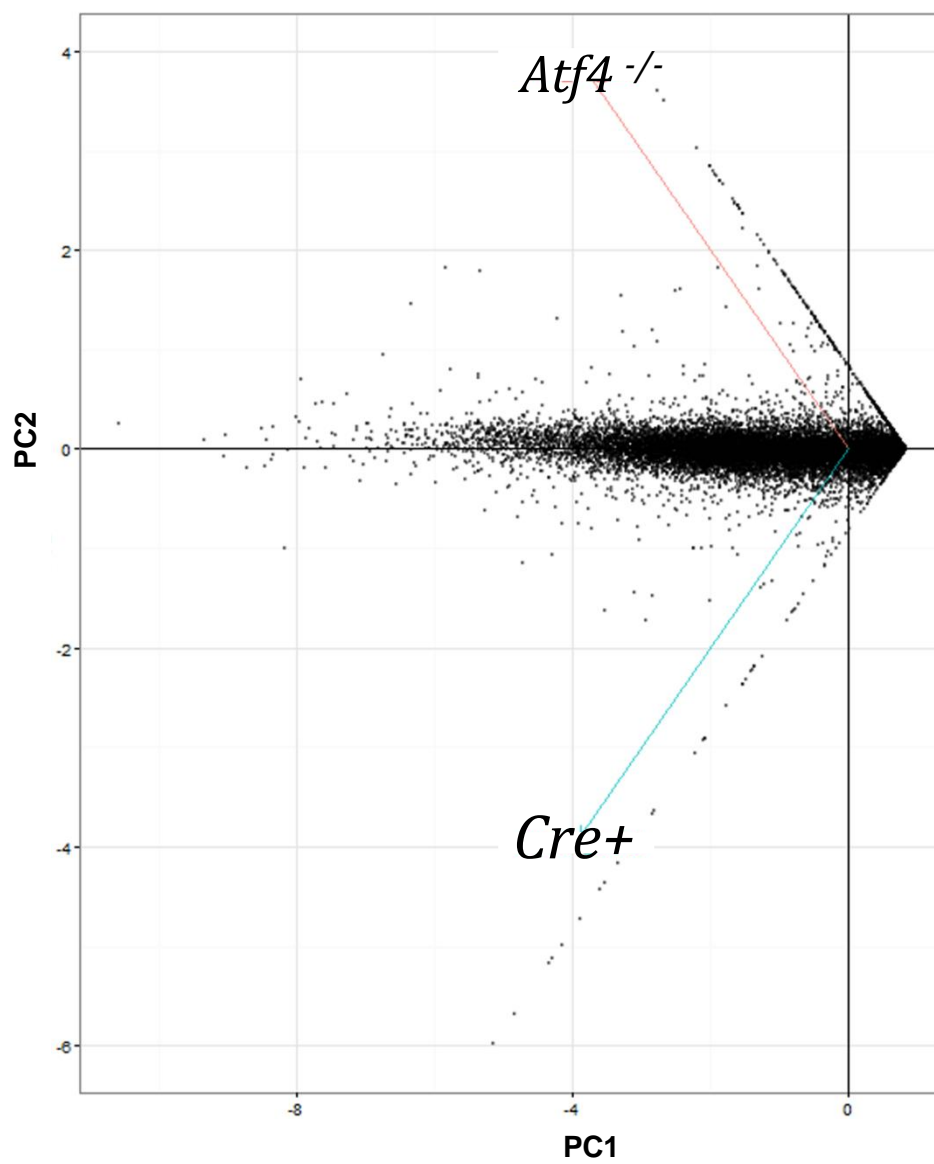
Figure 2

Figure 2

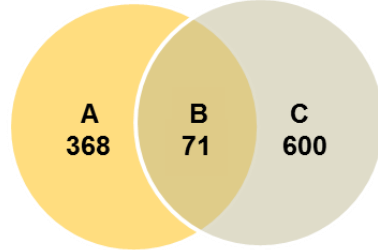
C



D

Basal condition

Cre+ vs Cre-

Atf4^{-/-} vs WT

Hepatic ATF4

Extra hepatic ATF4

A

368

B

71

C

600



E

Ingenuity Canonical Pathways

-log(p-value)

	A	B	C	
Nicotine Degradation III	4.8	2.3	1.4	0
Nicotine Degradation II	4.3	2.2	1.7	1
Melatonin Degradation I	3.8	2.3		2
Inositol Pyrophosphates Biosynthesis	3.7			3
Superpathway of Melatonin Degradation	3.6	2.2		4
Hepatic Fibrosis / Hepatic Stellate Cell Activation	3.4		4.2	5
ATM Signaling	3.2		2.8	6
Acyl-CoA Hydrolysis	3			7
VEGF Signaling	3			8
ILK Signaling	2.9		2.2	
STAT3 Pathway	2.7			
VEGF Family Ligand-Receptor Interactions	2.7			
eNOS Signaling	2.5			
Actin Cytoskeleton Signaling	2.4		2.5	
ERK/MAPK Signaling	2.3		1.4	
p53 Signaling	2.2			
Signaling by Rho Family GTPases	2.1		1.5	
VDR/RXR Activation	1.9			
AMPK Signaling	1.9		2.3	
mTOR Signaling	1.8			
Phospholipases	1.8			
FXR/RXR Activation	1.8	1.5		
Thrombin Signaling	1.7			
Myc Mediated Apoptosis Signaling	1.7			
PXR/RXR Activation	1.6	2.1	3.4	
Cell Cycle: G1/S Checkpoint Regulation	1.6			
Stearate Biosynthesis I (Animals)	1.6			
Integrin Signaling	1.6			
NF-κB Signaling	1.5			
NRF2-mediated Oxidative Stress Response	1.5	2.2	2.8	
Xenobiotic Metabolism Signaling	1.4	1.7	2.2	
LPS/IL-1 Mediated Inhibition of RXR Function		6.4	5.1	
Acetone Degradation I (to Methylglyoxal)	2.9	1.6		
Unfolded protein response	2.2			
Fatty Acid β-oxidation III (Unsaturated, Odd Number)	2.1			
Superoxide Radicals Degradation	1.8			
LXR/RXR Activation	1.6	1.8		
Glutaryl-CoA Degradation	1.6			
p38 MAPK Signaling	1.6	1.4		
Isoleucine Degradation I	1.5			
Valine Degradation I	1.4			
Endoplasmic Reticulum Stress Pathway	1.4			
Tryptophan Degradation III (Eukaryotic)	1.3			
Calcium Signaling			7.7	
Glutathione-mediated Detoxification			5.4	
Superpathway of Cholesterol Biosynthesis			5	
Epithelial Adherens Junction Signaling			4.2	
Complement System			3.5	
Glycolysis I			3.3	
Gluconeogenesis I			3.3	
Acute Phase Response Signaling			3.1	
Retinol Biosynthesis			2.8	
Retinoate Biosynthesis I			2.7	
Cell Cycle: G2/M DNA Damage Checkpoint Regulation			2.5	
Intrinsic Prothrombin Activation Pathway			2.1	
TR/RXR Activation			2	
PPARα/RXRα Activation			1.6	
Ketogenesis			1.5	

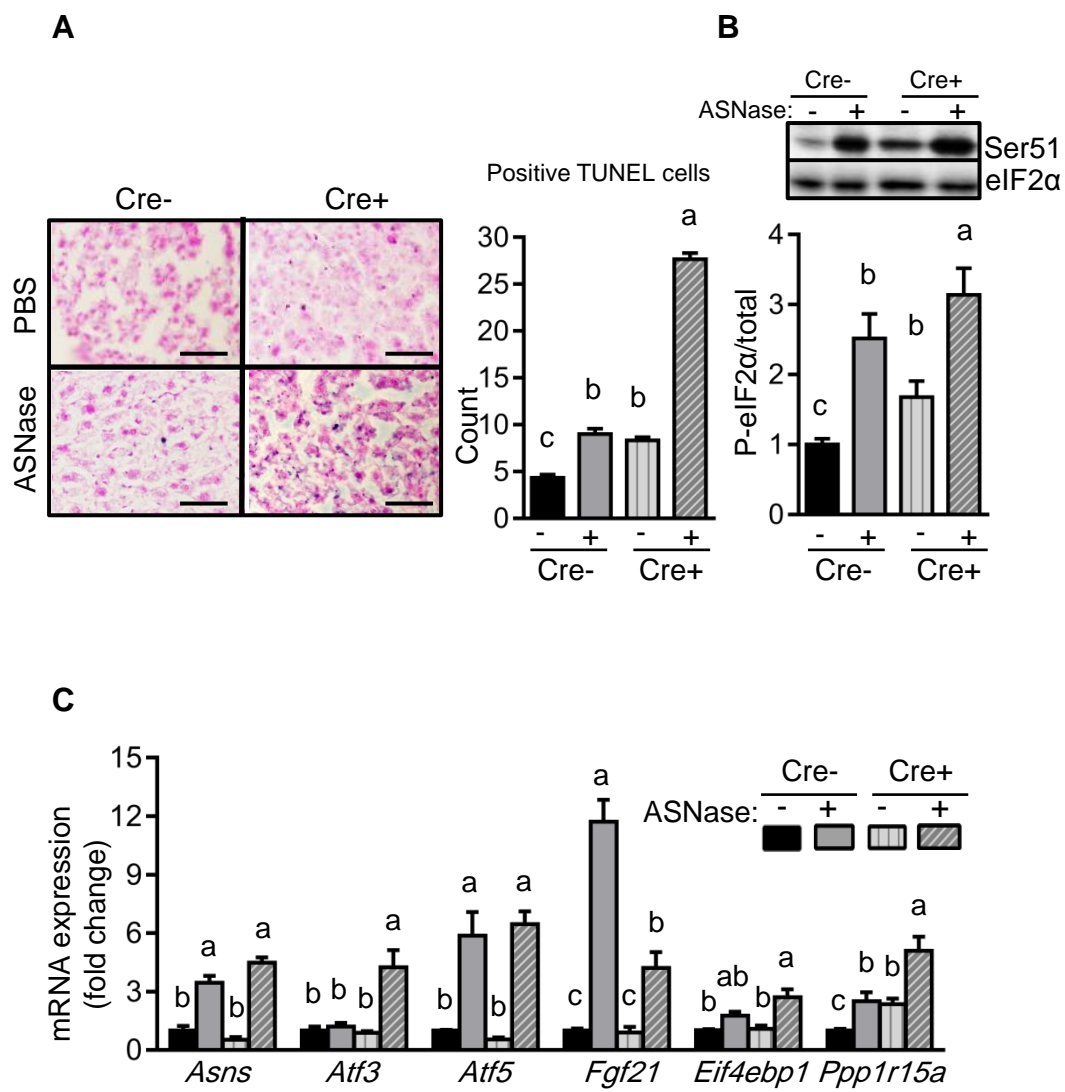
Figure 3

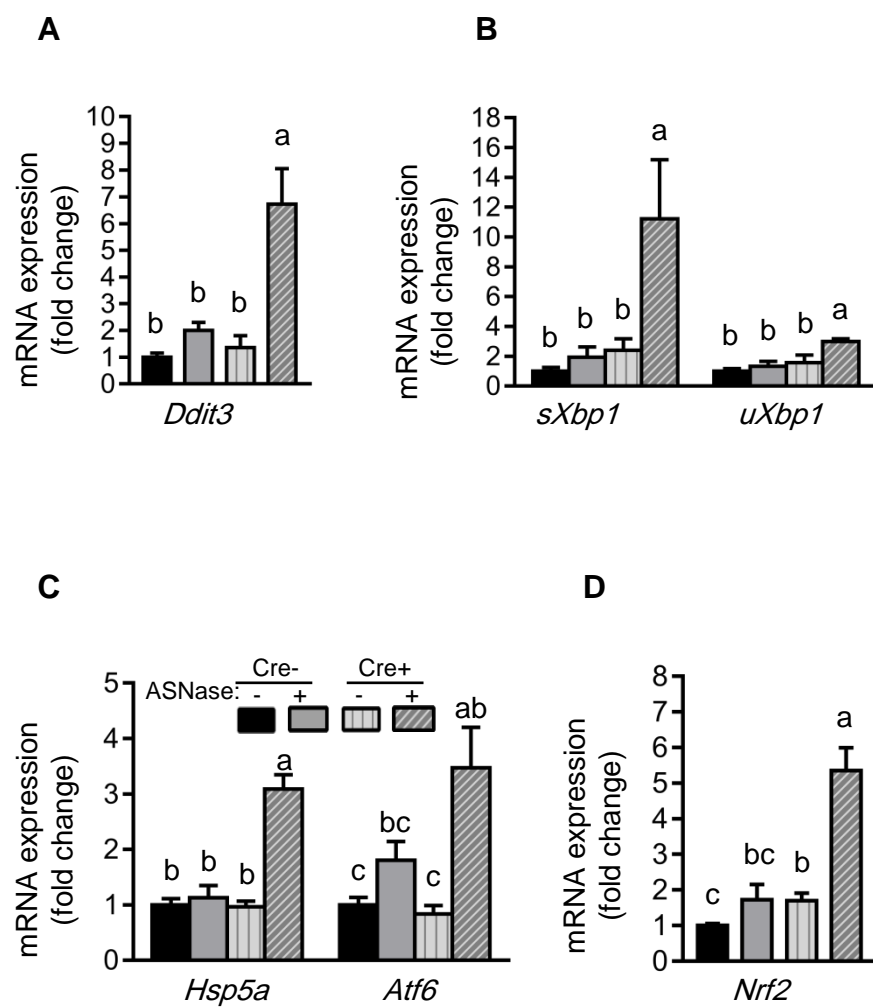
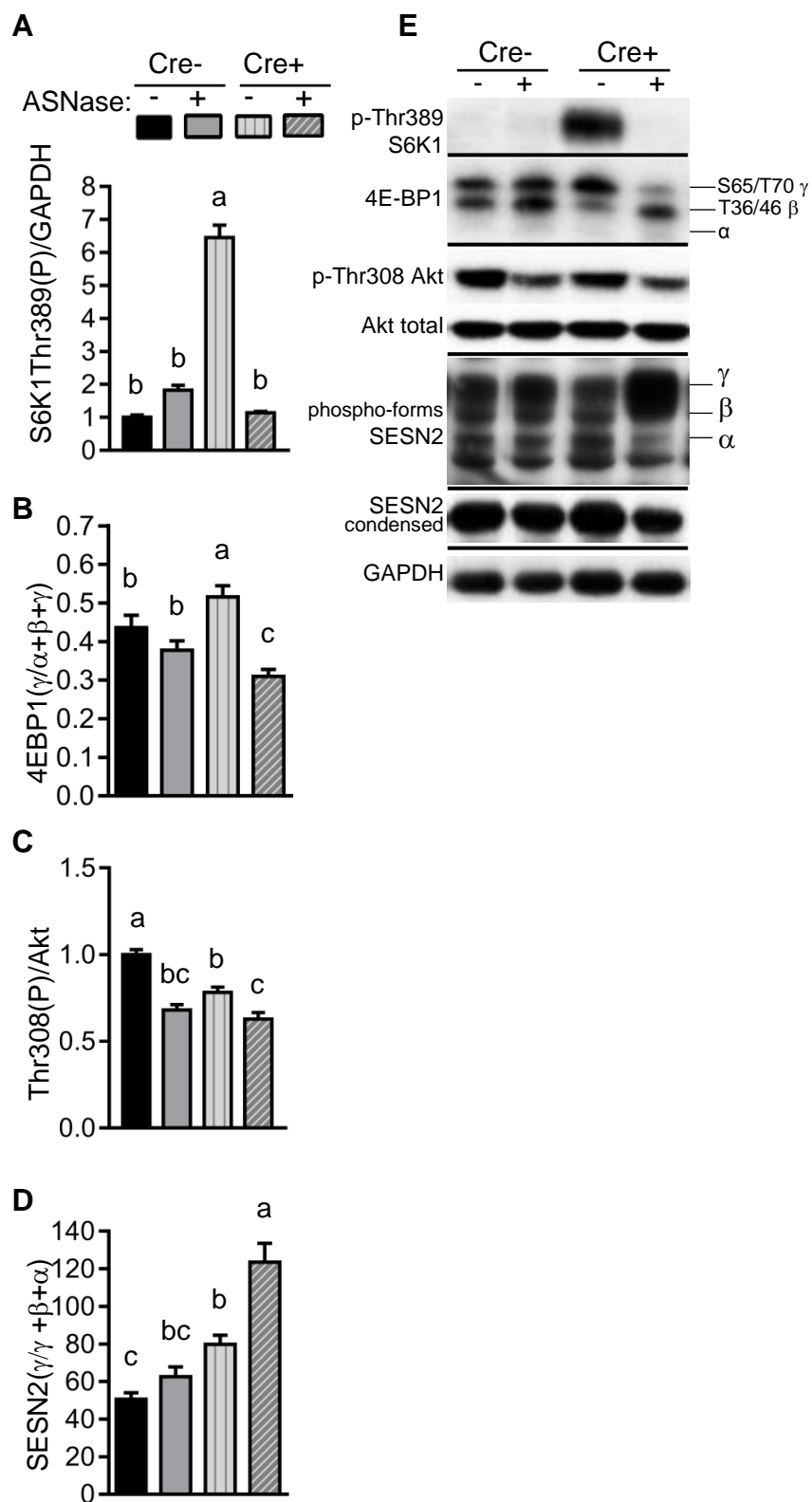
Figure 4

Figure 5

Overall Summary

The diagnosis of ALL in a child or adult can be devastating to a family especially if the treatment is without high safety margin. ASNase is one of the most efficient chemotherapies to survive the ALL but patients suffer comorbidities including liver failure (Appel et al., 2008), coagulopathy and thromboembolism (Wani et al., 2010; Pui and Evans, 2006; Payne and Vora, 2007; Merlen et al., 2015), neurological and cardiovascular complications (Kieslich et al., 2003), hyperglycemia and pancreatitis (Knoderer et al., 2010; Spinola-Castro et al., 2009). However, hepatotoxicity is characterized as the most life-threatening side effect of ASNase (Douer et al., 2007; Rosen et al., 2003, Vetro et al., 2014). This can lead to severe secondary events including thromboembolism (Ettinger et al., 1995), liver failure, and encephalopathy (Rytting et al., 2010). Thus, there exists a critical need to develop therapies that prevent or mitigate the adverse metabolic effects of ASNase based on its molecular mechanism of action in affected tissues.

ASNase functions by degrading two amino acids, asparagine and glutamine (Wilson et al., 2013) that are essential to cancer cells to survive. Decreasing amino acid level in the cells sensitized by GCN2 kinase which then phosphorylates eIF2 α inhibiting the global protein translation except for some proteins like ATF4 (Vattem and Wek, 2004), that is part of ISR response (Harding et al., 2003). As part of ISR, in response to amino acid depletion, ATF4 activates transcriptional program AAR that functions to restore homeostasis (Kilberg et al.,

2012). My dissertation project sought to determine the influence of global versus partial loss of ATF4 on liver toxicity in ASNase-treated mice.

Aim 1 of this dissertation compared the role of ATF4 versus GCN2 in the liver basally as well as in response to ASNase. My work revealed that ATF4 only partially mediates the effect of Gcn2 in liver. I also showed that intact ATF4 is of extreme importance to adapt to ASNase treatment, and resulted in severe maladaptive responses. Specifically, global *Atf4* loss amplified the AAR and induced ER stress to ASNase. In contrast, *Gcn2* deleted mice failed to activate the AAR and do not exhibit ER stress in response to amino acid depletion by ASNase. Unexpectedly, *Atf4*^{-/-} mice behaved similar to WT mice regarding mTORC1 signaling pathway. Whilst loss of *Atf4* does not affect mTORC1 in response to ASNase, lack of *Gcn2* highly activates mTORC1 induction.

Aim 2 of this dissertation was conducted to assess if *Atf4* heterozygosity altered the ISR response to ASNase and induced hepatotoxicity. My results emphasized the importance of full *Atf4* gene expression to avoid ASNase-induced hepatotoxicity. My findings revealed that loss of one allele of *Atf4* gene is also detrimental in that it induced AAR amplification, ER stress, liver steatosis, and cell death in response to ASNase. The results of my experiments demonstrated that defective ISR exacerbate the ASNase side effects and can predispose ALL patients towards severe deleterious metabolic events under this chemotherapy treatment.

Finally, in Aim 3 I examined the impact of *Atf4* deletion in liver both on basal gene expression and on the AAR to ASNase. In addition, I compared

genetic loss of *Atf4* in the liver versus the whole body under nonstressed conditions, revealing the critical role that ATF4 serves in regulating the liver transcriptome basally. In these studies, I discovered that liver deletion of *Atf4* induces AAR and ER stress to ASNase similar to whole body deletion of *Atf4*. Furthermore, I found that mTORC1 signaling is not altered in mice with liver deletion of *Atf4* and hepatic ATF4 is not required to increase Sestrin2 phosphorylation or inhibit mTORC1 in response to ASNase. Importantly, these responses were similar to whole body deletion of *Atf4*. Overall, I concluded that hepatic deletion of *Atf4* augmented liver toxicity to ASNase similar to whole body deletion of *Atf4*.

My results indicate a need to screen ALL patients' genetic backgrounds for ASNase may not be ideal to treat this disease in patients with defects or mutations in the ISR. This is consistent with recent human studies that identify single nucleotide polymorphisms in *Atf5* and *Asns* and correlate their incidence with adverse events to asparaginase (Rousseau et al., 2011; Pastorczak et al., 2013). Early identification of symptoms or biological markers related to these defects applies knowledge that helps to determine patients harboring silent potential inabilities to handle the stress associated with ASNase. This allows physicians to identify at risk ALL patients to be treated with different chemotherapy that they can tolerate given their specific genetic risk. In addition, future recommendation to improve the ASNase safety by applying a concomitant therapy protocol that may include for example; synthetic antioxidants to mitigate oxidative stress, and or chaperones to alleviate ER stress.

Further studies are required to unravel some questions raised in my dissertation. For example, I suggest to carrying out a study to understand the reason behind the stress that the *Atf4* deleted mice suffered under nonstressed conditions. This might be done by conducting experiments to compare wildtype to *Atf4* deleted mice basally by using more advanced analyses. The RNA-Seq that I done in the dissertation might be followed by metabolomics, proteomics and/or other analyses that may help to reveal the real time protein activity in the cell.

Future studies are also required to indicate the role of other factors that might compensate the absence of the ATF4 function in *Atf4*^{-/-} mice. For examples, I found that *Nrf2* gene expression is highly elevated in the *Atf4* deleted mice that might supersede the ATF4 effect in driving the response to oxidative stress. Studies can be done to investigate NRF2 protein expression in these mice compared to wildtype mice by conducting western blotting or chip seq analyses to assure this idea. Also, I found high induction of *Atf6* mRNA expression in the *Atf4*^{-/-} mice that its protein might take over ATF4 role in inducing the ER stress response as I previously ascertained by measuring the ATF6 cleavage in the *Atf4* knockout mice (Fusakio et al., 2016).

Other studies might be conducted by following the redundant pathways that were highlighted by the IPA analyses to figure out candidates that might be controlled by the *Atf4* gene to regulate metabolism. For example, the recognition of nuclear receptors as being ATF4 regulated gene products suggest a mechanism for how ATF4 regulates metabolism in response to amino acid

starvation.

In addition to the global transcriptomic analyses that I have conducted in this dissertation, future areas of investigation include comparing the global transcriptional response in liver to other profiling modalities (i.e. proteomic or metabolic, and in normal tissues and/or cancer cell lines) and using this information to discover novel treatments or therapies to prevent metabolic toxicities to ASNase. In conclusion, the suggested studies might help to indicate other factors that can be targeted to improve ASNase treatment as chemotherapy in defected *Atf4* individuals.

Literature Cited

- Douer D, Yampolsky H, Cohen LJ, Watkins K, Levine AM, Periclou AP, Avramis VI. Pharmacodynamics and safety of intravenous pegaspargase during remission induction in adults aged 55 years or younger with newly diagnosed acute lymphoblastic leukemia. *Blood* 2007;109:2744–50.
- Ettinger LJ, Kurtzberg J, Voute PA, Jurgens H, Halpern SL. An open-label, multicenter study of polyethylene glycol-L-asparaginase for the treatment of acute lymphoblastic leukemia. *Cancer* 1995;75:1176–81.
- Fusakio ME, Willy JA, Wang Y, Mirek ET, Al Baghdadi RJ, Adams CM, et al. Transcription factor ATF4 directs basal and stress-induced gene expression in the unfolded protein response and cholesterol metabolism in the liver. *Mol Biol Cell*. 2016 May 1;27(9):1536-51.
- Harding HP, Zhang Y, Zeng H, Novoa I, Lu PD, Calton M, Sadri N, Yun C, Popko B, Paules R, Stojdl DF, Bell CJ, Hettmann T, Leiden JM, Ron D, An integrated stress response regulates amino acid metabolism and resistance to oxidative stress, *Mol. Cell* 11 (2003) 619–633.
- Kilberg MS, Balasubramanian M, Fu L, Shan J The transcription factor network associated with the amino acid response in mammalian cells. *Adv Nutr*. 2012 May 1;3(3):295-306. doi: 10.3945/an.112.001891.
- Pastorczyk A, Fendler W, Zalewska-Szewczyk B, Górniak P, Lejman M, Trelińska J, Walenciak J, Kowalczyk J, Szczepanski T, Mlynarski W; Polish Pediatric Leukemia/Lymphoma Study Group. Asparagine synthetase (ASNS) gene polymorphism is associated with the outcome of childhood acute lymphoblastic leukemia by affecting early response to treatment. *Leuk Res*. 2014 Feb;38(2):180-3. doi: 10.1016/j.leukres.2013.10.027. Epub 2013 Nov 5. PMID: 24268318
- Rosen O, Muller HJ, Gokbuget N, et al. Pegylated asparaginase in combination with high-dose methotrexate for consolidation in adult acute lymphoblastic leukaemia in first remission: a pilot study. *Br J Haematol* 2003;123:836–41.
- Rousseau J, Gagné V, Labuda M, Beaubois C, Sinnett D, Laverdière C, Moghrabi A, Sallan SE, Silverman LB, Neuberg D, Kutok JL, Krajcinovic M. ATF5 polymorphisms influence ATF function and response to treatment in children with childhood acute lymphoblastic leukemia. *Blood*. 2011 Nov 24;118(22):5883-90. doi: 10.1182/blood-2011-05-355560. Epub 2011 Oct 4.

- Rytting M. Peg-asparaginase for acute lymphoblastic leukemia. *Expert Opin Biol Ther* 2010;10:833–9.
- Vattem KM, Wek RC. Reinitiation involving upstream ORFs regulates ATF4 mRNA translation in mammalian cells. *Proc Natl Acad Sci U S A*. 2004;11269–74.
- Vetro C, Giulietti G, Calafiore V, Romano A, Di Raimondo F. A snapshot of asparaginase-induced liver insufficiency. *Eur J Haematol*. 2014 Mar;92(3):271-2. doi: 10.1111/ejh.12251. Epub 2014 Jan 10.
- Wilson GJ, Bunpo P, Cundiff JK, Wek RC, Anthony TG. The eukaryotic initiation factor 2 kinase GCN2 protects against hepatotoxicity during ASNase treatment. *Am J Physiol Endocrinol Metab*. 2013 Nov 1;305(9):E1124-33. doi: 10.1152/ajpendo.00080.2013. Epub 2013 Sep 3.